sensors

MDPI

Article

Characterization of RAP Signal Patterns, Temporal Relationships, and Artifact Profiles Derived from Intracranial Pressure Sensors in Acute Traumatic Neural Injury

Abrar Islam [1,*], Amanjyot Singh Sainbhi [1], Kevin Y. Stein [1,2], Nuray Vakitbilir [1], Alwyn Gomez [3,4], Noah Silvaggio [4], Tobias Bergmann [1], Mansoor Hayat [3], Logan Froese [5] and Frederick A. Zeiler [1,3,4,5,6,7]

[1] Department of Biomedical Engineering, Price Faculty of Engineering, University of Manitoba, Winnipeg, MB R3T 2N2, Canada; amanjyot.s.sainbhi@gmail.com (A.S.S.); steink34@myumanitoba.ca (K.Y.S.); vakitbir@myumanitoba.ca (N.V.); bergmant@myumanitoba.ca (T.B.); frederick.zeiler@umanitoba.ca (F.A.Z.)
[2] Undergraduate Medicine, Rady Faculty of Health Sciences, University of Manitoba, Winnipeg, MB R3T 2N2, Canada
[3] Section of Neurosurgery, Department of Surgery, Rady Faculty of Health Sciences, University of Manitoba, Winnipeg, MB R3T 2N2, Canada; gomeza35@myumanitoba.ca (A.G.); mansoor.hayat@umanitoba.ca (M.H.)
[4] Department of Human Anatomy and Cell Science, Rady Faculty of Health Sciences, University of Manitoba, Winnipeg, MB R3T 2N2, Canada; silvaggn@myumanitoba.ca
[5] Department of Clinical Neurosciences, Karolinksa Institutet, 171 77 Stockholm, Sweden; log.froese@gmail.com
[6] Pan Am Clinic Foundation, Winnipeg, MB R3M 3E4, Canada
[7] Division of Anaesthesia, Department of Medicine, Addenbrooke's Hospital, University of Cambridge, Cambridge CB2 1TN, UK
* Correspondence: islama9@myumanitoba.ca

Abstract: Goal: Current methodologies for assessing cerebral compliance using pressure sensor technologies are prone to errors and issues with inter- and intra-observer consistency. RAP, a metric for measuring intracranial compensatory reserve (and therefore compliance), holds promise. It is derived using the moving correlation between intracranial pressure (ICP) and the pulse amplitude of ICP (AMP). RAP remains largely unexplored in cases of moderate to severe acute traumatic neural injury (also known as traumatic brain injury (TBI)). The goal of this work is to explore the general description of (a) RAP signal patterns and behaviors derived from ICP pressure transducers, (b) temporal statistical relationships, and (c) the characterization of the artifact profile. Methods: Different summary and statistical measurements were used to describe RAP's pattern and behaviors, along with performing sub-group analyses. The autoregressive integrated moving average (ARIMA) model was employed to outline the time-series structure of RAP across different temporal resolutions using the autoregressive (p-order) and moving average orders (q-order). After leveraging the time-series structure of RAP, similar methods were applied to ICP and AMP for comparison with RAP. Finally, key features were identified to distinguish artifacts in RAP. This might involve leveraging ICP/AMP signals and statistical structures. Results: The mean and time spent within the RAP threshold ranges ([0.4, 1], (0, 0.4), and [−1, 0]) indicate that RAP exhibited high positive values, suggesting an impaired compensatory reserve in TBI patients. The median optimal ARIMA model for each resolution and each signal was determined. Autocorrelative function (ACF) and partial ACF (PACF) plots of residuals verified the adequacy of these median optimal ARIMA models. The median of residuals indicates that ARIMA performed better with the higher-resolution data. To identify artifacts, (a) ICP q-order, AMP p-order, and RAP p-order and q-order, (b) residuals of ICP, AMP, and RAP, and (c) cross-correlation between residuals of RAP and AMP proved to be useful at the minute-by-minute resolution, whereas, for the 10-min-by-10-min data resolution, only the q-order of the optimal ARIMA model of ICP and AMP served as a distinguishing factor. Conclusions: RAP signals derived from ICP pressure

check for updates

Received: 18 December 2024
Revised: 14 January 2025
Accepted: 15 January 2025
Published: 20 January 2025

Citation: Islam, A.; Sainbhi, A.S.; Stein, K.Y.; Vakitbilir, N.; Gomez, A.; Silvaggio, N.; Bergmann, T.; Hayat, M.; Froese, L.; Zeiler, F.A. Characterization of RAP Signal Patterns, Temporal Relationships, and Artifact Profiles Derived from Intracranial Pressure Sensors in Acute Traumatic Neural Injury. *Sensors* **2025**, *25*, 586. https://doi.org/10.3390/s25020586

sensor technology displayed reproducible behaviors across this population of TBI patients. ARIMA modeling at the higher resolution provided comparatively strong accuracy, and key features were identified leveraging these models that could identify RAP artifacts. Further research is needed to enhance artifact management and broaden applicability across varied datasets.

Keywords: traumatic brain injury; cerebral compliance; RAP; Signal Processing; Cerebral Dynamics

1. Introduction

Acute biomechanical traumatic neural injury, also termed traumatic brain injury (TBI), is a significant global health concern, causing over 50 million cases annually and incurring worldwide costs of approximately CAD 540 billion [1]. In Canada and globally, TBI remains a leading cause of death and disability [2]. The impact of moderate to severe TBI involves both primary and secondary injuries. Primary injuries occur at the moment of impact, causing immediate structural brain damage. In contrast, secondary injuries develop over time through systemic and cellular processes that exacerbate brain tissue damage. Unlike primary injuries, secondary injury mechanisms may respond to therapeutic interventions, offering opportunities to enhance patient outcomes. To prevent secondary injury across patient populations, current management strategies for moderate to severe TBI focus on guideline-based interventions that target physiological parameters using data from invasive pressure sensor technologies [2–5]. A key focus is maintaining intracranial pressure (ICP) below 22 mmHg, triggering therapeutic measures when exceeded [2,3]. ICP, which is often derived from invasive strain-gauge pressure sensors, is also used as an indicator of intracranial compliance, with the bedside manual visual inspection of pulse waveform morphology for assessing compensatory reserve. Intracranial compliance/compensatory reserve is a parameter that provides insight into the brain's ability to adapt to changes in volume while maintaining stable pressure levels [6,7]. However, these methods are prone to errors, along with inter-observer and intra-observer consistency issues.

As a result, the RAP index was derived using signal sources from ICP pressure sensors, and has the potential for usage in TBI. RAP is a metric of intracranial compensatory reserve (and therefore compliance) derived using the moving correlation between ICP and the pulse amplitude of ICP (AMP) from any ICP pressure sensor technology [8–12]. In recent hydrocephalus studies, RAP (the correlation [R] between AMP [A] and ICP [P]) helped predict shunt failure in patients [8–11]. In addition, this index can be continuously calculated at the bedside in those patients with continuous ICP monitoring, optimally positioning it for use in TBI monitoring. As RAP values are the Pearson correlation coefficients, they range from -1 to $+1$, with lower positive values indicating good compliance, while higher positive and negative values suggest poor and exhausted compliance, respectively [8,9]. However, RAP has not been thoroughly investigated in moderate to severe TBI populations. Specifically, there is a lack of understanding of the general statistical behaviors of RAP in relation to ICP and AMP, its temporal time-series structure, and the characterization of its artifact profiles [7,13].

Therefore, this study aims to explore the following: (A) the general description of RAP signal patterns and behaviors, (B) the temporal statistical profile of RAP, and (C) the characterization of RAP artifact profiles. Gaining more profound insights into these aspects is essential for advancing the future integration of the RAP index into bedside monitoring,

enhancing patient trajectory modeling, and supporting clinical intervention studies based on RAP values.

2. Materials and Methods

2.1. Patients

As with previous studies from our lab group [14,15], the data were retrospectively obtained from the TBI database prospectively maintained at the Multi-omic Analytics and Integrative Neuroinformatics in the HUman Brain (MAIN-HUB) Lab at the University of Manitoba. This study included patient data collected from January 2018 to March 2023. All patients in this cohort experienced moderate to severe TBI (Glasgow Coma Score < 12). Invasive ICP and arterial blood pressure (ABP) monitoring were conducted as per Brain Trauma Foundation (BTF) guidelines [2].

2.2. Ethics

Data collection was conducted with full approval from the University of Manitoba Health Research Ethics Board (H2017:181, H2017:188, and H2024:266).

2.3. Data Collection

In line with our previous work [14,15], all physiological data were recorded and digitized at a high frequency of 100 Hz or higher using Intensive Care Monitoring 'Plus' (ICM+ v8.5.4.6) data acquisition software, with analog-to-digital converters (Data Translations, DT9804 or DT9826) employed as needed. ABP was captured via radial arterial lines, while ICP was measured invasively using intra-parenchymal strain gauge probes (Codman ICP MicroSensor; Codman & Shurtleff Inc., Raynham, MA, USA) placed in the frontal lobe or using external ventricular drains (Medtronic, Minneapolis, MN, USA) in four cases.

For this study, demographic information at admission was extracted according to existing prognostic models in TBI. The collected demographic data included age, biological sex, admission pupillary response (bilaterally reactive, unilaterally reactive, or bilaterally unreactive), Marshall computed tomography (CT) grade, and Glasgow Outcome Scale-Extended (GOSE) grade.

2.4. Signal Processing

Post-acquisition processing of the above signals was conducted using ICM+, in keeping with our previously published methodology. ICP and ABP were initially decimated using 10 s moving averages updated every 10 s to avoid data overlap [14–16]. Mean arterial pressure (MAP) was subsequently calculated from ABP. AMP was obtained through Fourier analysis of the fundamental harmonic of the ICP waveform [7,17,18]. RAP was derived via the moving Pearson correlation coefficient between 30 consecutive 10 s mean windows (i.e., each calculation window was 5 min) of the parent signals (ICP and AMP), updated every minute according to previously validated methods [9,19–21]. This analysis also included cerebrovascular reactivity. The pressure reactivity index (PRx) is a continuous measure for assessing cerebrovascular reactivity [6,22,23]. Likewise, PRx was determined using the Pearson correlation coefficient between ICP and MAP, where the update period (i.e., one minute) and the calculation window size (i.e., 5 min) were similar to those of RAP [14,24,25].

2.5. Analysis of the Patterns and Behaviours of RAP

Alongside RAP, the analysis also included ICP, MAP, AMP, and CPP signals, since ICP and AMP were used to derive RAP [8,19], while MAP and cerebral perfusion pressure (CPP) helped establish standard thresholds used in RAP analysis in this field [2,26]. Firstly,

Panda's (a Python library) [27] describe function [28] from Python was used to find the summary measurements for each signal in all patients. Following this, a custom script was executed to find the time spent on RAP within certain threshold ranges (0.4 to 1, 0 to 0.4, and −1 to 0), based on a systematic review study previously conducted by our lab [19]. Afterwards, a comparative sub-group analysis was conducted based on age, biological sex, pupillary response, Marshall CT grade, outcome (GOSE grade), ICP, AMP, and PRx values. Threshold lines for these comparisons were established using commonly referenced values from prior studies [29–32] in related fields, as follows:

- Age—less than 40 years, 40 to 60 years, and above 60 years;
- Pupillary response—bilateral reactive, bilateral unreactive, and unilateral unreactive;
- Marshall CT grade—grade II, grade III, grade IV, and grade V;
- Outcome GOSE grade—alive/dead (2 or higher vs. 1) and favorable/unfavorable (5 or higher vs. 4 or less);
- ICP thresholds—below 20 mmHg and above 22 mmHg;
- AMP thresholds—below 1, between 1 and 3, and above 3;
- PRx thresholds—less than 0 vs. greater than 0 and less than 0.25 vs. greater than 0.25

Mann–Whitney U-test was utilized for the formal comparison since none of the groups showed normal distributions. One-way ANOVA was used to compare more than two groups. To run these operations, Python's (version 3.7.16) mannwhitneyu [33] and f_oneway [34] functions from scipy.stats library were used, respectively.

2.6. Analysis of RAP Time-Series Structures

2.6.1. Application of ARIMA Model

The autoregressive integrated moving average (ARIMA) model is a widely used statistical method for time-series forecasting [35–38]. It works by combining three main components, as follows: autoregression (AR), differencing to make data stationary (I for Integrated), and a moving average (MA). The model aims to capture the underlying patterns in time-series data and predict future values based on historical observations [35–38]. The AR part is controlled by the parameter p, representing the number of lagged observations in the model. It refers to the regression of the variable on its own lagged (previous) values. The parameter d represents the number of times the data need to be differenced to achieve stationarity. The MA part is controlled by parameter q, representing the number of lagged error terms in the model. It refers to modeling the error (or residual) term as a linear combination of previous error terms [35–38]. An ARIMA model is usually written as ARIMA(p, d, q). Assuming the signal is stationary (d-order = 0), a general autoregressive moving average model for a physiological signal, X, can be represented using Equation (1). In this model, p is the autoregressive order, q is the moving average order, X_t is the signal at time t, X_{t-i} is the signal at time $t - i$, ε_t is the error at time t, ε_{t-j} is the error at time $t - j$, φ is the autoregressive coefficient at time $t - i$, and θ is the moving average coefficient at time $t - j$ [14].

$$X_t = c + \varepsilon_t + \sum_{i=1}^{p} \varphi_i X_{t-i} + \sum_{j=1}^{q} \theta_j \varepsilon_{t-j} \quad (1)$$

This ARIMA model was employed to capture the structure of time-series signals. ARIMA was chosen since it provides interpretability in terms of temporal dependencies (p, d, q), making it particularly suited for understanding signal dynamics, comparing temporal structure among signals and identifying artifacts. It is also a similar methodology to those used for determining the more basic aspects of cerebral blood flow physiologies [14,15]. According to previous works from the lab, both the p-order and q-order for determining the optimal ARIMA model varied from 0 to 10 [14,15]. The analysis was run on the differenced data

(discussed in Section 2.6.3), and therefore, the *d*-order was set to 0, which effectively acted as *d*-order = 1. The ARIMA function from the statsmodels module [39] of Python was used for this analysis. Each combination of the orders was evaluated to find the optimal model for each signal and each patient.

2.6.2. Statistical Metrics for ARIMA Analysis

Akaike Information Criterion (AIC), Bayesian Information Criterion (BIC), and Log-Likelihood (LL) were calculated to assess whether the models effectively captured the structure of the signal. These are statistical metrics used to evaluate the quality and goodness-of-fit of an ARIMA model, helping to assess how well the model captures the underlying structure of the time-series data [14,40,41]. Each of these metrics has its own characteristics and significance in model selection. AIC measures the goodness-of-fit of a model while penalizing for model complexity (the number of parameters). It balances model fit and complexity to avoid overfitting. BIC is similar to AIC but applies a more substantial penalty for models with more parameters, making it more conservative in terms of model complexity. LL measures the likelihood that the model could have generated the observed data. It reflects the fit of the model without penalizing for complexity. Lower AIC and BIC values indicate a better model, while higher LL values indicate a better fit [14,40,41].

According to a previous study from our lab, BIC is more stringent than AIC and LL [14]. On the other hand, models based on LL were more complex and could potentially overfit the data, leading to better residuals [14]. Given this, AIC was considered the most balanced option for model selection, as it strikes a middle ground between the stringency of BIC and the leniency of LL. For this reason, AIC was chosen to find the optimal ARIMA models for the signals.

2.6.3. Stationarity Analysis

Since the ARIMA model is built on the assumption of the stationarity of time series, the data need to be stationary to apply an ARIMA model. Hence, stationarity analysis was carried out. Like in the previous work from our lab [16], Augmented Dickey–Fuller (ADF) and Kwiatkowski–Phillips–Schmidt–Shin (KPSS) tests were used to check the stationarity of all the signals. The ADF test indicates whether a time series is trend-stationary, while the KPSS test determines if the series remains stationary around a linear trend [36,42]. If the *p*-value from the ADF test is less and the *p*-value from the KPSS test is higher than a certain threshold, the time series is considered stationary. In line with previous studies [16], the threshold was set at 0.05 for both tests. The adfuller and kpss functions from the statsmodels module [39] in Python were used to perform the tests at the patient level. Additionally, due to the ADF and KPSS test results on the original data (discussed in Section 3.2.1), these tests were performed on each patient's first-order-differenced data. It is noteworthy that the differenced data were achieved after temporal resolution.

2.6.4. Generation of Different Temporal Resolutions of Data

ICP, AMP, and RAP were calculated across various temporal resolutions for a comprehensive analysis and to examine the impact of the temporal resolution reduction on the results. Subsequently, the optimal ARIMA model at the patient level was calculated for each parameter for every temporal resolution. The temporal resolutions applied in this study included minute-by-minute, 10 min intervals, 30 min intervals, and hour-by-hour intervals. The primary derived data were at minute-by-minute intervals. Afterward, Panda's resample function [43] was used to reduce the resolution. The primary data (i.e., minute-by-minute resolution) mean of 10 min data points was determined as a single non-overlapping point in 10 min intervals. Similarly, for the 30 min and 1 h intervals, the

means of 30 consecutive data points and 60 consecutive data points, respectively, were used to represent each interval.

2.6.5. Evaluation Tools

After deriving the optimal ARIMA model for each patient, the median optimal ARIMA model for each signal was calculated based on those models (i.e., median p-order and median q-order values were calculated). The choice of the median value for optimal models across the whole population ensured a more representative summary across the examples while reducing the impact of outliers. To confirm the adequacy of the median optimal ARIMA models, the magnitude of residuals, autocorrelation function (ACF), and partial ACF (PACF) plots of residuals were examined by comparing the raw data to the modeled data [14,36]. Residuals represent the differences between actual data points and model-predicted values. The ACF measures the relationship between a time series and its past values, while the PACF indicates the correlation between a time series and its lagged values, excluding the effects of intermediate lags. For a well-fitted ARIMA model, residuals should be minimal, and the ACF and PACF plots should show no significant spikes at any lags, indicating that the model has captured the underlying structure [14,36]. Additionally, this analysis included the calculation of the overall variance in data, the residual variance, and the count of significant spikes to justify that the data had been modeled well.

2.7. RAP Artifact Segment Analysis

2.7.1. Separating True Artifact Segments

For this section, true artifacts had to be calculated. Previously, to obtain clean and artifact-free data, artifacts were manually detected and removed from the raw collected data by experts in cerebral physiologic signal analysis and neurophysiology. Therefore, while comparing clean data with non-clean data, any additional data present in the non-clean version but absent in the clean version should be taken as representing artifacts. This step was performed by comparing timestamps of clean and non-clean data. Afterwards, identified artifact segments were saved into different comma-separated value (CSV) files.

2.7.2. Analysis of Clean Data and Artifact Segments

The optimal models for the clean signal have already been obtained in the previous section. The optimal models for the artifact segments were calculated for each signal of each patient using the same methodology. Finally, a comparison between clean data and artifact segments based on temporal structure was conducted using various statistical techniques. The temporal resolutions applied in this analysis included minute-by-minute and 10 min intervals. The remaining resolutions were excluded from this analysis because, at such low resolutions, the quantity of artifact data would be insufficient to yield significant results in this section.

This analysis focused on three key areas:

(i) Comparing optimal ARIMA models—The optimal models for the clean data were obtained in the previous section (i.e., Section 2.6). The optimal models for the artifact segments were also computed for each signal of each patient using the same methodology. These models for clean data and artifact segments are expected to differ, resulting in varying p-orders and q-orders between the two groups for each patient. A formal comparison of the groups' ARIMA orders for each signal was conducted using the Mann–Whitney U test, with scatterplots provided for visual representation;

(ii) Comparing the residuals—Using the median optimal ARIMA model calculated for clean data in Section 2.6, residuals for clean and artifact segments were computed and formally compared at the patient level. The results are expected to indicate significant

differences in the mean residuals and variance of residuals between the clean and artifact groups;

(iii) Comparing the cross-correlation of residuals—If cross-correlation is calculated between RAP residuals and ICP/AMP residuals, the expectation is that the maximum correlation value between clean RAP and clean ICP/AMP residuals would be higher than that between clean RAP and artifact ICP/AMP residuals. Since RAP is derived from ICP and AMP, their residuals should naturally show a strong correlation. However, this correlation is expected to decrease when considering the artifact segments of ICP/AMP, as these segments do not accurately represent true ICP/AMP values. The *correlate* function from the *Numpy* library was used to calculate the cross-correlations, and it measured the similarity between two signals (or datasets) as a function of the time lag applied to one of them (i.e., calculated dot product).

2.7.3. Evaluating Identified Features

After analyzing the data to identify features with the potential to effectively distinguish artifacts, a simple sliding window approach was applied to the non-clean data to assess the success rate of these features in identifying artifacts within the signal. The success rate of capturing artifacts within the signal was calculated as (captured artifacts/true artifacts) $\times$ 100%.

3. Results

3.1. Patient Demographics

As reported in Table 1, 109 TBI patients were included in this study, with a median recording duration of 4125.13 min. The median age of the patients was 43 years (interquartile range (IQR): 29 to 57), and 89 of the patients were male (81.65%). The median Glasgow Coma Scale (GCS) score was 7 (IQR: 4 to 8), while the median motor sub-score was 4 (IQR: 2 to 5).

Table 1. Demographic data.

Variable	Median (IQR) or Number (%)
Duration of Recording (min)	4125.13 (1714.99–7250.14)
Number of Patients	109
Age (years)	43 (29–57)
Sex (Male)	89 (81.65%)
GCS	7 (4–8)
GCS Motor	4 (2–5)
Pupils	
Bilateral Reactive	65 (59.63%)
Unilateral Reactive	25 (22.93%)
Bilateral Unreactive	19 (17.43%)
Marshall CT Score	
V	55 (50.46%)
IV	20 (18.34%)
III	31 (28.44%)
II	3 (2.75%)

CT, computerized tomography; GCS, Glasgow Coma Score; IQR, interquartile range.

3.2. General RAP Patterns and Behaviours

3.2.1. Summary Measurements

There were some unrealistic values of ICP and MAP in the data that could lead to erroneous CPP, AMP, and RAP values, since they are derived from them. Therefore,

according to the previous studies [44], data points with ICP > 100 mmHg or <−15 mmHg and MAP > 200 mmHg or <0 mmHg were excluded from this analysis. Afterwards, summary measures of the aforementioned parameters were calculated and are depicted in Table A1 of Appendix A. Notably, RAP had a mean of 0.632 ± 0.483.

Based on our previous study, RAP was classified into three distinct states according to its value [19], which were as follows: (i) state 1, representing a healthy condition, was characterized by small positive RAP values close to zero; (ii) state 2, which was most commonly observed in TBI patients, reflected impaired intracranial compliance and compensatory reserve, with elevated RAP values (RAP > 0.4), and (iii) state 3 occurred in more severe conditions, indicating the further deterioration of compensatory reserve, cerebrovascular reactivity, and cerebral autoregulation. This state was associated with a significant number of fatal outcomes and was marked by declining RAP values, including, in some cases, negative RAP [19]. Based on the mean RAP obtained in this study, it can be stated that the mean RAP fell into state 2, indicating impaired cerebral compliance and compensatory reserve. This finding is consistent with our previous study, wherein state 2 was also the most commonly observed condition among TBI patients [19].

3.2.2. Time Spent Within Thresholds

According to the threshold ranges outlined in Section 2.5, the percentage of time spent within each range was calculated for all patients and is presented in Table A2 of Appendix A. So, using the RAP index, the highest percentage of time spent was in the impaired state (ranging from RAP of 0.4 to 1), which was 78.091% and corresponds to state 2, as previously defined [19].

3.2.3. Sub-Group Analysis

The sub-group analysis results are shown in Appendix A Tables A3–A15. In the age groups analysis, for the first age comparison (i.e., age above and below 40 years), only ICP showed a significant difference ($p = 0.048$) between the two groups, with AMP having a near-significant p-value of 0.065227, as depicted in Table A3 of Appendix A. In the second age comparison (age below 40 years, 40 to 60 years, and above 60 years), AMP and RAP were significantly different ($p = 0.046$, $p = 0.005$), while ICP showed no significant difference ($p = 0.284$) (Table A4 of Appendix A).

In the M/F sex groups, only CPP ($p = 0.008$) was significantly different (Table A5 of Appendix A). For pupillary response, none of the parameters showed significant differences (Table A6 of Appendix A). In Marshall CT grade groupings, ICP, AMP, and RAP were significantly different across groups ($p = 0.002$, $p = 0.0003$, $p = 0.00001$) (Table A7 of Appendix A). RAP increased from grade II to IV, but at grade V, it decreased. A similar case was observed for ICP and AMP.

For outcome comparison, the GOSE grade was assessed at 1-month and 6-month intervals (Tables A8–A11 of Appendix A). In the alive/dead comparison, for both cases, AMP significantly differentiated the groups in both intervals ($p = 0.003$, $p = 0.01$), while ICP and CPP were only significant in the 1-month GOSE results ($p = 0.033$, $p = 0.032$). However, RAP was not significant in either case. In the favorable/unfavorable cases, ICP, CPP, and AMP were significantly different for both intervals, but RAP again showed no significant difference in either case ($p = 0.294$, $p = 0.403$).

In the subgroup analysis for ICP, all parameters showed significant differences between the two groups (p = close to 0 for both groups). The group with ICP > 22 mmHg had higher RAP and AMP values than the other group. Similarly, in the AMP analysis, both ICP and RAP increased as AMP rose, reflecting the findings from the ICP subgroup analysis, with all parameters displaying significant differences.

Finally, in PRx analysis, the first comparison showed that RAP had a lower mean value when PRx > 0 compared to PRx < 0, though ICP and AMP were higher. This finding suggests that impaired cerebrovascular reactivity (PRx > 0) was associated with reduced RAP, aligning with the results of our systematic review [19]. This decrease in RAP corresponded to state 3 of RAP [19], as defined in Section 3.2.1. Similarly, in the second comparison, using a PRx threshold of 0.25, a comparable pattern emerged, with lower RAP being associated with higher PRx values (i.e., PRx > 0.25). Similar to the ICP and AMP threshold analyses, all parameters demonstrated significant differences between sub-groups in the PRx threshold analysis (p = close to 0 for all cases). The results of these three threshold analyses are presented in Tables A12–A15 of Appendix A.

3.3. Optimal ARIMA Structure Analysis

3.3.1. Stationarity Assessment

As discussed in Section 2.6.3, ADF and KPSS tests were performed for each patient and signal to check the stationarity of the signals. Initially, these tests were applied to the original data. Tables A16 and A17 of Appendix B illustrate the p-values for each patient's test results at the minute-by-minute data resolution. Additionally, Tables A20 and A21 of Appendix C show the summarized results. As shown in the tables, while most of the signals appeared stationary according to the ADF tests, the KPSS test indicated that most were non-stationary. This suggests that the signals are largely trend-stationary, but likely non-stationary around a linear trend. However, for ARIMA model analysis, the data need to be stationary in terms of both cases. Therefore, a first-order difference was applied to the original data after temporal resolution. Tables A18 and A19 of Appendix B show the p-values for each patient's test results at the minute-by-minute data resolution. The resulting outcomes are summarized in Tables A22 and A23 of Appendix C.

As evident from the tables, after applying first-order differencing, nearly all the data, with a few exceptions, were assessed as stationary in both tests. Therefore, these differenced data were suitable for ARIMA model analysis.

3.3.2. Determination of Optimal ARIMA Models

Appendix D provides the optimal ARIMA models for each signal at each resolution for each patient, detailing the p-, d-, and q-orders along with their AIC values. Based on these results, the population global median optimal models in each resolution were calculated and are shown in Table 2. As shown in the table, the models for each signal were quite similar in the case of 10-min resolution and below.

Table 2. Global population median optimal models for each resolution.

Temporal Resolution	ICP	AMP	RAP
Minute-by-minute	5, 1, 1	3, 1, 5	3, 1, 3
10-min-by-10-min	2, 1, 2	2, 1, 3	1, 1, 1
30-min-by-30-min	2, 1, 2	2, 1, 2	1, 1, 1
Hour-by-hour	2, 1, 2	1, 1, 1	1, 1, 1

AMP, pulse amplitude of ICP; ICP, intracranial pressure; RAP, compensatory reserve index.

3.3.3. Evaluation of Optimal ARIMA Models

With the median optimal ARIMA models now determined, the quality of these models can be assessed using the residuals, ACF, and PACF plots of residuals. Figure 1 represents a patient example of the ACF and PACF plots of residuals for RAP at 1 min intervals for pre- and post-ARIMA modeled data.

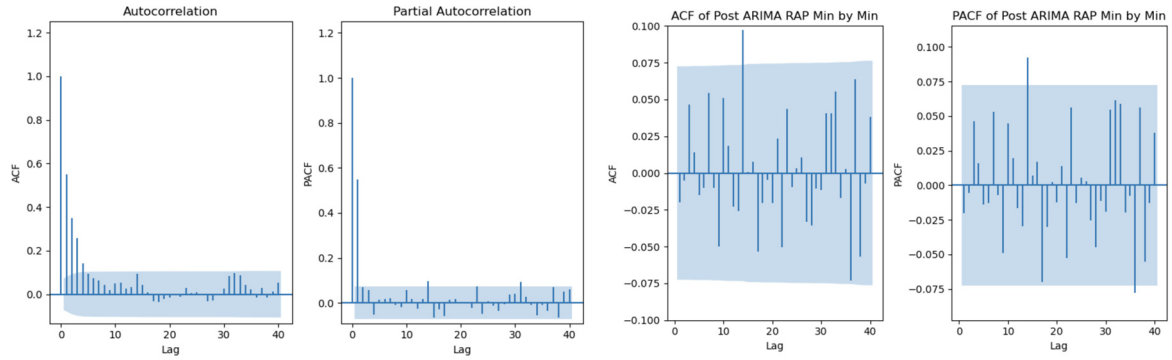

Figure 1. ACF and PACF plots at minute-by-minute temporal resolution—patient example. (**a**) RAP pre-ARIMA plots, (**b**) RAP post-ARIMA (3, 1, 3) plots.

The figure corresponds to the residuals of the RAP signal (a) before and (b) after ARIMA. The original plots had significant spikes in both ACF and PACF plots, while the spikes in post-ARIMA (3, 1, 3) were mostly within the 95% confidence interval, indicating that the model moderately accounts for the RAP structure.

ACF, autocorrelative function; ARIMA, autoregressive integrated moving average; PACF, partial autocorrelative function; RAP, compensatory reserve index.

Figure 1a corresponds to the original RAP data since the orders were set to zero (ARIMA (0, 0, 0)). Figure 1b utilizes the median optimal ARIMA model for RAP (ARIMA (3, 1, 3)). It is evident that the ACF plot of the residuals using the original data showed a gradual decay, while the PACF plot had significant spikes at various lags, indicating that the ARIMA (0, 0, 0) model did not effectively capture the signal's structure. On the contrary, after applying the median optimal ARIMA model for RAP (3, 1, 3), only two significant spikes were present at lag 15, with another after lag 30 in the PACF plot. Otherwise, most of the ACF and PACF values fell within the 95% confidence interval, implying that any autocorrelation left in the residuals is not statistically significant and suggesting that the calculated ARIMA model successfully captured the structure of the signal.

Figures A1 and A3 of Appendix E illustrate a patient example of ACF and PACF plots with this comparison for ICP and AMP signals, and demonstrate similar results, proving that the calculated median optimal ARIMA model captures the time-series structure with moderate performance.

While visually, the performance of the optimal ARIMA model is satisfactory, the global population median of residuals was compared with it to provide a better description between the original data and those yielded after optimal ARIMA model application for all signals, as reported in Table 3.

Table 3. Global population median residuals of the signals.

Parameter	Original	Optimal ARIMA Model
ICP	0.63008	0.17941
AMP	0.49329	0.13549
RAP	0.32493	0.12564

AMP, pulse amplitude of ICP; ARIMA, autoregressive integrated moving average; ICP, intracranial pressure; RAP, compensatory reserve index.

While calculating, the absolute value of the residuals of each data point was taken for the betterment of the calculation. The median residual of the optimal ARIMA model was substantially less than that of the original data for all signals, which further emphasizes the

ARIMA model's success in capturing the signal structure. Additionally, the variance of the overall data, variance in the residuals, and the number of significant spikes were calculated and are shown in Table A25 of Appendix E. It can be seen that the variance of the residuals was smaller than that of the original data. Furthermore, both ACF and PACF plots for the modeled data had only one significant spike, in contrast to the original ACF and PACF plots, which had seven and two spikes, respectively. These values align with the results from Figure 1 and Table 3, further proving that the data are being modeled. The values of these parameters were calculated for each signal of each patient at the minute-by-minute resolution, as shown in Tables A27, A29 and A30 of Appendix E. Subsequently, the means and medians were determined, as presented in Tables A31 and A32 of Appendix E. The attribute values in these tables indicate that the data were adequately modeled. The values of the variance in the residuals and the number of significant spikes in ACF and PACF plots were much smaller than those of the original data.

A similar analysis was performed at different temporal resolutions for the same patients. Figure 2 shows a patient example of the ACF and PACF plots of the residuals for RAP at the remaining temporal resolutions. Even though all the lags were within the 95% confidence interval at all the resolutions (which was also justified by the result in Table A26 of Appendix E), the ACF and PACF plots exhibited comparatively significant spikes with higher magnitudes than those at the minute-by-minute temporal resolution (depicted in Figure 1b). This indicates that while the optimal ARIMA model captures the time-series structure in both cases, it is more successful at the minute-by-minute resolution than at other lower temporal resolutions. Figures A2 and A4 of Appendix E present these comparative figures for ICP and AMP at the 10 min, 30 min and 1 h intervals, which also displayed similar characteristics in the ACF and PACF plots of the residuals.

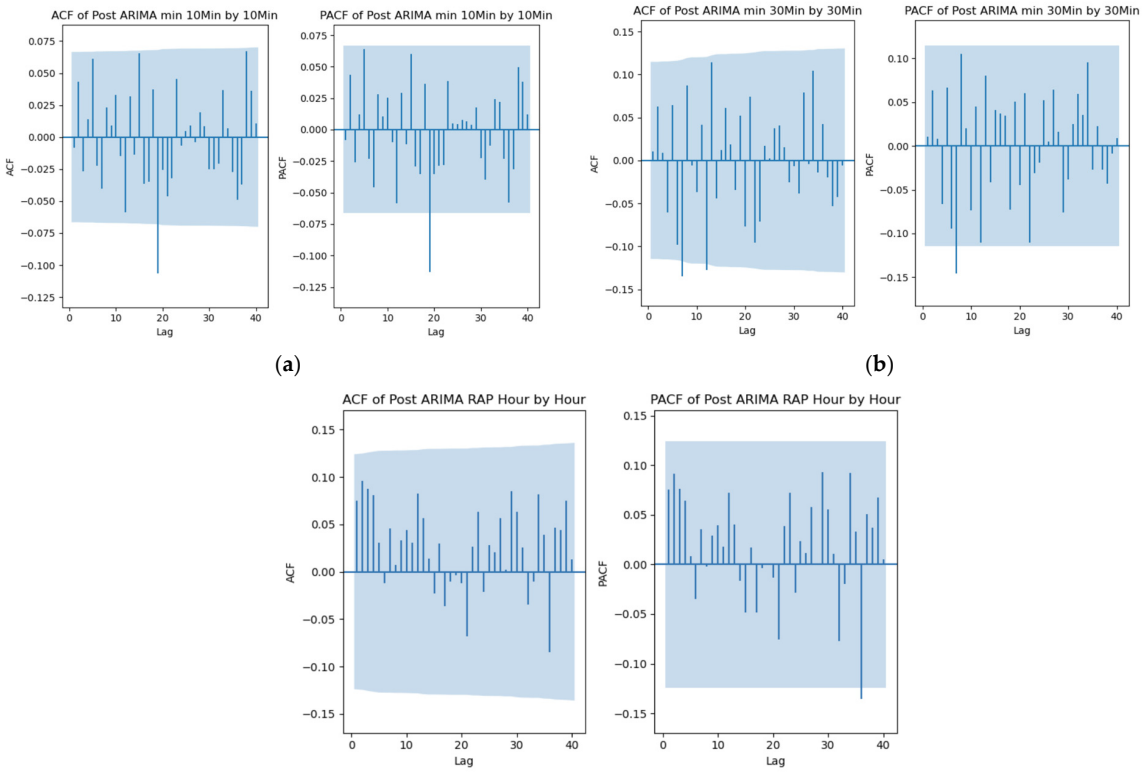

Figure 2. ACF and PACF plots at different resolutions—patient example. (**a**) At 10-min-by-10-min resolution with ARIMA (1, 1, 1), (**b**) at 30-min-by-30-min resolution with ARIMA (1, 1, 1), (**c**) at hour-by-hour resolution with ARIMA (1, 1, 1).

The figure documents the ACF and PACF of the residuals of the RAP-mapped ARIMA structure in the (a) 10-min-by-10-min, (b) 30-min-by-30-min, and (c) hour-by-hour relationships.

ACF, autocorrelative function; ARIMA, autoregressive integrated moving average; PACF, partial autocorrelative function; RAP, compensatory reserve index.

3.4. Assessment of the Features for Identifying Artifacts

3.4.1. Comparing Optimal ARIMA Models

Initially, the optimal ARIMA models for the artifact segments of each signal of each patient were calculated. The results are depicted in Table A34 of Appendix F. Afterwards, the medians and means of the orders of the ARIMA models for the two groups were calculated. Tables A35 and A36 of Appendix F contain the median and the mean results for the 1 min and 10 min temporal resolutions. *d*-order was not included in the analysis, as it was set to 1 across all cases. While calculating optimal models for the artifact segments of 10 min data, five examples (i.e., patients) could not provide any result because of the inadequacy of data (i.e., artifact segments). As both tables show, the median and mean orders of all clean and artifact data parameters differed significantly, particularly for the minute-by-minute data. The Mann–Whitney U test that was conducted on these two groups of orders could provide a clear statistical comparison. The resulting *p*-values are as follows.

As reported in Table 4, since *p*-value < 0.05 indicates a significant difference between the two groups, it can be concluded that in the case of minute-by-minute data, both the *p*-orders (p = close to 0) and *q*-orders (p = 0.01526) of the RAP ARIMA model can serve as effective indicators for distinguishing artifact segments from clean data. However, only the *q*-order of ICP (p = 0.00058) and the *p*-order of AMP (p = 0.00501) demonstrated a significant difference between the two groups. For the lower-resolution data, RAP did not appear to show any notable differences across any orders. However, the *q*-orders of ICP (p = close to 0) and AMP (p = 0.00032) exhibited significant differences.

Table 4. A comparative analysis between clean and artifact segments' optimal ARIMA models (*p*-values from Mann–Whitney U-test).

Parameter	Minute-by-Minute		10-min-by-10-min	
	***p*-Order**	***q*-Order**	***p*-Order**	***q*-Order**
ICP	0.60996	**0.00058**	0.49778	**close to 0**
AMP	**0.00501**	0.20620	0.23175	**0.00032**
RAP	**close to 0**	**0.01526**	0.88808	0.94798

All the significant *p*-values are marked in bold. AMP, pulse amplitude of ICP; ARIMA, autoregressive integrated moving average; ICP, intracranial pressure; RAP, compensatory reserve index.

To visually represent the data, scatterplots comparing the orders of the two groups are shown in Figure 3. As seen in the figure, there are only a few patient examples wherein the clean and artifact segment orders overlap in the minute-by-minute resolution (Figure 3a). The majority of them differ, confirming that the optimal models for the parameters of clean and artifact segments are quite distinct. In the case of the 10 min resolution data, although many instances show non-overlapping orders, there are more examples of overlap compared to the minute-by-minute resolution. Scatterplots for RAP *q*-order and the rest of the signals are demonstrated in Appendix F Figures A6–A8. They also displayed similar results, with both of the orders differing between the two groups and the minute-by-minute resolution showing a more pronounced distinction.

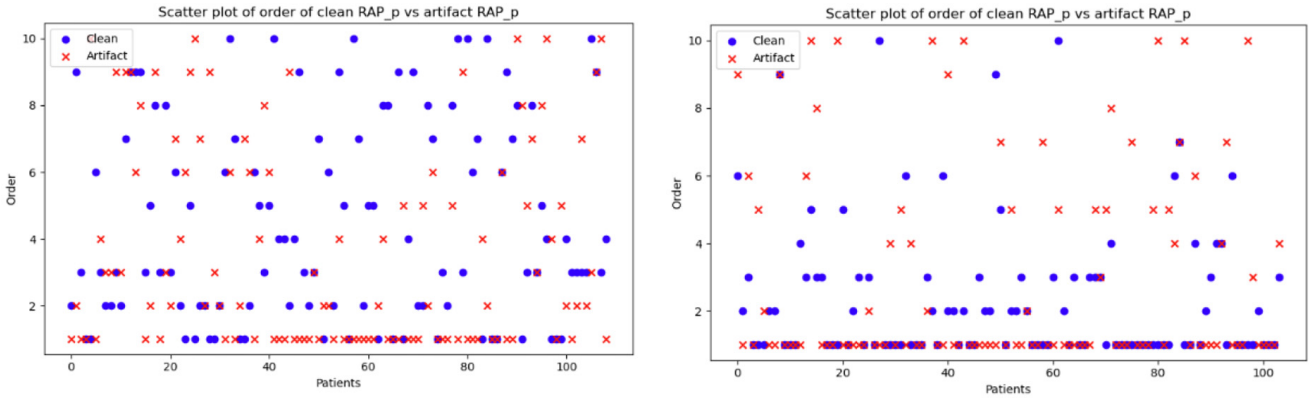

(**a**) (**b**)

Figure 3. Scatterplots for RAP *p*-orders at different resolutions for each patient. (**a**) at minute-by-minute resolution, (**b**) at 10-min-by-10-min resolution.

The figure demonstrates the values of the *p*-orders from the ARIMA model of the clean vs. artifact for each patient at (a) minute-by-minute resolution and (b) 10-min-by-10-min resolution. The blue circles correspond to the *p*-orders of the cleaned data, whereas the red crosses represent the *p*-orders of the artifact segment. If a red cross overlaps a blue circle, the value of the order for that patient is the same. If they do not overlap, the values differ.

ARIMA, autoregressive integrated moving average; RAP, compensatory reserve index.

As seen from the figures, there are only a few patient examples wherein the clean and artifact segment orders overlap in the minute-by-minute resolution (Figure 3a). The majority of them differ, confirming that the optimal models for the parameters of clean and artifact segments are quite distinct. In the case of the 10-min resolution data, although many instances show non-overlapping orders, there are more examples of overlap compared to the minute-by-minute resolution. Scatterplots for RAP *q*-order and the rest of the signals are demonstrated in Appendix F Figures A6–A8. They also display similar results, with most of the orders differing between the two groups and the minute-by-minute resolution showing a more pronounced distinction.

To assess the success rate of artifact identification, the sliding window method was applied at the patient level. For minute-by-minute data, a window size of 100 with a sample size of 50 was used, while for 10-min-by-10-min data, a window size of 50 with a sample size of 25 was employed. Within each window, the optimal ARIMA model was calculated, and artifacts were identified in the window if any of the calculated orders (p, d, or q) differed by more than three from those of the clean data optimal model. Using this approach, the average success rates for artifact identification were 65.258% for ICP, 65.258% for AMP, and 84.038% for RAP at the minute-by-minute resolution. The average success rates for artifact identification at the 10-min-by-10-min resolution were 55.336% for ICP, 54.128% for AMP, and 43.089% for RAP. Tables A37 and A38 of Appendix G depict the average success rates for artifact identification in both temporal resolutions.

3.4.2. Comparing the Residuals

Using the median optimal model described in Table 5, the residuals of clean data and artifact segments were calculated for all patients. The difference between the two groups was determined using the Mann–Whitney U test for each patient. The result is summarized below, where significant corresponds to $p < 0.05$ and insignificant is otherwise.

Table 5. Significant and insignificant counts after a Mann–Whitney U test between clean and artifact residuals.

Parameter	Minute-by-Minute		10-min-by-10-min	
	Significant	Insignificant	Significant	Insignificant
ICP	63	45	17	79
AMP	64	45	22	74
RAP	65	44	8	96

AMP, pulse amplitude of ICP; ICP, intracranial pressure; RAP, compensatory reserve index.

As seen from the table, most cases showed significant differences at the minute-by-minute resolution while comparing clean residuals with artifact residuals. On the contrary, the result was the opposite in the 10-min temporal resolution, with the majority of examples belonging to the insignificant group.

While calculating residuals, a few patient examples had inadequate data points (1 patient at the minute-by-minute data resolution for ICP and 13 patients at the 10 min data resolution across all signals). Consequently, the residuals for those patients could not be calculated, and the analysis was carried out excluding them.

Additionally, to consider residuals as a feature to identify artifacts, the residuals of all the clean data should be low. In other words, they need to be consistent and should be fitted by the median optimal ARIMA model calculated for the clean data. To check this, the variance of the residuals of each patient was calculated (Table 6). The same was done for the artifact data (whose expected variance should be higher). The median and mean values of variance of each group were calculated as shown below.

Table 6. Medians and means of the variance of the residuals.

Parameter	Minute-by-Minute				10-min-by-10-min			
	Median		Mean		Median		Mean	
	Clean	Artifact	Clean	Artifact	Clean	Artifact	Clean	Artifact
ICP	1.41843	24.83865	2.00069	266.45723	4.56886	35.47967	10.2683	1837.70208
AMP	0.04842	0.61611	0.08891	2.29946	0.11453	0.09194	0.27448	3.60461
RAP	0.10523	0.20676	0.10882	0.21222	0.08715	0.10794	0.09471	0.11736

AMP, pulse amplitude of ICP; ICP, intracranial pressure; RAP, compensatory reserve index.

As shown in the table, the expected outcome was observed for both resolutions. Particularly, ICP showed the largest difference among the signals. However, the median results of AMP at the 10-min-by-10-min data resolution deviated from the expected result.

The sliding window method was applied at the patient level to evaluate the success rate of artifact identification for this feature. A window size of 50 with a sample size of 25 was used for both minute-by-minute and 10-min-by-10-min resolution. At first, the variance of residuals within each window was calculated, and artifacts were identified if the variance of residuals exceeded the median variance of the total data for a single patient. Using this method, the average success rates for identifying artifacts across the entire population were 70.212% for ICP, 56.916% for AMP and 91.666% for RAP at the minute-by-minute resolution, and 85.092% for ICP, 74.264% for AMP and 84.411% for RAP at the 10-min-by-10-min resolution, as illustrated in Tables A37 and A38 of Appendix G.

3.4.3. Comparing the Cross-Correlation of Residuals

The groups for this analysis were formed as outlined in Section 2.7.2. After calculating the cross-correlation of total signals for each case and patient, the maximum values from the results were recorded. Next, the median and mean values of the maximum cross-correlation between RAP and ICP/AMP residuals were calculated across the total population for both the clean and artifact cases, as follows below.

Table 7 demonstrates that for the minute-by-minute data, the maximum RAP–AMP cross-correlation of residuals was expectedly higher in clean–clean cases compared to clean–artifact cases, based on both median and mean values. However, this was not the case for RAP–ICP; even though the mean value of clean–clean cases was slightly higher, the median was lower. On the other hand, for the 10-min-by-10-min data, none of the clean–clean cases had considerably higher values in RAP–ICP (median and mean) cross-correlation. In contrast, RAP–AMP cross-correlation showed higher values in clean–clean cases in terms of both median and mean.

Table 7. Medians and means of the maximum cross-correlations of residuals.

Parameter	Minute-by-Minute				10-min-by-10-min			
	Median		Mean		Median		Mean	
	Clean and Clean	Clean and Artifact	Clean and Clean	Clean and Artifact	Clean and Clean	Clean and Artifact	Clean and Clean	Clean and Artifact
RAP-ICP	14.48875	23.01389	77.319716	46.14512	26.92	32.46088	36.9293	121.002
RAP–AMP	137.63467	28.61530	415.91384	51.74234	4.4332	1.55919	5.83130	3.97946

Clean and clean refers to the cross-correlation between clean RAP and clean ICP (RAP–ICP) or clean RAP and clean AMP (RAP–AMP), whereas clean and artifact refers to clean RAP and artifact ICP (RAP–ICP) or clean RAP and artifact AMP (RAP–AMP).

A Mann–Whitney U test was subsequently performed to compare the two groups—maximum cross-correlation of clean RAP residuals with clean ICP/AMP residuals vs. clean RAP residuals with artifact ICP/AMP residuals. For RAP–ICP, the p-values were 0.02809 for the minute-by-minute resolution and 0.31919 for the 10 min resolution. In contrast, for RAP–AMP, the p-values were close to 0 for both resolutions.

Additionally, the maximum cross-correlations of the two groups (i.e., RAP–ICP clean–clean residuals vs. clean–artifact residuals and RAP–AMP clean–clean residuals vs. clean–artifact residuals) were compared at the patient level. The expected result was that the clean–clean maximum cross-correlation of residuals should be greater than the clean–artifact maximum cross-correlation of residuals, as explained in Section 2.7.2. The numbers of patients (out of 108 patients in total) in each case that showed greater values in clean–clean cases are as follows: (i) RAP–ICP, 34 cases and (ii) RAP–AMP, 95 cases at the minute-by-minute resolution; (i) RAP–ICP, 41 cases and (ii) RAP–AMP, 69 cases at the 10-min-by-10-min resolution.

The outcome of this analysis aligns with the findings of the overall (median and mean) result presented in Table 7, showing that the RAP–AMP cross-correlation at the minute-by-minute resolution demonstrated the greatest number of patients (95 cases) with higher values of maximum cross-correlation in clean–clean cases, alongside RAP–AMP cross-correlation at the 10-min-by-10-min resolution demonstrating 69 cases. On the contrary, RAP–ICP failed to achieve such large numbers at both resolutions.

In the success rate findings of this feature, RAP–ICP and RAP–AMP cross-correlations were calculated within each window. The window sizes and sample sizes were similar to the previous feature (i.e., 50 and 25, respectively). Artifacts were predicted within a window if the maximum cross-correlation was lower than the median of the maximum cross-correlation values between clean and artifact groups of the total recording for a single

patient. Using this method, the median success rates for identifying artifacts across the entire population were 37.011% for RAP–ICP and 61.6% for RAP–AMP cross-correlation at the minute-by-minute resolution, whereas at the 10-min-by-10-min resolution, they were 6.512% and 35.829%, respectively.

4. Discussion

We set out to explore the RAP compensatory reserve index, derived from ICP pressure sensors, to better understand some critical aspects of such cerebral data streams. First, we comprehensively characterized the general nature of RAP signals with respect to other cerebral physiologic parameters, including subgroup analysis. Second, we outlined the time-series statistical structures of RAP in relation to its constituent signals (ICP and AMP). Finally, we leveraged our enhanced understanding of the time-series structures of RAP data streams to explore signal artifact detection. Throughout this process, some important aspects of RAP and the use of such sensor data streams deserve to be highlighted.

4.1. RAP's Patterns and Behaviours

First, based on the results in Appendix A, TBI patients generally demonstrated an impaired compensatory reserve, as they spent most of their time within the range of 0.4 to 1, as measured by the RAP index (illustrated in Table A2 of Appendix A), corresponding to state 2 of RAP [19], as defined in Section 3.2.1. Regarding age comparison, Tables A3 and A4 of Appendix A indicate that RAP increased with age. For Marshall CT grades, grades I through IV represent progressively worsening brain injuries [15]; thus, RAP would be expected to increase from grade I to IV, as supported by the analysis in Table A7 of Appendix A. In grade V, patients underwent brain surgery whereby mass lesions were removed [15]. This may or may not have resulted in a higher RAP than grade IV, depending on the surgery's outcome, and can explain the reduced RAP value observed in grade V.

4.2. Time Series Structure Analysis

Second, during the time series analysis, it was clear that RAP signal sources were non-stationary and carried substantial trend features inherent within their data streams. We were able to demonstrate this across two different temporal resolutions of RAP data, emphasizing that this was present even at low temporal resolutions. This is critical for the future use of RAP in physiologic modeling, as not accounting for such a trend would lead to model inaccuracies, and most work in the field to date ignores such features.

RAP data streams displayed inherent autoregressive features, consistent with optimal ARIMA models with non-zero autocorrelative and moving average orders (p-orders and q-orders, respectively). Also of interest, the optimal ARIMA model orders for RAP differed from both ICP and AMP, and its constituent signals, highlighting that RAP contains different information compared to ICP or AMP alone. This was the case across the population, highlighting again the need to account not just for the data trend, but also for more complex autoregressive features, in future modeling using temporally resolved RAP data. However, it must be noted that the median optimal model calculated for the dataset may not accurately represent all patients. For instance, RAP at minute-by-minute resolution had a median optimal ARIMA model of (3, 1, 3). However, one patient individually obtained an optimal ARIMA model (8, 1, 3). Hence, applying the ARIMA (3, 1, 3) model to this patient's RAP signal may not effectively capture the data's structure due to the substantial difference in the p-order. Examining this patient's ACF and PACF plots shown in Figure A5 of Appendix E reveals spikes between lags 0 to 5 that fall outside the confidence intervals, highlighting further limitations of using the median optimal ARIMA model. Nevertheless, the spikes out of the confidence intervals had very small magnitudes compared to the

spikes seen in the ACF and PACF plots from the original data. Therefore, the median optimal ARIMA model obtained in this analysis could contribute to the identification of the features that helped distinguish clean data from artifact segments.

4.3. Comparison Among Different Resolutions

Third, during ARIMA model generation, including stationarity tests, some examples failed to return a *p*-value due to insufficient data points, which were most commonly observed at the hour-by-hour temporal resolution. Similarly, most of the non-stationary results were also found at this lowest resolution in both the original and differenced data. Additionally, while calculating the optimal ARIMA model for each signal of each patient, some cases failed to yield results due to insufficient data, mainly at lower resolutions. These observations highlight the critical role of data point quantity in each step of determining the optimal ARIMA model. It also suggests that lower resolutions may be associated with higher residuals, indicating a comparatively less accurate model. The medians of the residuals for each resolution were calculated with the results summarized in Table A33 of Appendix E. All of these findings emphasize the importance of a proper understanding of the statistical structures of such data streams from pressure sensors and their derived metrics (such as RAP). Throughout Table 2, the loss of RAP lags can be observed in the median optimal ARIMA models for lower resolutions (i.e., order numbers are smaller). Additionally, Tables 5 and 6 show the lower importance of artifact management, since the difference between clean and artificial groups was not significantly different at lower resolutions. This suggests that the lower resolutions lose the dynamic aspects of the data (ICP/AMP/RAP).

This trend can also be observed in Table A24 of Appendix D, which details the optimal models for each signal and resolution for each patient. Lower resolutions tend to have simpler optimal models with lower order (p, d, q) values, leading to underfitting. This occurred because the ARIMA analysis, constrained by fewer data points, could not find a suitable model to capture the data fully. In contrast, higher resolutions, with more data points, yielded better results. The presence of spikes with higher magnitudes in the ACF and PACF plots of residuals at lower resolutions from Figure 2 and Appendix F further supports this statement.

4.4. Identifying Artifacts

Finally, building on the results from the time-series modeling of RAP, ICP, and AMP, we aimed to identify potential features capable of distinguishing artifacts from clean data. To qualify as a potential identifier of artifact profiles, a feature must show significant differences between the clean and artifact groups in every case; for instance, in a Mann–Whitney U-test analysis, the *p*-value between the two groups should be less than 0.05. Firstly, according to Table 4, the *p*-values for ICP *q*-order, AMP *p*-order, and RAP *p*-orders and *q*-orders were less than 0.05 (i.e., significant difference) while comparing optimal ARIMA models of clean and artifact data at the minute-by-minute resolution, suggesting that these orders are strong candidates for identifying artifacts. Conversely, ICP *p*-orders and AMP *q*-orders from the optimal models could be excluded as potential features due to insignificant differences between the clean and artifact groups (p-value > 0.05). However, at the 10-min-by-10-min data resolution, only the *q*-order of optimal ARIMA models of ICP (p-value = close to 0) and AMP (p-value = 0.00032) proved to be a potential distinguishing factor, while other orders showed no significant differences.

Secondly, while comparing the residuals of clean and artifact profiles at the patient level, Table 5 shows that the majority of cases exhibited significant differences for each signal at the minute-by-minute resolution. Specifically, significant differences were observed

in 63, 64, and 65 cases out of 108 for ICP, AMP, and RAP, respectively. In contrast, at the 10-min-by-10-min resolution, most cases showed no significant differences for all signals. This indicates that though residuals could be a strong feature for distinguishing artifact profiles at the minute-by-minute resolution, they are less effective at the 10 min resolution. Table 6 further supports this finding, as the medians and means of the variance of residuals across the population were consistently lower for clean data and higher for artifact segments at both resolutions. This consistency suggests that clean data were moderately well-modeled. Therefore, residuals could be considered as a reliable feature for artifact identification.

The third and final analysis focused on comparing the maximum cross-correlation of residuals between clean–clean and clean–artifact combinations for RAP–ICP and RAP–AMP. This analysis was conducted in three parts. It was hypothesized that the maximum cross-correlation between clean RAP and clean ICP/AMP residuals would be higher than that between clean RAP and artifact ICP/AMP residuals, as RAP is derived from ICP and AMP, and their residuals are expected to exhibit strong correlations. Firstly, the medians and means of the maximum cross-correlations were calculated. Among these, only the RAP–AMP cross-correlation consistently showed higher values in clean–clean cases for both median and mean. Thus, the RAP–AMP maximum cross-correlation emerged as a potential feature for both minute-by-minute and 10-min-by-10-min resolutions. Secondly, a Mann–Whitney U test was performed across the entire population to compare the groups. The test revealed significant differences ($p < 0.05$) between clean–clean and clean–artifact residuals for each case except RAP–ICP at the 10-min-by-10-min resolution. Finally, maximum cross-correlations were compared at the patient level, with the expectation that clean–clean maximum cross-correlations would be greater than clean–artifact correlations. This was confirmed for RAP–AMP cross-correlation at both the minute-by-minute and 10-min-by-10-min resolutions, where the majority of patients exhibited higher clean–clean values. In conclusion, combining these three parts, between RAP–ICP and RAP–AMP, the cross-correlation of the latter at both resolutions could serve as a strong feature for identifying artifacts.

Fourthly, a detailed treatment-based sub-group assessment is required. This analysis did not include the effects of different therapeutic interventions, such as decompressive craniectomy, pCO_2 changes or mannitol infusion. Though ICP treatments have an immediate impact on ICP (the minutes after treatment), their long-term impact on ICP modeling and other derived ICP measures (like PRx) is quite limited [45–47]. Therefore, when modeling and assessing RAP physiological factors over larger periods of time and over whole populations, ICP treatment factors can likely be largely ignored. However, when robust minute-by-minute RAP is being modeled (looking at individual moments of patient state), these factors should be considered.

Finally, while the success rate of capturing artifacts showed promising results, some non-artifact data points were mistakenly identified as artifacts (i.e., false positives). The number of false positives at each parameter and each analysis is demonstrated in Tables A37 and A38 of Appendix G. Removing these non-artifact data points could result in the loss of valuable information from the signal. Further work is needed to address this issue, either by refining the thresholds and parameters in the sliding window approach, or by utilizing machine learning (ML) methods and incorporating these identified features into the model.

5. Limitations

The population sample size is relatively small despite representing the largest study to date comprehensively characterizing RAP data features. Such small sample sizes limit the ability to extrapolate such findings to other populations where ICP sensor technology is

applied, and RAP can be measured. For instance, as discussed in the previous section, the median optimal model identified for the clean data may not fully represent all patients. Secondly, the number of data points for each patient constrains the results at lower resolutions. The reduction in data points at lower resolutions, due to calculation methods, led many optimal models at these resolutions to return ARIMA (1, 1, 1), indicating insufficient data points to capture the signal structure and resulting in underfitting. This is supported by the table showing higher residuals at lower resolutions (Table A32 of Appendix E). Additionally, several examples failed to return optimal ARIMA models, residuals, or *p*-values in the Mann–Whitney U-test, further decreasing the data size at lower resolutions. Moreover, it remains unclear why RAP at lower resolutions did not show significant order differences between clean and artifact groups, while RAP at higher resolutions did. This could be due to RAP's derivation method, which results in 80% overlapping data, or due to insufficient data points at lower resolutions. Thirdly, the heterogeneity in TBI characteristics and the diversity of treatments administered could have influenced the physiological response observed in the signals, which might make it difficult to identify consistent patterns and draw generalized conclusions Finally, the data originate from a single-center archive, limiting generalizability, as findings may not apply to other centers with different patient populations, treatment protocols, or equipment.

6. Future Directions

Future work on ICP pressure sensor-based signal sources, including RAP, needs to include larger multi-center high-frequency signal databases. With improved sample sizes, the validation of the above general RAP behavior, its time-series structure and artifact detection methods need to occur. Such future work could include non-linear methods and future sub-group analysis based on injury or disease patterns. Further, artifact detection methods could be enhanced to include not just the time-series methods explored within this manuscript, but also layered approaches, including signal morphological assessments, wavelet decomposition methods, and ML techniques. Finally, for RAP data to be temporally modeled, a proper understanding of its time-domain statistical features is key. Such larger multi-center studies would be optimally positioned to define RAP statistical features more robustly.

7. Conclusions

RAP signals, derived from ICP sensor technology, displayed reproducible and characteristic patterns in this population of moderate/severe TBI patients, with most displaying features of impaired compensatory reserve. The time-series statistical features of RAP demonstrated inherent autoregressive features and data trends, regardless of temporal resolution. Such time-domain statistical features of RAP signals can be used to identify artifactual segments in RAP data streams. Future work is required in larger populations to validate such findings.

Author Contributions: Conceptualization, F.A.Z.; methodology, A.I. and F.A.Z.; data curation, A.S.S., K.Y.S., A.G. and T.B.; writing—original draft, A.I.; writing—review and editing, A.S.S., K.Y.S., N.V., A.G., N.S., T.B., M.H., L.F. and F.A.Z.; supervision, F.A.Z.; funding acquisition, F.A.Z. All authors have read and agreed to the published version of the manuscript.

Funding: This work was directly supported through the University of Manitoba Endowed Manitoba Public Insurance (MPI) Chair in Neuroscience and the Natural Sciences and Engineering Research Council of Canada (NSERC; ALLRP-578524-22, ALLRP 597708-24).

Institutional Review Board Statement: All procedures performed in studies involving human participants were in accordance with the ethical standards of the institutional and/or national research

committee (University of Manitoba Research Ethics Board; H2017:1818, H2017:188, H2020:118) and with the 1964 Helsinki declaration and its later amendments or comparable ethical standards.

Informed Consent Statement: For this type of study, formal consent is not required. No identifying participant information is present in this study.

Data Availability Statement: Data are contained within the article.

Acknowledgments: FAZ is supported through the Endowed Manitoba Public Insurance (MPI) Chair in Neuroscience/TBI Research Endowment, NSERC (DGECR-2022-00260, RGPIN-2022-03621, ALLRP-578524-22, ALLRP-576386-22, I2IPJ 586104-23, ALLRP 586244-23, ALLRP 590680-2023, ALLRP 597442-24, ALLRP 597708-24), Canadian Institutes of Health Research (CIHR), the MPI Neuroscience Research Operating Fund, the Health Sciences Centre Foundation Winnipeg, the Canada Foundation for Innovation (CFI) (Project #: 38583), Research Manitoba (Grant #: 3906, 5429, 5914) and the Pan Am Clinic Foundation of Winnipeg. AI is supported through NSERC (ALLRP-578524-22). ASS is supported through NSERC (RGPIN-2022-03621). NV is supported by the University of Manitoba Graduate Fellowship (UMGF)—Biomedical Engineering, NSERC (ALLRP-576386-22, ALLRP 586244-23, ALLRP 597442-24), AG is supported by the CIHR Fellowship Program. KYS is supported through the NSERC CGS-D program (CGS D-579021-2023), University of Manitoba R.G. and E.M. Graduate Fellowship (Doctoral) in Biomedical Engineering, and the University of Manitoba MD/PhD program. NS is support through the University of Manitoba Graduate Fellowship (UMGF)—Human Anatomy and Cell Science. TB is supported through the NSERC CGS-M program and NSERC (ALLRP-578524-22), University of Manitoba Graduate Enhancement of Tri-Agency Stipends (GETS) program. MH is supported through Research Manitoba (Grant #: 5429). LF is supported through the NSERC Post-Doctoral Fellowship (PDF) program.

Conflicts of Interest: F.A.Z. currently has NSERC Alliance Advantage grant support in partnership with Medtronic's Patient Monitoring Division for work that is in part related to this manuscript. Funding from the partner organization is provided to match NSERC governmental funding only, in keeping with NSERC policies. Medtronic does not direct the research objectives, data collection, analysis, interpretation or publication of the findings in any way. All other authors assert that they have no conflicts of interest to disclose regarding this work, confirming the absence of any financial interests, affiliations, or personal relationships that may have influenced or biased this research.

Abbreviations

ADF, Augmented Dickey–Fuller; AMP, pulse amplitude of ICP; ARIMA, auto-regressive integrated moving average; ICP, intracranial pressure; KPSS, Kwiatkowski–Phillips–Schmidt–Shin; MAP, mean arterial blood pressure; RAP, compensatory reserve index; std, standard deviation.

Appendix A. Summary Measurements, Time Spent Within Thresholds, and Analysis of ICP/AMP/RAP

The following appendix contains the tables for summary measurements and percentage of time spent within certain thresholds, across the whole population. All the significant *p*-values were marked bold.

AMP, pulse amplitude of ICP; CPP, cerebral perfusion pressure; CT, computed tomography; GOSE, Glasgow outcome scale-extended; ICP, intracranial pressure; MAP, mean arterial blood pressure; PRx, pressure reactivity index; RAP, compensatory reserve index; std, standard deviation.

Table A1. Summary measurements.

Metrics	ICP	MAP	CPP	AMP	RAP
mean	10.818	85.374	74.555	2.244	0.632
std	7.564	13.881	14.049	1.855	0.483
min	−15	0.035	−34.26	0	−1
25%	6.138	76.69	66.5005	0.9977	0.49635
50%	10.17	83.94	73.03	1.711	0.8578
75%	14.74	92.65	81.69	2.91	0.9646
max	80.06	200	197.362	22.41	1

Table A2. Time spent within threshold.

Ranges	Time Spent (Unit)	% Time Spent	Total Time (Unit)
[0.4, 1]	267.578	78.091	342.646
(0, 0.4)	30.889	9.014	
[0, −1]	43.166	12.597	

Table A3. Sub-group analysis—age (first comparison).

Condition	ICP	MAP	CPP	AMP	RAP
Below 40 years (n = 46)	10.56481 ± 6.85241	84.44187 ± 7.36121	73.68225 ± 7.94464	1.71982 ± 1.21450	0.60043 ± 0.18153
Above 40 years (n = 63)	8.51253 ± 6.63832	84.07349 ± 7.70570	76.12142 ± 8.49570	2.40335 ± 1.82718	0.53754 ± 0.20982
p-value	**0.047852**	0.710493	0.136793	0.065227	0.119867

Table A4. Sub-group analysis—age (second comparison).

Condition	ICP	MAP	CPP	AMP	RAP
Below 40 years (n = 46)	10.56481 ± 6.85241	84.44187 ± 7.36121	73.68225 ± 7.94464	1.71982 ± 1.21450	0.60043 ± 0.18153
Between 40 and 60 years (n = 39)	8.71919 ± 7.12835	86.03822 ± 8.03764	77.66581 ± 9.36177	2.21371 ± 1.61825	0.59274 ± 0.19015
Above 60 years (n = 24)	8.17672 ± 5.88620	80.88080 ± 6.01193	73.61179 ± 6.25669	2.71151 ± 2.12438	0.44784 ± 0.21301
p-value	0.28399	**0.02818**	0.05323	**0.04624**	**0.00459**

Table A5. Sub-group analysis—M/F Sex.

Condition	ICP	MAP	CPP	AMP	RAP
Male (n = 89)	8.90705 ± 6.30729	84.74958 ± 7.90121	76.15799 ± 8.24657	2.02947 ± 1.54173	0.55111 ± 0.20298
Female (n = 20)	11.47718 ± 8.42448	81.91215 ± 5.12074	70.34861 ± 7.02543	2.49502 ± 1.96119	0.62181 ± 0.17918
p-value	0.333628	0.192417	**0.00805**	0.483515	0.164657

Table A6. Sub-group analysis—pupillary response.

Condition	ICP	MAP	CPP	AMP	RAP
Bilat Reactive (n = 65)	9.68200 ± 6.32553	84.11428 ± 7.34526	74.95088 ± 7.44597	2.25631 ± 1.76652	0.59983 ± 0.19003
Bilat Unreactive (n = 19)	7.21860 ± 6.62510	85.25445 ± 10.43550	77.67136 ± 10.39840	1.84440 ± 1.38851	0.51583 ± 0.19264
Unilateral Unreactive (n = 25)	10.23149 ± 7.88851	83.74773 ± 5.33723	73.49879 ± 8.63051	1.95276 ± 1.41453	0.50780 ± 0.21717
p-value	0.29519	0.79378	0.25327	0.53557	0.07446

Table A7. Sub-group analysis—Marshall CT grade.

Condition	ICP	MAP	CPP	AMP	RAP
Grade II (*n* = 3)	8.41885 ± 1.46502	88.19054 ± 2.95348	79.67350 ± 4.20626	1.10567 ± 0.32360	0.53874 ± 0.23926
Grade III (*n* = 31)	10.10747 ± 5.75164	85.77724 ± 7.99221	75.28605 ± 6.88824	2.34405 ± 1.30344	0.65335 ± 0.16089
Grade IV (*n* = 20)	13.85727 ± 7.61941	86.37602 ± 7.24507	73.34250 ± 8.89201	3.30238 ± 2.28233	0.67305 ± 0.16134
Grade V (*n* = 55)	7.39158 ± 6.41152	82.35945 ± 7.18358	75.36899 ± 9.00899	1.60895 ± 1.28146	0.47552 ± 0.19312
p-value	**0.00227**	0.06480	0.60516	**0.00028**	**0.00001**

Table A8. Sub-group analysis—alive/dead (1-month GOSE).

Condition	ICP	MAP	CPP	AMP	RAP
Alive (*n* = 71)	8.08183 ± 5.20270	84.54202 ± 7.87658	76.48282 ± 8.44677	1.65068 ± 1.01478	0.57072 ± 0.19835
Dead (*n* = 38)	11.98871 ± 8.45046	83.68252 ± 7.01954	72.27488 ± 7.38769	2.96776 ± 2.15609	0.55279 ± 0.20754
p-value	**0.033485**	0.668784	**0.031911**	**0.002865**	0.604539

Table A9. Sub-group analysis—favorable/unfavorable (1-month GOSE).

Condition	ICP	MAP	CPP	AMP	RAP
Favourable (*n* = 52)	7.29237 ± 5.30263	84.20479 ± 7.90128	77.03737 ± 8.74621	1.44024 ± 0.79148	0.54361 ± 0.20245
Unfavorable (*n* = 57)	11.46599 ± 7.36347	84.27194 ± 7.30886	73.11250 ± 7.46122	2.73982 ± 1.94607	0.58373 ± 0.19920
p-value	0.001883	1.0	0.016348	0.000358	0.294478

Table A10. Sub-group analysis—alive/dead (6-month GOSE).

Condition	ICP	MAP	CPP	AMP	RAP
Alive (*n* = 68)	8.42374 ± 5.18191	84.72952 ± 7.98240	76.32846 ± 8.45665	1.66250 ± 1.02750	0.58264 ± 0.19200
Dead (*n* = 41)	11.37039 ± 8.47379	83.53319 ± 7.27248	72.68237 ± 7.72236	2.83479 ± 2.12879	0.53877 ± 0.21121
p-value	0.169741	0.562849	0.065448	**0.010051**	0.258864

Table A11. Sub-group analysis—favorable/unfavorable (6-month GOSE).

Condition	ICP	MAP	CPP	AMP	RAP
Favourable (*n* = 25)	8.12572 ± 5.14666	84.64676 ± 8.09823	76.55841 ± 8.59283	1.67795 ± 1.04272	0.57845 ± 0.19602
Unfavorable (*n* = 64)	11.61034 ± 8.23577	83.83620 ± 6.72062	72.72268 ± 7.47357	2.77978 ± 2.10187	0.54720 ± 0.20960
p-value	**0.048501**	0.738688	**0.041701**	**0.01456**	0.4034

Table A12. ICP thresholds.

Condition	ICP	MAP	CPP	AMP	RAP
ICP > 22	28.34662 ± 7.12649	91.16469 ± 17.08712	62.81109 ± 17.58897	4.99916 ± 3.26314	0.72418 ± 0.43710
ICP < 20	9.34625 ± 5.61682	84.79938 ± 13.48051	75.54584 ± 13.34231	2.06319 ± 1.57050	0.62705 ± 0.48596
***p*-value**	**Close to 0**	**Close to 0**	**Close to 0**	**Close to 0**	**Close to 0**

Table A13. AMP thresholds.

Condition	ICP	MAP	CPP	AMP	RAP
AMP < 1	6.99299 ± 5.69411	84.26304 ± 14.03507	77.38008 ± 13.74575	0.58311 ± 0.26164	0.43376 ± 0.55036
1 < AMP < 3	10.94096 ± 7.58453	85.39152 ± 13.89387	74.56503 ± 14.06739	2.31228 ± 1.93635	0.63582 ± 0.48283
AMP > 3	15.60541 ± 8.33541	86.79509 ± 14.63808	71.22871 ± 14.81692	5.01951 ± 1.90360	0.78769 ± 0.36104
***p*-value**	**Close to 0**	**Close to 0**	**Close to 0**	**Close to 0**	**Close to 0**

Table A14. PRx thresholds (first comparison).

Condition	ICP	MAP	CPP	AMP	RAP	PRx
PRx < 0	10.44394 ± 6.53201	85.41019 ± 12.90041	74.88617 ± 12.82014	2.22166 ± 1.73685	0.68340 ± 0.44809	−0.42581 ± 0.26188
PRx > 0	11.25437 ± 8.56936	85.55157 ± 14.99946	74.20460 ± 15.28773	2.27123 ± 1.98214	0.57066 ± 0.51977	0.42869 ± 0.27811
***p*-value**	**Close to 0**	**Close to 0**	**Close to 0**	**Close to 0**	**Close to 0**	**Close to 0**

Table A15. PRx thresholds (second comparison).

Condition	ICP	MAP	CPP	AMP	RAP	PRx
PRx < 0.25	10.82641 ± 7.57303	85.47692 ± 13.93089	74.56473 ± 14.04217	2.24505 ± 1.85682	0.63016 ± 0.48653	−0.02201 ± 0.50469
PRx > 0.25	11.77002 ± 9.13674	85.55960 ± 15.74818	73.67751 ± 16.11601	2.34873 ± 2.09150	0.55701 ± 0.52997	0.57686 ± 0.21250
***p*-value**	**Close to 0**	**Close to 0**	**Close to 0**	**0.002642**	**Close to 0**	**Close to 0**

Appendix B. Stationarity Test Analysis—ADF/KPSS Tests for Original and Differenced Data

The following are specific *p*-values for stationary tests at the minute-by-minute resolution, confirming that, for the most part, the data were stationary after the first ordered differencing for both ADF and KPSS tests.

ADF, Augmented Dickey–Fuller; AMP, pulse amplitude of ICP; ICP, intracranial pressure; KPSS, Kwiatkowski–Phillips–Schmidt–Shin; RAP, compensatory reserve index.

Table A16. ADF test *p*-values for original data at the minute-by-minute resolution.

Patient	ICP	AMP	RAP
TBI_001	close to 0	close to 0	close to 0
TBI_002	close to 0	close to 0	close to 0
TBI_003	0.01	0.16	close to 0
TBI_004	close to 0	close to 0	close to 0
TBI_007	0.02	0.59	close to 0
TBI_008	0.33	close to 0	close to 0
TBI_009	close to 0	0.08	close to 0
TBI_010	close to 0	0.01	close to 0
TBI_011	close to 0	close to 0	close to 0
TBI_012	close to 0	close to 0	close to 0
TBI_013	0.19	0.14	close to 0
TBI_014	0.98	0.72	close to 0
TBI_015	close to 0	close to 0	close to 0
TBI_016	0.04	0.01	close to 0
TBI_017	0.03	0.09	close to 0
TBI_018	0.55	0.17	close to 0
TBI_019	0.47	0.25	0.03
TBI_020	close to 0	close to 0	close to 0
TBI_021	0.58	0.22	close to 0
TBI_022	0.02	0.02	close to 0
TBI_023	close to 0	close to 0	close to 0
TBI_024	close to 0	close to 0	close to 0
TBI_025	0.26	0.27	close to 0
TBI_026	close to 0	close to 0	close to 0
TBI_027	0.12	0.16	close to 0
TBI_028	close to 0	close to 0	close to 0

Table A16. *Cont.*

Patient	ICP	AMP	RAP
TBI_029	close to 0	close to 0	close to 0
TBI_030	close to 0	close to 0	close to 0
TBI_031	0.1	0.04	close to 0
TBI_032	0.23	0.05	close to 0
TBI_033	close to 0	close to 0	close to 0
TBI_034	0.01	0.01	close to 0
TBI_036	close to 0	close to 0	close to 0
TBI_037	close to 0	close to 0	close to 0
TBI_038	close to 0	close to 0	close to 0
TBI_039	close to 0	close to 0	close to 0
TBI_040	close to 0	0.02	close to 0
TBI_041	close to 0	close to 0	close to 0
TBI_042	close to 0	close to 0	close to 0
TBI_043	close to 0	close to 0	close to 0
TBI_044	0.03	0.1	close to 0
TBI_045	close to 0	close to 0	close to 0
TBI_046	close to 0	close to 0	close to 0
TBI_047	close to 0	0.14	close to 0
TBI_048	0.54	0.63	close to 0
TBI_049	close to 0	close to 0	close to 0
TBI_050	close to 0	close to 0	close to 0
TBI_051	0.33	0.42	close to 0
TBI_052	0.68	0.12	close to 0
TBI_053	0.01	0.01	close to 0
TBI_054	0.05	0.01	close to 0
TBI_055	close to 0	close to 0	close to 0
TBI_056	0	close to 0	close to 0
TBI_057	close to 0	close to 0	close to 0
TBI_058	0	close to 0	close to 0
TBI_059	0.06	0.05	close to 0
TBI_060	close to 0	close to 0	close to 0
TBI_061	close to 0	0.08	close to 0
TBI_062	0.01	0.27	close to 0
TBI_063	close to 0	0.01	close to 0
TBI_064	0	0.42	close to 0
TBI_065	0.03	0.04	close to 0
TBI_066	0	close to 0	close to 0
TBI_067	close to 0	close to 0	close to 0
TBI_068	0	0.12	close to 0
TBI_069	close to 0	close to 0	close to 0
TBI_070	0.42	0.99	close to 0
TBI_071	close to 0	close to 0	close to 0
TBI_072	0.05	0.37	close to 0
TBI_073	close to 0	close to 0	close to 0
TBI_074	close to 0	close to 0	close to 0
TBI_075	close to 0	close to 0	close to 0
TBI_076	close to 0	close to 0	close to 0

Table A16. *Cont.*

Patient	ICP	AMP	RAP
TBI_077	close to 0	close to 0	close to 0
TBI_078	close to 0	0.28	close to 0
TBI_079	0.49	close to 0	close to 0
TBI_080	close to 0	close to 0	close to 0
TBI_081	close to 0	close to 0	close to 0
TBI_082	0.72	0.17	close to 0
TBI_083	0.02	0.06	close to 0
TBI_084	0.05	0.06	close to 0
TBI_085	close to 0	close to 0	close to 0
TBI_086	close to 0	close to 0	close to 0
TBI_087	0.01	0.06	close to 0
TBI_088	close to 0	close to 0	close to 0
TBI_089	close to 0	close to 0	close to 0
TBI_090	0	0.01	close to 0
TBI_091	close to 0	close to 0	close to 0
TBI_092	close to 0	close to 0	close to 0
TBI_093	close to 0	close to 0	close to 0
TBI_094	0.57	close to 0	close to 0
TBI_095	close to 0	close to 0	close to 0
TBI_096	0.29	close to 0	close to 0
TBI_097	0.02	0.04	close to 0
TBI_098	close to 0	0.01	close to 0
TBI_099	close to 0	close to 0	close to 0
TBI_100	close to 0	close to 0	close to 0
TBI_101	0.55	close to 0	close to 0
TBI_102	0.02	0.2	close to 0
TBI_103	close to 0	close to 0	close to 0
TBI_104	close to 0	close to 0	close to 0
TBI_105	0.04	close to 0	close to 0
TBI_106	close to 0	close to 0	close to 0
TBI_107	0.1	close to 0	close to 0
TBI_108	close to 0	close to 0	close to 0
TBI_109	0.01	close to 0	close to 0
TBI_110	close to 0	close to 0	close to 0
TBI_111	close to 0	close to 0	close to 0
TBI_112	0.07	close to 0	close to 0

Table A17. KPSS test *p*-values for original data at minute-by-minute resolution.

Patient	ICP	AMP	RAP
TBI_001	0.01	0.01	0.01
TBI_002	0.01	0.01	0.01
TBI_003	0.01	0.01	0.01
TBI_004	0.08	0.1	0.1
TBI_007	0.01	0.01	0.1
TBI_008	0.01	0.07	0.1
TBI_009	0.01	0.01	0.01

Table A17. *Cont.*

Patient	ICP	AMP	RAP
TBI_010	0.1	0.01	0.01
TBI_011	0.01	0.01	0.01
TBI_012	0.02	0.01	0.1
TBI_013	0.03	0.07	0.1
TBI_014	0.01	0.01	0.01
TBI_015	0.01	0.01	0.1
TBI_016	0.01	0.01	0.01
TBI_017	0.01	0.1	0.1
TBI_018	0.01	0.01	0.01
TBI_019	0.01	0.01	0.01
TBI_020	0.01	0.01	0.01
TBI_021	0.01	0.01	0.01
TBI_022	0.01	0.01	0.01
TBI_023	0.01	0.01	0.01
TBI_024	0.01	0.01	0.02
TBI_025	0.01	0.01	0.1
TBI_026	0.03	0.01	0.01
TBI_027	0.1	0.1	0.01
TBI_028	0.01	0.1	0.01
TBI_029	0.01	0.01	0.01
TBI_030	0.01	0.01	0.1
TBI_031	0.03	0.05	0.01
TBI_032	0.01	0.01	0.08
TBI_033	0.01	0.02	0.03
TBI_034	0.01	0.01	0.01
TBI_036	0.01	0.01	0.01
TBI_037	0.01	0.01	0.01
TBI_038	0.01	0.01	0.01
TBI_039	0.01	0.01	0.01
TBI_040	0.01	0.01	0.02
TBI_041	0.01	0.01	0.1
TBI_042	0.01	0.02	0.01
TBI_043	0.01	0.01	0.09
TBI_044	0.01	0.01	0.1
TBI_045	0.01	0.01	0.01
TBI_046	0.01	0.01	0.1
TBI_047	0.01	0.01	0.1
TBI_048	0.01	0.01	0.01
TBI_049	0.01	0.01	0.1
TBI_050	0.01	0.1	0.1
TBI_051	0.01	0.01	0.1
TBI_052	0.01	0.01	0.01
TBI_053	0.01	0.01	0.01
TBI_054	0.02	0.01	0.1
TBI_055	0.01	0.01	0.01
TBI_056	0.02	0.1	0.1
TBI_057	0.01	0.01	0.01

Table A17. *Cont.*

Patient	ICP	AMP	RAP
TBI_058	0.01	0.01	0.01
TBI_059	0.01	0.01	0.01
TBI_060	0.01	0.01	0.01
TBI_061	0.01	0.01	0.1
TBI_062	0.01	0.01	0.07
TBI_063	0.01	0.01	0.1
TBI_064	0.01	0.01	0.01
TBI_065	0.01	0.01	0.01
TBI_066	0.01	0.01	0.01
TBI_067	0.1	0.09	0.1
TBI_068	0.01	0.01	0.01
TBI_069	0.01	0.01	0.01
TBI_070	0.01	0.01	0.02
TBI_071	0.01	0.01	0.01
TBI_072	0.01	0.01	0.01
TBI_073	0.1	0.01	0.01
TBI_074	0.01	0.01	0.01
TBI_075	0.05	0.01	0.01
TBI_076	0.01	0.01	0.1
TBI_077	0.1	0.1	0.01
TBI_078	0.02	0.01	0.1
TBI_079	0.01	0.01	0.01
TBI_080	0.01	0.01	0.1
TBI_081	0.01	0.02	0.01
TBI_082	0.01	0.01	0.02
TBI_083	0.01	0.01	0.01
TBI_084	0.01	0.01	0.1
TBI_085	0.01	0.01	0.1
TBI_086	0.01	0.01	0.01
TBI_087	0.01	0.01	0.01
TBI_088	0.02	0.01	0.01
TBI_089	0.01	0.01	0.01
TBI_090	0.01	0.02	0.01
TBI_091	0.01	0.01	0.01
TBI_092	0.01	0.01	0.01
TBI_093	0.01	0.01	0.01
TBI_094	0.01	0.01	0.09
TBI_095	0.01	0.01	0.01
TBI_096	0.1	0.1	0.01
TBI_097	0.01	0.01	0.05
TBI_098	0.01	0.01	0.05
TBI_099	0.02	0.01	0.01
TBI_100	0.05	0.01	0.02
TBI_101	0.01	0.01	0.01
TBI_102	0.01	0.01	0.01
TBI_103	0.01	0.01	0.02
TBI_104	0.01	0.01	0.01

Table A17. *Cont.*

Patient	ICP	AMP	RAP
TBI_105	0.01	0.01	0.01
TBI_106	0.01	0.01	0.1
TBI_107	0.01	0.09	0.01
TBI_108	0.01	0.01	0.01
TBI_109	0.09	0.01	0.1
TBI_110	0.01	0.01	0.01
TBI_111	0.01	0.01	0.01
TBI_112	0.01	0.01	0.02

Table A18. ADF test *p*-values for differenced data at minute-by-minute resolution.

Patient	ICP	AMP	RAP
TBI_001	close to 0	close to 0	close to 0
TBI_002	close to 0	close to 0	close to 0
TBI_003	close to 0	close to 0	close to 0
TBI_004	close to 0	close to 0	close to 0
TBI_007	close to 0	close to 0	close to 0
TBI_008	close to 0	close to 0	close to 0
TBI_009	close to 0	close to 0	close to 0
TBI_010	close to 0	close to 0	close to 0
TBI_011	close to 0	close to 0	close to 0
TBI_012	close to 0	close to 0	close to 0
TBI_013	close to 0	close to 0	close to 0
TBI_014	close to 0	close to 0	close to 0
TBI_015	close to 0	close to 0	close to 0
TBI_016	close to 0	close to 0	close to 0
TBI_017	close to 0	close to 0	close to 0
TBI_018	close to 0	close to 0	close to 0
TBI_019	close to 0	close to 0	close to 0
TBI_020	close to 0	close to 0	close to 0
TBI_021	close to 0	close to 0	close to 0
TBI_022	close to 0	close to 0	close to 0
TBI_023	close to 0	close to 0	close to 0
TBI_024	close to 0	close to 0	close to 0
TBI_025	close to 0	close to 0	close to 0
TBI_026	close to 0	close to 0	close to 0
TBI_027	close to 0	close to 0	close to 0
TBI_028	close to 0	close to 0	close to 0
TBI_029	close to 0	close to 0	close to 0
TBI_030	close to 0	close to 0	close to 0
TBI_031	close to 0	close to 0	close to 0
TBI_032	close to 0	close to 0	close to 0
TBI_033	close to 0	close to 0	close to 0
TBI_034	close to 0	close to 0	close to 0
TBI_036	close to 0	close to 0	close to 0
TBI_037	close to 0	close to 0	close to 0
TBI_038	close to 0	close to 0	close to 0

Table A18. *Cont.*

Patient	ICP	AMP	RAP
TBI_039	close to 0	close to 0	close to 0
TBI_040	close to 0	close to 0	close to 0
TBI_041	close to 0	close to 0	close to 0
TBI_042	close to 0	close to 0	close to 0
TBI_043	close to 0	close to 0	close to 0
TBI_044	close to 0	close to 0	close to 0
TBI_045	close to 0	close to 0	close to 0
TBI_046	close to 0	close to 0	close to 0
TBI_047	close to 0	close to 0	close to 0
TBI_048	close to 0	close to 0	close to 0
TBI_049	close to 0	close to 0	close to 0
TBI_050	close to 0	close to 0	close to 0
TBI_051	close to 0	close to 0	close to 0
TBI_052	close to 0	close to 0	close to 0
TBI_053	close to 0	close to 0	close to 0
TBI_054	close to 0	close to 0	close to 0
TBI_055	close to 0	close to 0	close to 0
TBI_056	close to 0	close to 0	close to 0
TBI_057	close to 0	close to 0	close to 0
TBI_058	close to 0	close to 0	close to 0
TBI_059	close to 0	close to 0	close to 0
TBI_060	close to 0	close to 0	close to 0
TBI_061	close to 0	close to 0	close to 0
TBI_062	close to 0	close to 0	close to 0
TBI_063	close to 0	close to 0	close to 0
TBI_064	close to 0	close to 0	close to 0
TBI_065	close to 0	close to 0	close to 0
TBI_066	close to 0	close to 0	close to 0
TBI_067	close to 0	close to 0	close to 0
TBI_068	close to 0	close to 0	close to 0
TBI_069	close to 0	close to 0	close to 0
TBI_070	close to 0	close to 0	close to 0
TBI_071	close to 0	close to 0	close to 0
TBI_072	close to 0	close to 0	close to 0
TBI_073	close to 0	close to 0	close to 0
TBI_074	close to 0	close to 0	close to 0
TBI_075	close to 0	close to 0	close to 0
TBI_076	close to 0	close to 0	close to 0
TBI_077	close to 0	close to 0	close to 0
TBI_078	close to 0	close to 0	close to 0
TBI_079	close to 0	close to 0	close to 0
TBI_080	close to 0	close to 0	close to 0
TBI_081	close to 0	close to 0	close to 0
TBI_082	close to 0	close to 0	close to 0
TBI_083	close to 0	close to 0	close to 0
TBI_084	close to 0	close to 0	close to 0
TBI_085	close to 0	close to 0	close to 0

Table A18. *Cont.*

Patient	ICP	AMP	RAP
TBI_086	close to 0	close to 0	close to 0
TBI_087	close to 0	close to 0	close to 0
TBI_088	close to 0	close to 0	close to 0
TBI_089	close to 0	close to 0	close to 0
TBI_090	close to 0	close to 0	close to 0
TBI_091	close to 0	close to 0	close to 0
TBI_092	close to 0	close to 0	close to 0
TBI_093	close to 0	close to 0	close to 0
TBI_094	close to 0	close to 0	close to 0
TBI_095	close to 0	close to 0	close to 0
TBI_096	0.05	close to 0	close to 0
TBI_097	close to 0	close to 0	close to 0
TBI_098	close to 0	close to 0	close to 0
TBI_099	close to 0	close to 0	close to 0
TBI_100	close to 0	close to 0	close to 0
TBI_101	close to 0	close to 0	close to 0
TBI_102	close to 0	close to 0	close to 0
TBI_103	close to 0	close to 0	close to 0
TBI_104	close to 0	close to 0	close to 0
TBI_105	close to 0	close to 0	close to 0
TBI_106	close to 0	close to 0	close to 0
TBI_107	close to 0	close to 0	close to 0
TBI_108	close to 0	close to 0	close to 0
TBI_109	close to 0	close to 0	close to 0
TBI_110	close to 0	close to 0	close to 0
TBI_111	close to 0	close to 0	close to 0
TBI_112	close to 0	close to 0	close to 0

Table A19. KPSS test *p*-values for differenced data at minute-by-minute resolution.

Patient	ICP	AMP	RAP
TBI_001	0.1	0.1	0.1
TBI_002	0.1	0.1	0.1
TBI_003	0.1	0.1	0.1
TBI_004	0.1	0.1	0.06
TBI_007	0.1	0.1	0.1
TBI_008	0.1	0.1	0.1
TBI_009	0.1	0.1	0.1
TBI_010	0.1	0.1	0.1
TBI_011	0.1	0.1	0.1
TBI_012	0.1	0.1	0.1
TBI_013	0.1	0.1	0.1
TBI_014	0.09	0.1	0.1
TBI_015	0.1	0.1	0.1
TBI_016	0.1	0.1	0.1
TBI_017	0.1	0.1	0.1
TBI_018	0.1	0.1	0.1

Table A19. *Cont.*

Patient	ICP	AMP	RAP
TBI_019	0.1	0.1	0.1
TBI_020	0.1	0.1	0.1
TBI_021	0.1	0.1	0.1
TBI_022	0.1	0.1	0.1
TBI_023	0.1	0.1	0.1
TBI_024	0.1	0.1	0.1
TBI_025	0.1	0.1	0.1
TBI_026	0.1	0.1	0.1
TBI_027	0.1	0.1	0.1
TBI_028	0.1	0.1	0.1
TBI_029	0.1	0.1	0.1
TBI_030	0.1	0.1	0.1
TBI_031	0.1	0.1	0.1
TBI_032	0.1	0.1	0.1
TBI_033	0.1	0.1	0.1
TBI_034	0.1	0.1	0.1
TBI_036	0.1	0.1	0.1
TBI_037	0.1	0.1	0.1
TBI_038	0.1	0.1	0.1
TBI_039	0.1	0.1	0.1
TBI_040	0.1	0.1	0.1
TBI_041	0.1	0.1	0.1
TBI_042	0.1	0.1	0.1
TBI_043	0.1	0.1	0.1
TBI_044	0.1	0.1	0.1
TBI_045	0.1	0.1	0.1
TBI_046	0.1	0.1	0.1
TBI_047	0.1	0.1	0.1
TBI_048	0.1	0.1	0.1
TBI_049	0.1	0.1	0.1
TBI_050	0.1	0.1	0.1
TBI_051	0.1	0.1	0.1
TBI_052	0.1	0.1	0.1
TBI_053	0.1	0.1	0.1
TBI_054	0.1	0.1	0.1
TBI_055	0.1	0.1	0.1
TBI_056	0.1	0.1	0.1
TBI_057	0.1	0.1	0.1
TBI_058	0.1	0.1	0.1
TBI_059	0.1	0.1	0.1
TBI_060	0.1	0.1	0.1
TBI_061	0.1	0.1	0.1
TBI_062	0.1	0.1	0.1
TBI_063	0.1	0.1	0.1
TBI_064	0.1	0.1	0.1
TBI_065	0.1	0.1	0.1

Table A19. *Cont.*

Patient	ICP	AMP	RAP
TBI_066	0.1	0.1	0.05
TBI_067	0.1	0.1	0.1
TBI_068	0.1	0.1	0.1
TBI_069	0.1	0.1	0.1
TBI_070	0.1	0.04	0.1
TBI_071	0.1	0.1	0.1
TBI_072	0.1	0.1	0.1
TBI_073	0.1	0.1	0.1
TBI_074	0.1	0.1	0.1
TBI_075	0.1	0.1	0.1
TBI_076	0.1	0.1	0.1
TBI_077	0.1	0.1	0.1
TBI_078	0.1	0.1	0.1
TBI_079	0.1	0.1	0.1
TBI_080	0.1	0.1	0.1
TBI_081	0.1	0.1	0.1
TBI_082	0.1	0.1	0.1
TBI_083	0.1	0.1	0.1
TBI_084	0.1	0.1	0.1
TBI_085	0.1	0.1	0.1
TBI_086	0.1	0.1	0.1
TBI_087	0.1	0.1	0.1
TBI_088	0.1	0.1	0.1
TBI_089	0.1	0.1	0.1
TBI_090	0.1	0.1	0.1
TBI_091	0.1	0.1	0.1
TBI_092	0.1	0.1	0.1
TBI_093	0.1	0.1	0.1
TBI_094	0.1	0.1	0.1
TBI_095	0.1	0.1	0.1
TBI_096	0.1	0.1	0.1
TBI_097	0.1	0.1	0.1
TBI_098	0.1	0.1	0.1
TBI_099	0.1	0.1	0.1
TBI_100	0.1	0.1	0.1
TBI_101	0.1	0.1	0.1
TBI_102	0.1	0.1	0.1
TBI_103	0.1	0.1	0.1
TBI_104	0.1	0.1	0.1
TBI_105	0.1	0.1	0.1
TBI_106	0.1	0.1	0.1
TBI_107	0.1	0.1	0.1
TBI_108	0.1	0.1	0.1
TBI_109	0.1	0.1	0.1
TBI_110	0.1	0.1	0.1
TBI_111	0.1	0.1	0.1
TBI_112	0.1	0.1	0.1

Appendix C. Summary of Stationarity Analysis Tests—ADF/KPSS Tests for Original and Differenced Data

This appendix highlights that after first-ordered differencing was applied, overall, the data became stationary at each resolution.

ADF, Augmented Dickey–Fuller; AMP, pulse amplitude of ICP; ICP, intracranial pressure; KPSS, Kwiatkowski–Phillips–Schmidt–Shin; RAP, compensatory reserve index.

Table A20. Stationarity check of the original data based on ADF.

Parameter	Minute-by-Minute			10-min-by-10-min			30-min-by-30-min			Hour-by-Hour		
	Stationary	Non-Stationary	N/A	Stationary	Non-Stationary	N/A	Stationary	Non-Stationary	N/A	Stationary	Non-Stationary	N/A
ICP	86	23	0	66	43	0	60	49	0	51	55	3
AMP	80	29	0	58	51	0	52	57	0	48	58	3
RAP	109	0	0	93	16	0	76	33	0	69	37	3

Table A21. Stationarity check of the original data based on KPSS.

Parameter	Minute-by-Minute			10-min-by-10-min			30-min-by-30-min			Hour-by-Hour		
	Stationary	Non-Stationary	N/A	Stationary	Non-Stationary	N/A	Stationary	Non-Stationary	N/A	Stationary	Non-Stationary	N/A
ICP	8	101	0	33	76	0	49	60	0	59	49	1
AMP	13	96	0	34	75	0	48	61	0	54	54	1
RAP	33	76	0	46	63	0	56	53	0	57	52	0

Table A22. Stationarity check of the first difference data based on ADF.

Parameter	Minute-by-Minute			10-min-by-10-min			30-min-by-30-min			Hour-by-Hour		
	Stationary	Non-Stationary	N/A	Stationary	Non-Stationary	N/A	Stationary	Non-Stationary	N/A	Stationary	Non-Stationary	N/A
ICP	108	1	0	106	3	0	104	4	1	91	14	4
AMP	109	0	0	108	1	0	101	7	1	89	16	4
RAP	109	0	0	107	2	0	100	8	1	92	13	4

Table A23. Stationarity check of the first difference data based on KPSS.

Parameter	Minute-by-Minute			10-min-by-10-min			30-min-by-30-min			Hour-by-Hour		
	Stationary	Non-Stationary	N/A	Stationary	Non-Stationary	N/A	Stationary	Non-Stationary	N/A	Stationary	Non-Stationary	N/A
ICP	109	0	0	108	1	0	106	3	0	98	8	3
AMP	108	1	0	105	4	0	105	4	0	99	7	3
RAP	108	1	0	103	6	0	100	9	0	93	13	3

Appendix D. Optimal ARIMA Models for Each Signal and Each Patient

The following shows the most significant ARIMA models (as informed through AIC) at individual patient levels for each resolution and each signal. Each cell has four values corresponding to p, d and q orders and associated AIC values for the model. m refers to minute and h refers to hour.

AIC, Akaike information criterion; AMP, pulse amplitude of ICP; ARIMA, autoregressive integrated moving average; ICP, intracranial pressure; RAP, compensatory reserve index.

Table A24. Optimal ARIMA models.

Patient	ICP m-by-m	ICP 10-m-by-10-m	ICP 30-m-by-30-m	ICP h-by-h	AMP m-by-m	AMP 10-m-by-10-m	AMP 30-m-by-30-m	AMP h-by-h	RAP m-by-m	RAP 10-m-by-10-m	RAP 30-m-by-30-m	RAP h-by-h
TBI_001	[10, 1, 3, '1531.771']	[6, 1, 1, '4255.733']	[4, 1, 3, '1522.509']	[2, 1, 4, '788.013']	[1, 1, 9, '35487.221']	[6, 1, 1, '1332.552']	[3, 1, 1, '498.284']	[6, 1, 7, '265.408']	[2, 1, 5, '14862.477']	[6, 1, 5, '−192.534']	[6, 1, 5, '−243.988']	[1, 1, 1, '−186.431']
TBI_002	[4, 1, 1, '301.383']	[3, 1, 1, '798.246']	[2, 1, 4, '312.842']	[2, 1, 3, '165.722']	[9, 1, 4, '7043.873']	[1, 1, 2, '390.750']	[8, 1, 1, '22.000']	[5, 1, 1, '99.766']	[9, 1, 3, '2469.440']	[2, 1, 1, '−52.852']	[1, 1, 1, '−55.084']	[1, 1, 1, '−29.913']
TBI_003	[6, 1, 1, '1091.937']	[4, 1, 3, '609.108']	[1, 1, 2, '221.819']	[1, 1, 5, '123.989']	[1, 1, 5, '3681.918']	[2, 1, 2, '−613.493']	[2, 1, 1, '−213.387']	[4, 1, 1, '−86.515']	[3, 1, 1, '−5762.879']	[3, 1, 4, '102.301']	[1, 1, 1, '10.314']	[1, 1, 2, '−5.858']
TBI_004	[1, 1, 1, '33.269']	[8, 1, 5, '19.483']	[2, 1, 1, '−15.142']	[1, 1, 1, '−5.331']	[1, 1, 1, '339.517']	[10, 1, 1, '−8.337']	[3, 1, 1, '−24.703']	[1, 1, 1, '−12.050']	[1, 1, 1, '68.348']	[1, 1, 1, '7.550']	[3, 1, 1, '4.856']	[1, 1, 1, '−10.030']
TBI_007	[2, 1, 1, '337.225']	[1, 1, 1, '341.530']	[1, 1, 1, '121.113']	[1, 1, 1, '58.863']	[1, 1, 1, '2403.149']	[1, 1, 1, '−42.308']	[1, 1, 1, '−21.910']	[10, 1, 2, '−29.149']	[1, 1, 1, '66.362']	[1, 1, 1, '29.447']	[1, 1, 2, '1.014']	[9, 1, 5, '2.568']
TBI_008	[7, 1, 2, '1230.670']	[6, 1, 7, '640.823']	[1, 1, 1, '292.706']	[1, 1, 1, '170.699']	[8, 1, 1, '3091.271']	[1, 1, 5, '−234.704']	[1, 1, 3, '−51.200']	[1, 1, 1, '−6.116']	[6, 1, 1, '−3794.499']	[1, 1, 1, '133.499']	[2, 1, 3, '19.027']	[1, 1, 2, '−0.816']
TBI_009	[3, 1, 1, '5942.191']	[3, 1, 1, '2728.697']	[2, 1, 5, '1043.663']	[7, 1, 2, '567.291']	[5, 1, 8, '17479.477']	[2, 1, 5, '−198.338']	[2, 1, 3, '37.041']	[4, 1, 4, '77.012']	[3, 1, 5, '−4518.618']	[2, 1, 3, '405.306']	[6, 1, 8, '−28.212']	[3, 1, 5, '−54.206']
TBI_010	[2, 1, 1, '−609.152']	[2, 1, 8, '829.657']	[2, 1, 4, '339.936']	[1, 1, 1, '174.663']	[4, 1, 10, '4585.005']	[8, 1, 2, '421.414']	[1, 1, 3, '208.454']	[1, 1, 1, '111.955']	[2, 1, 8, '1342.374']	[2, 1, 4, '−123.974']	[1, 1, 1, '−106.847']	[2, 1, 3, '−67.124']
TBI_011	[9, 1, 2, '2021.678']	[4, 1, 1, '3969.556']	[8, 1, 7, '34.000']	[2, 1, 3, '616.790']	[3, 1, 10, '34337.153']	[5, 1, 5, '1322.034']	[10, 1, 10, '472.085']	[2, 1, 3, '262.872']	[2, 1, 7, '10386.355']	[9, 1, 1, '−66.064']	[4, 1, 5, '−104.843']	[3, 1, 5, '−120.804']
TBI_012	[3, 1, 1, '120.069']	[3, 1, 3, '932.354']	[2, 1, 1, '350.342']	[2, 1, 4, '190.127']	[10, 1, 10, '6289.455']	[3, 1, 4, '170.531']	[1, 1, 3, '99.561']	[1, 1, 1, '57.176']	[3, 1, 4, '615.635']	[1, 1, 1, '34.510']	[6, 1, 3, '−57.594']	[2, 1, 3, '−41.261']
TBI_013	[3, 1, 1, '−704.728']	[1, 1, 1, '285.451']	[2, 1, 1, '129.206']	[10, 1, 4, '61.929']	[2, 1, 4, '1008.086']	[1, 1, 1, '116.816']	[5, 1, 2, '59.733']	[10, 1, 6, '11.389']	[2, 1, 4, '−430.580']	[1, 1, 1, '−111.659']	[1, 1, 1, '−49.679']	[1, 1, 1, '−30.654']
TBI_014	[5, 1, 2, '913.826']	[6, 1, 2, '705.939']	[1, 1, 1, '341.638']	[1, 1, 4, '200.105']	[8, 1, 7, '3008.562']	[4, 1, 1, '170.705']	[7, 1, 3, '80.471']	[3, 1, 2, '53.547']	[7, 1, 8, '−803.703']	[1, 1, 1, '149.620']	[1, 1, 4, '25.501']	[1, 1, 1, '−6.100']
TBI_015	[9, 1, 1, '3613.128']	[4, 1, 10, '3273.361']	[10, 1, 8, '1261.074']	[7, 1, 2, '711.312']	[10, 1, 9, '15518.215']	[6, 1, 7, '887.067']	[10, 1, 9, '464.622']	[2, 1, 8, '316.652']	[9, 1, 9, '−2847.042']	[4, 1, 1, '325.832']	[2, 1, 1, '53.187']	[1, 1, 1, '24.501']
TBI_016	[2, 1, 1, '701.730']	[4, 1, 5, '577.298']	[2, 1, 2, '190.466']	[1, 1, 1, '108.708']	[7, 1, 7, '32.000']	[2, 1, 6, '92.695']	[1, 1, 1, '30.722']	[1, 1, 1, '12.994']	[9, 1, 10, '1331.935']	[3, 1, 5, '35.309']	[1, 1, 1, '1.111']	[1, 1, 1, '2.441']
TBI_017	[1, 1, 1, '889.808']	[1, 1, 2, '841.047']	[2, 1, 3, '274.709']	[1, 1, 1, '142.480']	[8, 1, 8, '2882.115']	[5, 1, 6, '−46.309']	[3, 1, 2, '−9.950']	[6, 1, 1, '−11.021']	[9, 1, 10, '−116.108']	[5, 1, 5, '144.457']	[1, 1, 1, '12.939']	[2, 1, 3, '7.099']
TBI_018	[1, 1, 5, '752.011']	[1, 1, 3, '433.669']	[2, 1, 2, '178.075']	[6, 1, 1, '91.705']	[9, 1, 9, '2441.415']	[1, 1, 2, '−13.491']	[1, 1, 1, '8.642']	[1, 1, 1, '7.812']	[3, 1, 4, '−629.140']	[3, 1, 3, '89.550']	[3, 1, 1, '26.384']	[1, 1, 4, '11.223']
TBI_019	[1, 1, 4, '498.112']	[2, 1, 6, '408.893']	[1, 1, 1, '148.683']	[1, 1, 1, '82.831']	[6, 1, 9, '3812.284']	[4, 1, 3, '13.428']	[1, 1, 3, '8.181']	[1, 1, 1, '8.756']	[5, 1, 7, '−287.769']	[8, 1, 7, '18.908']	[2, 1, 2, '−3.921']	[2, 1, 3, '−5.043']
TBI_020	[8, 1, 1, '1784.103']	[8, 1, 3, '4486.602']	[2, 1, 9, '1865.086']	[1, 1, 2, '1012.086']	[8, 1, 3, '28969.156']	[1, 1, 3, '5.157']	[2, 1, 4, '357.707']	[1, 1, 1, '256.960']	[8, 1, 10, '−17023.134']	[3, 1, 1, '−23.169']	[9, 1, 2, '−194.386']	[2, 1, 2, '−182.112']
TBI_021	[6, 1, 1, '1098.804']	[1, 1, 2, '2075.738']	[3, 1, 4, '862.914']	[1, 1, 3, '477.400']	[9, 1, 10, '9002.559']	[1, 1, 3, '−1094.246']	[1, 1, 2, '−174.995']	[1, 1, 1, '−30.954']	[3, 1, 10, '−13874.873']	[1, 1, 2, '−105.751']	[1, 1, 2, '−195.491']	[1, 1, 1, '−112.378']
TBI_022	[10, 1, 2, '4169.616']	[3, 1, 4, '2732.960']	[6, 1, 8, '1014.211']	[4, 1, 3, '570.046']	[5, 1, 8, '17558.366']	[6, 1, 3, '−1294.473']	[1, 1, 2, '−303.740']	[2, 1, 4, '−117.154']	[8, 1, 8, '−14891.883']	[1, 1, 2, '339.065']	[1, 1, 1, '−4.223']	[1, 1, 1, '−54.605']
TBI_023	[2, 1, 1, '1588.588']	[5, 1, 8, '2102.452']	[3, 1, 1, '722.915']	[2, 1, 5, '342.677']	[4, 1, 1, '10881.139']	[2, 1, 2, '286.001']	[3, 1, 8, '109.017']	[7, 1, 10, '51.368']	[3, 1, 5, '−5418.788']	[1, 1, 1, '140.425']	[4, 1, 4, '−45.122']	[4, 1, 3, '−65.264']
TBI_024	[4, 1, 2, '772.025']	[2, 1, 2, '1977.338']	[2, 1, 7, '759.301']	[2, 1, 4, '405.739']	[1, 1, 5, '9235.961']	[3, 1, 7, '213.528']	[4, 1, 8, '193.197']	[2, 1, 4, '94.872']	[6, 1, 8, '−3654.987']	[5, 1, 1, '46.978']	[3, 1, 2, '−101.452']	[1, 1, 1, '−52.779']
TBI_025	[5, 1, 4, '813.208']	[5, 1, 7, '673.930']	[1, 1, 1, '246.431']	[1, 1, 1, '128.190']	[7, 1, 1, '536.739']	[2, 1, 1, '−187.712']	[1, 1, 1, '−67.705']	[1, 1, 1, '−45.265']	[2, 1, 3, '−3299.656']	[1, 1, 1, '182.025']	[4, 1, 5, '−2.759']	[1, 1, 1, '−20.589']
TBI_026	[7, 1, 1, '5398.748']	[3, 1, 1, '3079.708']	[4, 1, 10, '1065.744']	[1, 1, 1, '561.883']	[5, 1, 6, '27609.011']	[4, 1, 7, '884.406']	[3, 1, 9, '277.779']	[3, 1, 3, '109.451']	[1, 1, 2, '12092.375']	[2, 1, 1, '282.125']	[2, 1, 3, '−83.756']	[1, 1, 1, '−79.607']
TBI_027	[5, 1, 1, '122.719']	[6, 1, 6, '3432.804']	[6, 1, 9, '1294.061']	[3, 1, 8, '688.991']	[1, 1, 1, '1913.341']	[8, 1, 9, '1810.299']	[5, 1, 5, '757.074']	[1, 1, 1, '417.487']	[5, 1, 5, '24.000']	[3, 1, 2, '46.304']	[1, 1, 1, '−5.930']	[4, 1, 1, '−57.306']
TBI_028	[10, 1, 1, '3115.825']	[6, 1, 5, '2481.023']	[2, 1, 8, '789.797']	[5, 1, 3, '388.397']	[7, 1, 8, '17153.619']	[1, 1, 1, '558.722']	[3, 1, 1, '152.829']	[2, 1, 1, '70.552']	[1, 1, 6, '872.965']	[1, 1, 1, '228.778']	[2, 1, 1, '−3.613']	[2, 1, 4, '−26.064']
TBI_029	[5, 1, 1, '3549.700']	[9, 1, 9, '3676.162']	[7, 1, 5, '1466.528']	[2, 1, 2, '810.891']	[3, 1, 2, '16689.107']	[4, 1, 6, '1817.830']	[7, 1, 4, '763.579']	[2, 1, 4, '467.189']	[2, 1, 10, '11026.043']	[3, 1, 1, '323.412']	[1, 1, 1, '−38.610']	[3, 1, 1, '−57.485']
TBI_030	[1, 1, 1, '689.969']	[2, 1, 5, '1440.883']	[3, 1, 3, '521.747']	[2, 1, 5, '265.548']	[1, 1, 4, '10910.172']	[2, 1, 1, '424.745']	[6, 1, 1, '178.014']	[6, 1, 1, '95.864']	[2, 1, 3, '1378.543']	[1, 1, 1, '125.002']	[1, 1, 1, '−38.493']	[1, 1, 1, '−42.582']
TBI_031	[2, 1, 1, '110.431']	[1, 1, 1, '116.934']	[8, 1, 9, '38.000']	[1, 1, 1, '0.909']	[1, 1, 1, '633.083']	[9, 1, 1, '65.009']	[4, 1, 1, '24.710']	[1, 1, 1, '−5.600']	[1, 1, 3, '133.559']	[10, 1, 1, '12.878']	[1, 1, 1, '4.687']	[1, 1, 1, '−12.100']
TBI_032	[3, 1, 1, '1373.186']	[4, 1, 6, '1243.360']	[10, 1, 5, '448.944']	[1, 1, 5, '229.956']	[10, 1, 9, '8316.565']	[8, 1, 6, '414.222']	[3, 1, 3, '179.034']	[2, 1, 2, '88.697']	[1, 1, 8, '1870.893']	[1, 1, 1, '90.492']	[2, 1, 3, '11.638']	[1, 1, 1, '−14.844']
TBI_033	[1, 1, 3, '1446.406']	[1, 1, 2, '556.279']	[1, 1, 2, '185.070']	[1, 1, 1, '85.864']	[1, 1, 4, '4367.810']	[1, 1, 1, '−196.827']	[1, 1, 6, '−67.299']	[1, 1, 1, '−27.247']	[2, 1, 4, '−1988.852']	[1, 1, 1, '134.205']	[1, 1, 1, '19.728']	[1, 1, 3, '0.756']

Table A24. *Cont.*

Patient	ICP m-by-m	ICP 10-m-by-10-m	ICP 30-m-by-30-m	ICP h-by-h	AMP m-by-m	AMP 10-m-by-10-m	AMP 30-m-by-30-m	AMP h-by-h	RAP m-by-m	RAP 10-m-by-10-m	RAP 30-m-by-30-m	RAP h-by-h
TBI_034	[3, 1, 1, '1534.139']	[2, 1, 5, '608.336']	[1, 1, 1, '246.840']	[1, 1, 1, '136.863']	[6, 1, 9, '2876.342']	[2, 1, 1, '−560.840']	[9, 1, 1, '−168.536']	[1, 1, 1, '−77.134']	[6, 1, 6, '−6995.116']	[1, 1, 1, '118.680']	[1, 1, 1, '14.645']	[1, 1, 1, '13.331']
TBI_036	[8, 1, 1, '1070.938']	[5, 1, 7, '6284.400']	[1, 1, 1, '2438.594']	[1, 1, 1, '1340.666']	[10, 1, 10, '29070.777']	[10, 1, 8, '2447.168']	[1, 1, 1, '1382.036']	[1, 1, 4, '838.793']	[10, 1, 10, '−5956.178']	[1, 1, 1, '−40.093']	[1, 1, 1, '−233.931']	[1, 1, 1, '−128.070']
TBI_037	[6, 1, 1, '2029.214']	[1, 1, 1, '3174.555']	[6, 1, 9, '1047.098']	[4, 1, 6, '548.494']	[1, 1, 9, '26139.197']	[1, 1, 2, '692.762']	[1, 1, 9, '231.005']	[7, 1, 1, '122.810']	[7, 1, 1, '3980.163']	[6, 1, 7, '186.534']	[2, 1, 3, '−50.336']	[1, 1, 1, '−22.760']
TBI_038	[1, 1, 3, '1137.245']	[3, 1, 10, '3651.071']	[2, 1, 5, '1274.656']	[6, 1, 5, '642.687']	[4, 1, 7, '24104.256']	[2, 1, 8, '1418.069']	[1, 1, 1, '563.827']	[6, 1, 5, '272.605']	[1, 1, 10, '6255.177']	[1, 1, 1, '163.865']	[1, 1, 1, '−51.497']	[1, 1, 1, '−89.936']
TBI_039	[8, 1, 1, '1246.661']	[1, 1, 1, '1373.530']	[3, 1, 3, '441.113']	[1, 1, 5, '210.307']	[1, 1, 9, '9913.909']	[1, 1, 2, '461.798']	[3, 1, 3, '117.948']	[1, 1, 1, '45.445']	[1, 1, 4, '2137.736']	[1, 1, 1, '147.763']	[1, 1, 5, '26.651']	[6, 1, 1, '2.691']
TBI_040	[6, 1, 1, '1058.681']	[1, 1, 3, '2388.786']	[1, 1, 1, '928.918']	[4, 1, 2, '447.237']	[1, 1, 5, '17070.922']	[3, 1, 4, '507.213']	[1, 1, 1, '284.378']	[8, 1, 2, '117.861']	[2, 1, 1, '−475.122']	[1, 1, 2, '98.532']	[1, 1, 1, '−51.851']	[1, 1, 1, '−46.974']
TBI_041	[6, 1, 1, '1725.814']	[1, 1, 1, '2322.222']	[1, 1, 1, '887.819']	[2, 1, 2, '490.180']	[6, 1, 8, '15273.113']	[1, 1, 3, '218.837']	[1, 1, 1, '131.967']	[1, 1, 1, '103.582']	[6, 1, 9, '−4903.485']	[3, 1, 1, '215.685']	[1, 1, 4, '−37.146']	[3, 1, 1, '−31.963']
TBI_042	[3, 1, 3, '2374.186']	[1, 1, 1, '1491.790']	[1, 1, 2, '497.446']	[1, 1, 4, '256.675']	[4, 1, 5, '12487.824']	[4, 1, 1, '275.034']	[3, 1, 3, '64.228']	[1, 1, 1, '40.204']	[5, 1, 5, '3175.527']	[2, 1, 3, '229.795']	[2, 1, 7, '7.164']	[1, 1, 1, '−5.512']
TBI_043	[9, 1, 1, '2253.945']	[1, 1, 1, '583.359']	[1, 1, 1, '232.064']	[1, 1, 1, '124.113']	[3, 1, 3, '4389.474']	[1, 1, 1, '−742.371']	[1, 1, 1, '−232.103']	[1, 1, 3, '−113.272']	[3, 1, 4, '−7498.478']	[1, 1, 2, '159.959']	[1, 1, 1, '22.316']	[1, 1, 1, '4.356']
TBI_044	[5, 1, 1, '863.795']	[3, 1, 4, '712.394']	[2, 1, 1, '274.918']	[1, 1, 1, '159.557']	[7, 1, 1, '5306.273']	[2, 1, 1, '165.178']	[2, 1, 1, '116.624']	[1, 1, 1, '72.517']	[5, 1, 2, '−377.611']	[6, 1, 1, '70.514']	[2, 1, 1, '−4.925']	[1, 1, 1, '−1.222']
TBI_045	[3, 1, 1, '1084.027']	[4, 1, 3, '1595.632']	[7, 1, 9, '603.971']	[3, 1, 2, '303.459']	[9, 1, 1, '11149.290']	[2, 1, 1, '125.979']	[3, 1, 7, '126.147']	[1, 1, 1, '65.471']	[10, 1, 3, '−2520.470']	[2, 1, 5, '13.006']	[3, 1, 1, '−52.951']	[1, 1, 1, '−34.911']
TBI_046	[2, 1, 1, '−376.596']	[2, 1, 8, '745.024']	[1, 1, 2, '291.109']	[1, 1, 1, '153.518']	[6, 1, 8, '3834.026']	[2, 1, 10, '340.444']	[1, 1, 4, '161.518']	[1, 1, 2, '85.585']	[4, 1, 1, '−513.709']	[2, 1, 2, '−91.210']	[1, 1, 1, '−80.802']	[4, 1, 1, '−42.388']
TBI_047	[1, 1, 1, '2007.200']	[3, 1, 1, '1124.876']	[1, 1, 1, '414.130']	[1, 1, 3, '209.099']	[3, 1, 7, '8677.843']	[7, 1, 10, '1.010']	[1, 1, 7, '42.471']	[1, 1, 3, '30.669']	[4, 1, 7, '−144.422']	[1, 1, 1, '179.101']	[1, 1, 1, '25.246']	[1, 1, 1, '8.012']
TBI_048	[3, 1, 7, '422.350']	[1, 1, 1, '233.857']	[2, 1, 3, '75.631']	[1, 1, 1, '35.737']	[1, 1, 1, '1613.809']	[1, 1, 2, '−20.787']	[3, 1, 1, '7.269']	[7, 1, 1, '−1.320']	[4, 1, 4, '−316.729']	[3, 1, 2, '43.998']	[8, 1, 2, '5.953']	[5, 1, 6, '−11.224']
TBI_049	[8, 1, 2, '5376.289']	[1, 1, 3, '1656.563']	[5, 1, 1, '590.479']	[4, 1, 2, '326.338']	[9, 1, 1, '12735.921']	[2, 1, 1, '−669.049']	[1, 1, 9, '−206.879']	[1, 1, 8, '−69.388']	[2, 1, 8, '−7883.849']	[1, 1, 2, '436.151']	[3, 1, 3, '55.406']	[1, 1, 1, '22.745']
TBI_050	[5, 1, 1, '944.591']	[2, 1, 4, '543.931']	[5, 1, 2, '177.022']	[10, 1, 1, '74.081']	[1, 1, 6, '4487.034']	[6, 1, 9, '7.473']	[1, 1, 1, '−7.671']	[1, 1, 1, '2.830']	[4, 1, 1, '−258.752']	[2, 1, 4, '75.450']	[2, 1, 1, '−19.339']	[1, 1, 1, '−12.623']
TBI_051	[10, 1, 1, '1667.820']	[2, 1, 2, '779.306']	[1, 1, 1, '325.370']	[2, 1, 1, '186.721']	[1, 1, 1, '4609.700']	[2, 1, 1, '−239.027']	[1, 1, 1, '−43.043']	[1, 1, 1, '−4.290']	[1, 1, 1, '−3481.606']	[1, 1, 2, '129.049']	[1, 1, 1, '40.426']	[1, 1, 2, '15.658']
TBI_052	[5, 1, 1, '1006.793']	[1, 1, 1, '420.971']	[3, 1, 1, '163.236']	[2, 1, 4, '90.520']	[4, 1, 1, '3439.819']	[2, 1, 10, '−111.112']	[2, 1, 6, '−6.848']	[1, 1, 2, '−0.973']	[1, 1, 2, '−412.020']	[1, 1, 1, '120.369']	[1, 1, 1, '33.371']	[1, 1, 1, '16.747']
TBI_053	[10, 1, 1, '1936.359']	[4, 1, 8, '1055.686']	[2, 1, 4, '413.145']	[2, 1, 3, '213.149']	[1, 1, 5, '6752.862']	[8, 1, 10, '−414.364']	[3, 1, 1, '−69.436']	[1, 1, 1, '−35.399']	[9, 1, 5, '−8195.877']	[3, 1, 7, '171.868']	[6, 1, 1, '35.312']	[3, 1, 3, '9.527']
TBI_054	[1, 1, 2, '97.217']	[4, 1, 3, '248.705']	[2, 1, 2, '98.762']	[8, 1, 1, '47.618']	[3, 1, 4, '2007.982']	[2, 1, 2, '−69.739']	[1, 1, 1, '2.627']	[1, 1, 2, '9.658']	[3, 1, 1, '−1096.791']	[2, 1, 3, '−34.805']	[9, 1, 2, '−27.100']	[8, 1, 1, '−17.537']
TBI_055	[3, 1, 6, '3047.808']	[1, 1, 1, '1387.897']	[2, 1, 8, '532.821']	[5, 1, 2, '289.671']	[5, 1, 10, '11484.450']	[1, 1, 4, '−662.759']	[1, 1, 2, '−150.499']	[4, 1, 1, '−56.964']	[1, 1, 10, '−8744.441']	[2, 1, 1, '240.594']	[1, 1, 1, '28.482']	[4, 1, 1, '14.028']
TBI_056	[3, 1, 10, '149.263']	[8, 1, 1, '26.408']	[2, 1, 2, '7.467']	[None, 1, None, 'inf']	[1, 1, 2, '160.266']	[6, 1, 1, '−13.890']	[3, 1, 1, '−7.409']	[None, 1, None, 'inf']	[2, 1, 1, '−138.260']	[9, 1, 1, '17.316']	[2, 1, 1, '−5.010']	[None, 1, None, 'inf']
TBI_057	[1, 1, 4, '226.678']	[9, 1, 9, '7011.416']	[5, 1, 2, '2492.357']	[1, 1, 5, '1296.788']	[1, 1, 10, '47415.546']	[7, 1, 1, '2779.937']	[1, 1, 10, '1061.677']	[2, 1, 6, '588.615']	[3, 1, 10, '14844.050']	[5, 1, 1, '443.905']	[1, 1, 1, '−340.513']	[3, 1, 10, '−260.502']
TBI_058	[5, 1, 2, '2732.924']	[1, 1, 1, '1432.209']	[5, 1, 5, '570.988']	[2, 1, 4, '308.583']	[3, 1, 3, '10142.468']	[2, 1, 2, '−44.341']	[3, 1, 3, '100.081']	[1, 1, 2, '70.793']	[7, 1, 7, '−2675.763']	[1, 1, 1, '146.171']	[1, 1, 1, '−31.155']	[2, 1, 3, '−28.780']
TBI_059	[1, 1, 2, '901.127']	[2, 1, 2, '383.868']	[9, 1, 2, '173.476']	[8, 1, 1, '101.238']	[3, 1, 2, '2550.066']	[1, 1, 1, '−221.804']	[1, 1, 3, '−80.575']	[1, 1, 2, '−32.740']	[1, 1, 1, '−741.986']	[1, 1, 1, '73.161']	[2, 1, 3, '0.247']	[1, 1, 1, '−6.916']
TBI_060	[5, 1, 1, '1531.158']	[1, 1, 2, '1363.277']	[1, 1, 1, '485.037']	[1, 1, 1, '218.728']	[1, 1, 7, '9299.601']	[1, 1, 5, '471.852']	[1, 1, 1, '188.544']	[1, 1, 1, '84.654']	[6, 1, 1, '1608.989']	[2, 1, 4, '35.108']	[2, 1, 3, '−40.964']	[1, 1, 1, '−37.416']
TBI_061	[1, 1, 4, '924.972']	[3, 1, 2, '258.540']	[1, 1, 1, '90.891']	[2, 1, 3, '50.873']	[2, 1, 1, '2468.625']	[1, 1, 7, '−451.396']	[1, 1, 3, '−131.510']	[1, 1, 1, '−58.715']	[2, 1, 1, '−3542.816']	[2, 1, 1, '84.490']	[1, 1, 1, '22.054']	[6, 1, 1, '16.638']
TBI_062	[3, 1, 4, '840.774']	[1, 1, 1, '401.476']	[1, 1, 1, '144.057']	[10, 1, 5, '59.231']	[3, 1, 6, '2105.820']	[3, 1, 7, '19.553']	[1, 1, 5, '2.998']	[3, 1, 1, '5.310']	[9, 1, 7, '−1379.051']	[3, 1, 3, '88.883']	[1, 1, 3, '16.904']	[6, 1, 1, '13.276']
TBI_063	[6, 1, 1, '1464.237']	[1, 1, 1, '1489.315']	[3, 1, 4, '475.502']	[2, 1, 3, '249.235']	[6, 1, 1, '8515.205']	[1, 1, 2, '35.883']	[8, 1, 1, '21.126']	[1, 1, 2, '20.784']	[5, 1, 1, '−1578.509']	[2, 1, 2, '40.785']	[5, 1, 6, '−59.043']	[4, 1, 10, '−64.118']
TBI_064	[9, 1, 1, '813.256']	[1, 1, 1, '274.303']	[1, 1, 1, '101.098']	[9, 1, 4, '45.068']	[5, 1, 1, '2593.017']	[2, 1, 2, '−79.875']	[2, 1, 2, '−15.617']	[6, 1, 2, '−1.653']	[1, 1, 1, '−724.017']	[1, 1, 1, '76.839']	[1, 1, 1, '30.018']	[1, 1, 1, '13.842']
TBI_065	[6, 1, 1, '439.493']	[1, 1, 2, '465.404']	[2, 1, 2, '170.347']	[1, 1, 2, '83.113']	[6, 1, 3, '3353.609']	[1, 1, 1, '120.083']	[1, 1, 2, '57.380']	[9, 1, 1, '24.896']	[10, 1, 7, '−13.545']	[1, 1, 1, '10.605']	[5, 1, 4, '−22.987']	[2, 1, 2, '−22.768']

Table A24. *Cont.*

Patient	ICP m-by-m	ICP 10-m-by-10-m	ICP 30-m-by-30-m	ICP h-by-h	AMP m-by-m	AMP 10-m-by-10-m	AMP 30-m-by-30-m	AMP h-by-h	RAP m-by-m	RAP 10-m-by-10-m	RAP 30-m-by-30-m	RAP h-by-h
TBI_066	[8, 1, 1, '2979.779']	[4, 1, 3, '1368.894']	[3, 1, 3, '531.940']	[10, 1, 2, '28.000']	[5, 1, 2, '9401.210']	[2, 1, 1, '−896.379']	[2, 1, 3, '−243.850']	[3, 1, 2, '−102.689']	[7, 1, 2, '−11537.109']	[1, 1, 1, '150.551']	[1, 1, 1, '−66.236']	[1, 1, 1, '−63.698']
TBI_067	[4, 1, 4, '384.851']	[7, 1, 1, '385.927']	[3, 1, 2, '133.193']	[2, 1, 2, '78.913']	[8, 1, 10, '3470.167']	[2, 1, 10, '158.461']	[1, 1, 3, '82.468']	[6, 1, 1, '51.740']	[2, 1, 5, '340.122']	[1, 1, 1, '33.999']	[2, 1, 1, '0.999']	[1, 1, 2, '−4.503']
TBI_068	[4, 1, 6, '3658.594']	[1, 1, 1, '1229.778']	[1, 1, 2, '436.566']	[2, 1, 1, '263.000']	[3, 1, 1, '11219.746']	[1, 1, 3, '−217.419']	[4, 1, 4, '−0.259']	[3, 1, 2, '13.244']	[5, 1, 1, '−6317.538']	[3, 1, 3, '296.879']	[1, 1, 1, '−1.660']	[2, 1, 1, '−32.790']
TBI_069	[9, 1, 1, '1746.409']	[3, 1, 4, '4544.290']	[9, 1, 8, '38.000']	[1, 1, 1, '753.053']	[1, 1, 3, '36583.517']	[1, 1, 2, '1296.419']	[4, 1, 7, '514.515']	[7, 1, 7, '305.057']	[5, 1, 1, '4522.254']	[10, 1, 1, '15.428']	[2, 1, 9, '−139.607']	[1, 1, 4, '−129.456']
TBI_070	[5, 1, 1, '371.028']	[1, 1, 4, '126.313']	[9, 1, 4, '55.252']	[5, 1, 2, '25.958']	[5, 1, 5, '866.349']	[1, 1, 1, '−26.652']	[1, 1, 1, '−4.945']	[5, 1, 1, '4.785']	[1, 1, 3, '−282.991']	[2, 1, 1, '49.412']	[1, 1, 1, '19.752']	[7, 1, 2, '12.056']
TBI_071	[9, 1, 2, '38.752']	[7, 1, 4, '6316.318']	[3, 1, 4, '2280.672']	[1, 1, 1, '1201.920']	[1, 1, 8, '44941.599']	[2, 1, 2, '2622.449']	[2, 1, 5, '1233.442']	[3, 1, 3, '717.558']	[8, 1, 3, '2079.592']	[1, 1, 1, '−38.552']	[1, 1, 10, '−347.219']	[1, 1, 1, '−249.390']
TBI_072	[2, 1, 1, '701.818']	[7, 1, 9, '36.000']	[1, 1, 1, '233.732']	[1, 1, 1, '119.949']	[1, 1, 2, '3653.861']	[6, 1, 9, '288.003']	[2, 1, 3, '128.512']	[1, 1, 1, '75.537']	[8, 1, 10, '1476.957']	[3, 1, 1, '75.470']	[2, 1, 1, '−7.223']	[3, 1, 1, '−2.434']
TBI_073	[8, 1, 3, '6044.737']	[2, 1, 3, '5265.377']	[8, 1, 9, '1972.521']	[1, 1, 1, '1102.534']	[1, 1, 9, '31152.953']	[3, 1, 5, '−1026.621']	[7, 1, 1, '163.573']	[5, 1, 1, '226.264']	[1, 1, 1, '−19788.132']	[1, 1, 1, '602.585']	[4, 1, 3, '−41.957']	[5, 1, 3, '−96.271']
TBI_074	[5, 1, 3, '2033.327']	[1, 1, 2, '2353.766']	[1, 1, 1, '658.238']	[1, 1, 1, '365.060']	[3, 1, 2, '9292.142']	[6, 1, 10, '−38.469']	[2, 1, 2, '−1.884']	[1, 1, 1, '7.819']	[9, 1, 1, '1484.169']	[1, 1, 1, '72.476']	[4, 1, 7, '−44.283']	[1, 1, 3, '−41.262']
TBI_075	[10, 1, 9, '1006.698']	[8, 1, 10, '40.000']	[1, 1, 1, '447.754']	[1, 1, 1, '254.442']	[2, 1, 8, '7379.604']	[3, 1, 6, '244.269']	[2, 1, 1, '110.424']	[1, 1, 1, '63.610']	[1, 1, 2, '1187.449']	[3, 1, 3, '93.193']	[1, 1, 1, '19.821']	[2, 1, 4, '16.645']
TBI_076	[6, 1, 1, '2015.329']	[1, 1, 2, '3795.065']	[5, 1, 5, '1281.480']	[3, 1, 6, '657.078']	[2, 1, 9, '32735.636']	[6, 1, 5, '668.983']	[6, 1, 3, '223.408']	[1, 1, 3, '113.712']	[4, 1, 1, '7345.278']	[3, 1, 1, '37.733']	[2, 1, 1, '−171.251']	[1, 1, 1, '−154.354']
TBI_077	[2, 1, 1, '2091.058']	[1, 1, 1, '2098.357']	[4, 1, 6, '694.607']	[2, 1, 1, '347.893']	[1, 1, 8, '16326.011']	[3, 1, 3, '643.225']	[1, 1, 2, '193.850']	[2, 1, 4, '88.605']	[9, 1, 1, '3221.436']	[3, 1, 1, '119.313']	[4, 1, 2, '−75.504']	[1, 1, 10, '−38.655']
TBI_078	[3, 1, 1, '1499.557']	[1, 1, 1, '561.375']	[2, 1, 4, '208.265']	[1, 1, 2, '113.232']	[4, 1, 1, '3817.208']	[3, 1, 9, '−312.053']	[2, 1, 6, '−56.841']	[2, 1, 2, '−9.575']	[2, 1, 1, '−4448.552']	[1, 1, 1, '131.781']	[1, 1, 3, '−3.660']	[2, 1, 2, '−12.584']
TBI_079	[9, 1, 3, '499.800']	[1, 1, 1, '989.121']	[2, 1, 3, '313.918']	[2, 1, 2, '149.683']	[4, 1, 5, '8679.081']	[1, 1, 1, '140.132']	[1, 1, 1, '78.511']	[2, 1, 1, '56.192']	[2, 1, 1, '−36.576']	[4, 1, 1, '37.465']	[3, 1, 4, '−45.035']	[2, 1, 2, '−54.737']
TBI_080	[8, 1, 1, '8519.552']	[3, 1, 1, '2914.104']	[8, 1, 2, '1121.896']	[3, 1, 4, '621.151']	[1, 1, 9, '23574.334']	[1, 1, 1, '−1450.861']	[1, 1, 1, '−513.780']	[1, 1, 1, '−215.740']	[8, 1, 2, '−9852.278']	[1, 1, 2, '532.785']	[1, 1, 1, '−6.488']	[3, 1, 1, '−65.627']
TBI_081	[6, 1, 2, '−192.512']	[8, 1, 8, '5232.541']	[5, 1, 6, '1827.975']	[3, 1, 1, '900.265']	[8, 1, 9, '41173.806']	[3, 1, 4, '1931.642']	[3, 1, 3, '771.634']	[1, 1, 1, '385.392']	[7, 1, 8, '3577.089']	[1, 1, 1, '49.576']	[1, 1, 1, '−249.189']	[2, 1, 3, '−201.320']
TBI_082	[6, 1, 7, '30.000']	[2, 1, 2, '324.380']	[1, 1, 1, '121.923']	[9, 1, 1, '72.337']	[2, 1, 1, '2085.297']	[1, 1, 3, '−106.536']	[1, 1, 1, '−21.566']	[10, 1, 5, '−15.568']	[1, 1, 1, '−902.423']	[1, 1, 1, '76.542']	[1, 1, 3, '−0.877']	[2, 1, 1, '−2.428']
TBI_083	[8, 1, 3, '1950.808']	[4, 1, 4, '615.931']	[6, 1, 3, '22.000']	[1, 1, 1, '94.761']	[1, 1, 3, '4618.665']	[1, 1, 1, '−480.234']	[1, 1, 1, '−177.361']	[1, 1, 1, '−83.381']	[3, 1, 1, '−3100.572']	[1, 1, 6, '182.994']	[2, 1, 1, '45.060']	[1, 1, 1, '5.575']
TBI_084	[9, 1, 3, '2452.702']	[1, 1, 1, '254.656']	[3, 1, 3, '160.261']	[7, 1, 4, '26.000']	[1, 1, 3, '992.612']	[1, 1, 1, '−724.082']	[7, 1, 1, '−277.703']	[2, 1, 1, '−150.735']	[2, 1, 1, '−5710.491']	[1, 1, 1, '227.432']	[1, 1, 1, '38.168']	[1, 1, 7, '−13.910']
TBI_085	[2, 1, 1, '1617.882']	[9, 1, 8, '3805.534']	[8, 1, 3, '1284.198']	[2, 1, 1, '639.988']	[1, 1, 6, '32483.590']	[8, 1, 7, '282.638']	[1, 1, 5, '273.116']	[1, 1, 3, '156.721']	[8, 1, 9, '−1157.248']	[1, 1, 1, '−56.330']	[1, 1, 2, '−220.808']	[1, 1, 1, '−154.243']
TBI_086	[8, 1, 1, '3759.659']	[4, 1, 9, '4333.346']	[3, 1, 4, '1525.961']	[3, 1, 2, '733.449']	[7, 1, 3, '30851.610']	[4, 1, 1, '43.771']	[2, 1, 3, '84.952']	[4, 1, 2, '−2.803']	[10, 1, 1, '−7510.855']	[1, 1, 2, '148.433']	[3, 1, 1, '−142.687']	[3, 1, 2, '−154.657']
TBI_087	[8, 1, 1, '3330.323']	[1, 1, 2, '2362.099']	[2, 1, 1, '1097.819']	[1, 1, 2, '649.338']	[3, 1, 7, '15117.197']	[4, 1, 2, '−1591.208']	[2, 1, 1, '−348.556']	[1, 1, 6, '−92.731']	[3, 1, 3, '−16709.147']	[1, 1, 1, '99.391']	[1, 1, 1, '−141.305']	[1, 1, 3, '−131.817']
TBI_088	[8, 1, 2, '−3676.644']	[3, 1, 4, '5733.186']	[3, 1, 3, '1977.226']	[2, 1, 1, '964.577']	[1, 1, 8, '47020.336']	[7, 1, 1, '1185.601']	[3, 1, 5, '477.970']	[1, 1, 1, '233.392']	[10, 1, 2, '1892.864']	[1, 1, 1, '−719.332']	[5, 1, 1, '−385.957']	[2, 1, 1, '−386.385']
TBI_089	[3, 1, 1, '5410.816']	[1, 1, 2, '2767.672']	[3, 1, 3, '830.000']	[4, 1, 4, '499.134']	[1, 1, 2, '26948.639']	[1, 1, 1, '−898.413']	[3, 1, 3, '−143.604']	[1, 1, 2, '−26.113']	[6, 1, 1, '−7917.505']	[1, 1, 1, '361.620']	[1, 1, 2, '−24.255']	[2, 1, 10, '−63.433']
TBI_090	[1, 1, 2, '1496.104']	[2, 1, 7, '2391.440']	[5, 1, 2, '876.949']	[1, 1, 1, '473.946']	[4, 1, 8, '20812.777']	[7, 1, 3, '605.383']	[3, 1, 2, '270.077']	[2, 1, 2, '171.229']	[7, 1, 3, '1453.419']	[1, 1, 1, '212.776']	[2, 1, 3, '−36.092']	[3, 1, 8, '−52.744']
TBI_091	[8, 1, 2, '−4326.074']	[7, 1, 2, '6128.983']	[1, 1, 6, '2341.587']	[6, 1, 2, '1206.340']	[8, 1, 5, '45969.072']	[5, 1, 7, '2342.235']	[7, 1, 2, '1126.075']	[1, 1, 1, '621.492']	[4, 1, 8, '9385.585']	[6, 1, 8, '−668.544']	[3, 1, 3, '−487.607']	[2, 1, 2, '−315.631']
TBI_092	[10, 1, 1, '2866.928']	[1, 1, 5, '3760.560']	[5, 1, 4, '1400.699']	[3, 1, 3, '733.603']	[7, 1, 4, '32217.740']	[3, 1, 4, '1543.450']	[1, 1, 3, '685.049']	[2, 1, 4, '393.198']	[3, 1, 5, '5891.441']	[7, 1, 2, '261.090']	[3, 1, 2, '17.611']	[1, 1, 1, '−56.554']
TBI_093	[10, 1, 1, '3214.846']	[1, 1, 2, '5118.541']	[1, 1, 1, '1505.439']	[1, 1, 1, '757.552']	[2, 1, 6, '46132.657']	[3, 1, 1, '1003.610']	[5, 1, 5, '24.000']	[1, 1, 4, '180.726']	[3, 1, 10, '10307.165']	[1, 1, 2, '279.230']	[2, 1, 2, '−66.665']	[3, 1, 3, '−68.089']
TBI_094	[5, 1, 1, '1137.523']	[6, 1, 6, '394.269']	[4, 1, 2, '123.858']	[2, 1, 1, '65.781']	[7, 1, 3, '3598.210']	[1, 1, 1, '54.721']	[3, 1, 2, '−7.700']	[1, 1, 1, '−1.032']	[1, 1, 3, '1028.863']	[1, 1, 1, '127.756']	[2, 1, 3, '7.444']	[1, 1, 1, '−6.719']
TBI_095	[1, 1, 2, '772.852']	[1, 1, 1, '2364.346']	[3, 1, 1, '910.020']	[1, 1, 2, '520.535']	[10, 1, 4, '20958.908']	[1, 1, 3, '126.146']	[9, 1, 6, '34.000']	[2, 1, 10, '91.484']	[10, 1, 2, '−1725.344']	[4, 1, 9, '9.800']	[1, 1, 1, '−138.419']	[1, 1, 1, '−117.862']
TBI_096	[1, 1, 8, '176.761']	[1, 1, 1, '96.413']	[5, 1, 1, '16.524']	[2, 1, 2, '6.240']	[4, 1, 4, '714.264']	[1, 1, 2, '34.204']	[5, 1, 1, '−11.838']	[5, 1, 1, '−5.110']	[1, 1, 1, '119.360']	[1, 1, 4, '4.547']	[6, 1, 2, '−21.070']	[2, 1, 1, '−4.530']

Table A24. *Cont.*

Patient	ICP m-by-m	ICP 10-m-by-10-m	ICP 30-m-by-30-m	ICP h-by-h	AMP m-by-m	AMP 10-m-by-10-m	AMP 30-m-by-30-m	AMP h-by-h	RAP m-by-m	RAP 10-m-by-10-m	RAP 30-m-by-30-m	RAP h-by-h
TBI_097	[1, 1, 3, '1772.148']	[2, 1, 7, '539.291']	[2, 1, 3, '254.764']	[5, 1, 7, '155.859']	[1, 1, 7, '2955.267']	[3, 1, 3, '−861.808']	[1, 1, 1, '−208.121']	[1, 1, 1, '−77.235']	[1, 1, 1, '−8073.485']	[2, 1, 1, '164.963']	[1, 1, 1, '−8.749']	[1, 1, 4, '−11.313']
TBI_098	[8, 1, 2, '3516.109']	[1, 1, 2, '1453.918']	[2, 1, 2, '495.557']	[3, 1, 3, '271.226']	[2, 1, 9, '7701.261']	[9, 1, 6, '−722.735']	[2, 1, 6, '−292.401']	[1, 1, 6, '−156.646']	[6, 1, 4, '−7365.467']	[3, 1, 1, '291.945']	[2, 1, 2, '7.306']	[5, 1, 5, '−6.385']
TBI_099	[10, 1, 1, '4428.079']	[4, 1, 6, '1044.266']	[2, 1, 4, '381.526']	[1, 1, 1, '201.112']	[2, 1, 3, '7677.228']	[5, 1, 5, '−1355.549']	[7, 1, 5, '−465.568']	[2, 1, 2, '−207.105']	[9, 1, 3, '−13088.411']	[4, 1, 4, '28.276']	[2, 1, 1, '−31.254']	[1, 1, 1, '−30.302']
TBI_100	[5, 1, 1, '−888.900']	[5, 1, 1, '5978.417']	[2, 1, 10, '2357.758']	[6, 1, 9, '1231.232']	[3, 1, 10, '35412.892']	[2, 1, 9, '2860.168']	[4, 1, 10, '1285.253']	[6, 1, 9, '671.428']	[3, 1, 9, '4643.162']	[4, 1, 6, '−204.319']	[3, 1, 1, '−229.001']	[1, 1, 2, '−229.658']
TBI_101	[3, 1, 1, '887.794']	[8, 1, 6, '32.000']	[2, 1, 2, '257.635']	[1, 1, 1, '146.425']	[1, 1, 2, '3901.882']	[1, 1, 3, '135.282']	[1, 1, 6, '60.055']	[1, 1, 3, '51.528']	[7, 1, 10, '731.290']	[1, 1, 2, '55.751']	[1, 1, 1, '3.045']	[1, 1, 1, '−9.219']
TBI_102	[4, 1, 2, '2788.047']	[1, 1, 1, '1168.088']	[1, 1, 1, '390.724']	[1, 1, 2, '219.561']	[1, 1, 6, '10221.411']	[6, 1, 2, '409.388']	[1, 1, 1, '211.116']	[2, 1, 1, '124.576']	[3, 1, 5, '4170.125']	[7, 1, 1, '166.367']	[1, 1, 3, '1.027']	[1, 1, 1, '−14.126']
TBI_103	[8, 1, 2, '2542.697']	[8, 1, 8, '8422.112']	[9, 1, 3, '2832.935']	[4, 1, 2, '1384.877']	[10, 1, 1, '59606.024']	[1, 1, 9, '4707.190']	[7, 1, 5, '1614.544']	[3, 1, 1, '791.598']	[10, 1, 1, '27946.372']	[6, 1, 2, '55.531']	[2, 1, 1, '−193.827']	[1, 1, 1, '−193.076']
TBI_104	[4, 1, 2, '3715.331']	[7, 1, 10, '1789.902']	[3, 1, 3, '601.941']	[1, 1, 1, '337.912']	[1, 1, 4, '16471.188']	[1, 1, 1, '486.303']	[1, 1, 2, '80.663']	[2, 1, 2, '22.752']	[9, 1, 1, '7244.001']	[1, 1, 2, '242.016']	[1, 1, 2, '1.158']	[1, 1, 1, '−14.056']
TBI_105	[6, 1, 1, '2386.668']	[1, 1, 2, '1976.162']	[3, 1, 3, '770.934']	[1, 1, 1, '374.930']	[1, 1, 8, '13743.443']	[1, 1, 2, '737.405']	[1, 1, 2, '359.042']	[2, 1, 3, '184.929']	[3, 1, 2, '14.000']	[1, 1, 1, '204.868']	[1, 1, 1, '−3.069']	[5, 1, 2, '−31.658']
TBI_106	[7, 1, 1, '5618.687']	[3, 1, 5, '1840.146']	[9, 1, 2, '696.184']	[3, 1, 5, '330.181']	[1, 1, 9, '16364.647']	[8, 1, 9, '−964.441']	[2, 1, 1, '−407.916']	[3, 1, 1, '−209.424']	[4, 1, 1, '−2092.997']	[1, 1, 1, '458.617']	[2, 1, 1, '30.024']	[1, 1, 5, '−16.150']
TBI_107	[10, 1, 1, '6173.907']	[5, 1, 6, '1661.255']	[2, 1, 4, '574.528']	[1, 1, 1, '318.744']	[1, 1, 6, '14679.800']	[5, 1, 1, '−602.737']	[2, 1, 1, '−215.790']	[1, 1, 1, '−105.277']	[8, 1, 1, '−466.665']	[1, 1, 1, '545.032']	[1, 1, 1, '86.081']	[1, 1, 1, '11.488']
TBI_108	[1, 1, 3, '2004.242']	[1, 1, 1, '648.972']	[1, 1, 1, '266.534']	[1, 1, 3, '140.861']	[2, 1, 8, '5369.098']	[1, 1, 1, '−625.873']	[3, 1, 3, '−153.625']	[1, 1, 1, '−72.004']	[1, 1, 1, '−5104.216']	[2, 1, 1, '96.404']	[1, 1, 1, '−25.264']	[1, 1, 1, '−32.791']
TBI_109	[6, 1, 3, '276.721']	[1, 1, 1, '335.184']	[10, 1, 2, '107.985']	[8, 1, 4, '45.989']	[1, 1, 8, '771.134']	[3, 1, 3, '14.186']	[1, 1, 1, '22.349']	[1, 1, 1, '13.994']	[3, 1, 3, '−79.196']	[1, 1, 6, '55.569']	[1, 1, 1, '7.995']	[6, 1, 1, '−5.137']
TBI_110	[6, 1, 6, '4470.392']	[4, 1, 8, '2406.468']	[8, 1, 9, '812.468']	[5, 1, 5, '440.770']	[1, 1, 7, '18946.739']	[6, 1, 5, '369.640']	[2, 1, 10, '94.481']	[3, 1, 1, '59.186']	[8, 1, 1, '917.587']	[1, 1, 2, '367.743']	[1, 1, 5, '−35.338']	[3, 1, 4, '−65.701']
TBI_111	[5, 1, 1, '−884.091']	[5, 1, 1, '3183.328']	[1, 1, 1, '1111.862']	[1, 1, 1, '574.672']	[8, 1, 2, '16406.020']	[5, 1, 1, '1905.199']	[1, 1, 1, '702.719']	[5, 1, 5, '359.829']	[3, 1, 9, '6931.459']	[1, 1, 1, '−224.253']	[1, 1, 1, '−191.500']	[1, 1, 1, '−121.690']
TBI_112	[5, 1, 1, '1860.804']	[2, 1, 7, '1897.303']	[5, 1, 3, '838.261']	[2, 1, 6, '485.937']	[9, 1, 6, '8815.433']	[9, 1, 10, '−324.208']	[4, 1, 1, '81.606']	[1, 1, 2, '77.601']	[5, 1, 7, '−9640.931']	[3, 1, 1, '58.025']	[1, 1, 2, '−87.276']	[1, 1, 3, '−78.763']

Appendix E. Residuals, ACF, and PACF Plots of Residuals and Analysis

This appendix contains the figures and tables for the evaluation of the median optimal ARIMA models. Included are comparative ACF/PACF plots of the residuals (original vs. post-ARIMA) for a single patient's ICP and AMP data at both minute-by-minute and hour-by-hour resolutions. Additionally, the variance of the overall data, the residual variance, and the count of significant spikes are provided both for an individual patient and as a summary of the entire population to demonstrate effective data modeling.

ACF, autocorrelative function; AMP, pulse amplitude of ICP; ARIMA, auto-regressive integrated moving average; ICP, intracranial pressure; PACF, partial ACF; RAP, compensatory reserve index.

The figure corresponds to the ACF and PACF plots of residuals of the ICP signal (a) before and (b) after ARIMA (5, 1, 1), demonstrating that the model moderately accounts for the ICP structure.

The figure documents the ACF and PACF of the residuals of the ICP-mapped ARIMA structure in the (a) 10-min-by-10-min, (b) 30-min-by-30-min, and (c) hour-by-hour relationships.

The figure corresponds to the ACF and PACF plots of residuals of the AMP signal (a) before and (b) after ARIMA (3, 1, 5), demonstrating that the model moderately accounts for the AMP structure.

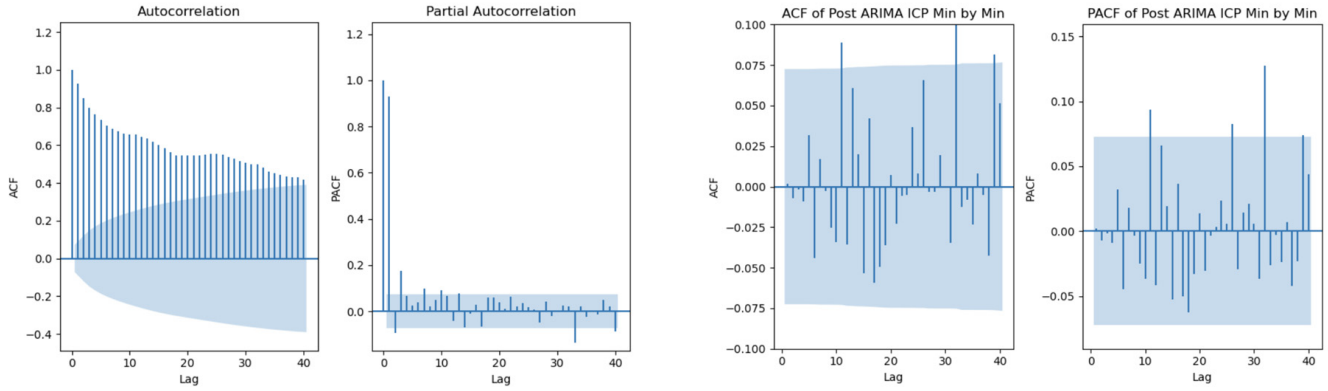

Figure A1. ACF and PACF plots for ICP at minute-by-minute resolution for an individual. (**a**) RAP pre-ARIMA plots, (**b**) RAP post-ARIMA (5, 1, 1) plots.

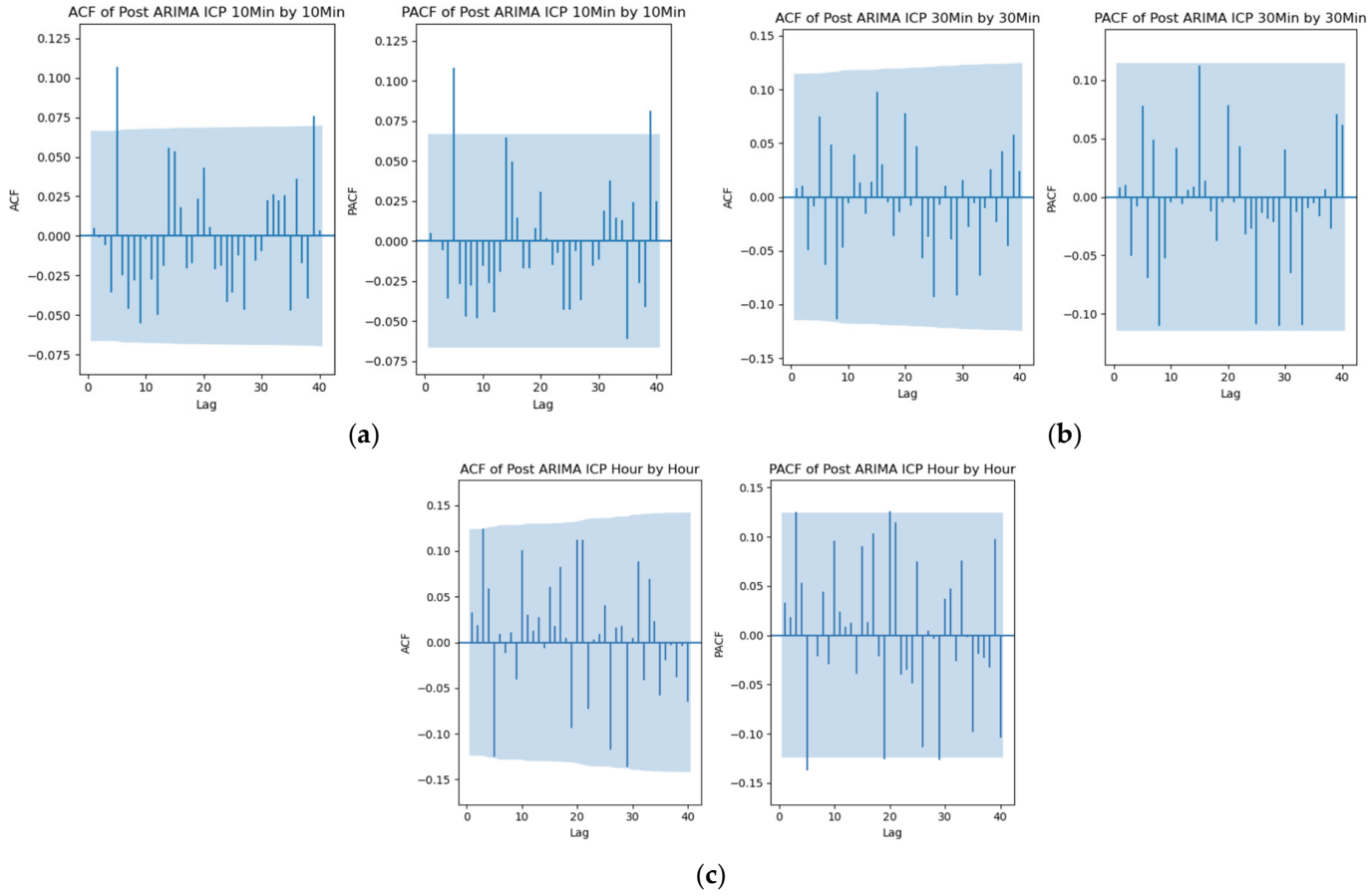

Figure A2. ACF and PACF plots for ICP at different resolutions for an individual. (**a**) At 10-min-by-10-min resolution with ARIMA (2, 1, 2), (**b**) at 30-min-by-30-min resolution with ARIMA (2, 1, 2), (**c**) at hour-by-hour resolution with ARIMA (2, 1, 2).

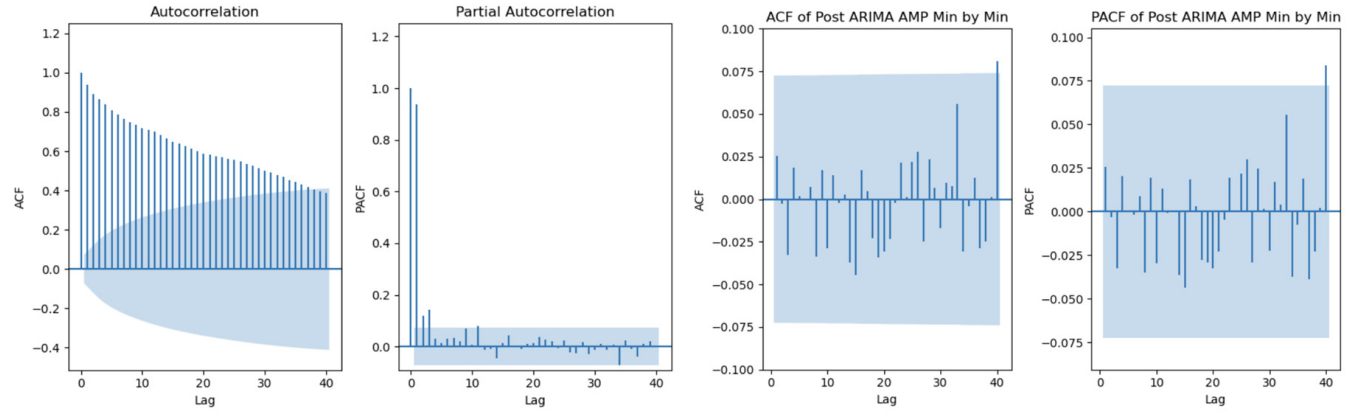

Figure A3. ACF and PACF plots for AMP at minute-by-minute resolution for an individual. (**a**) AMP pre-ARIMA plots, (**b**) AMP post-ARIMA (3, 1, 5) plots.

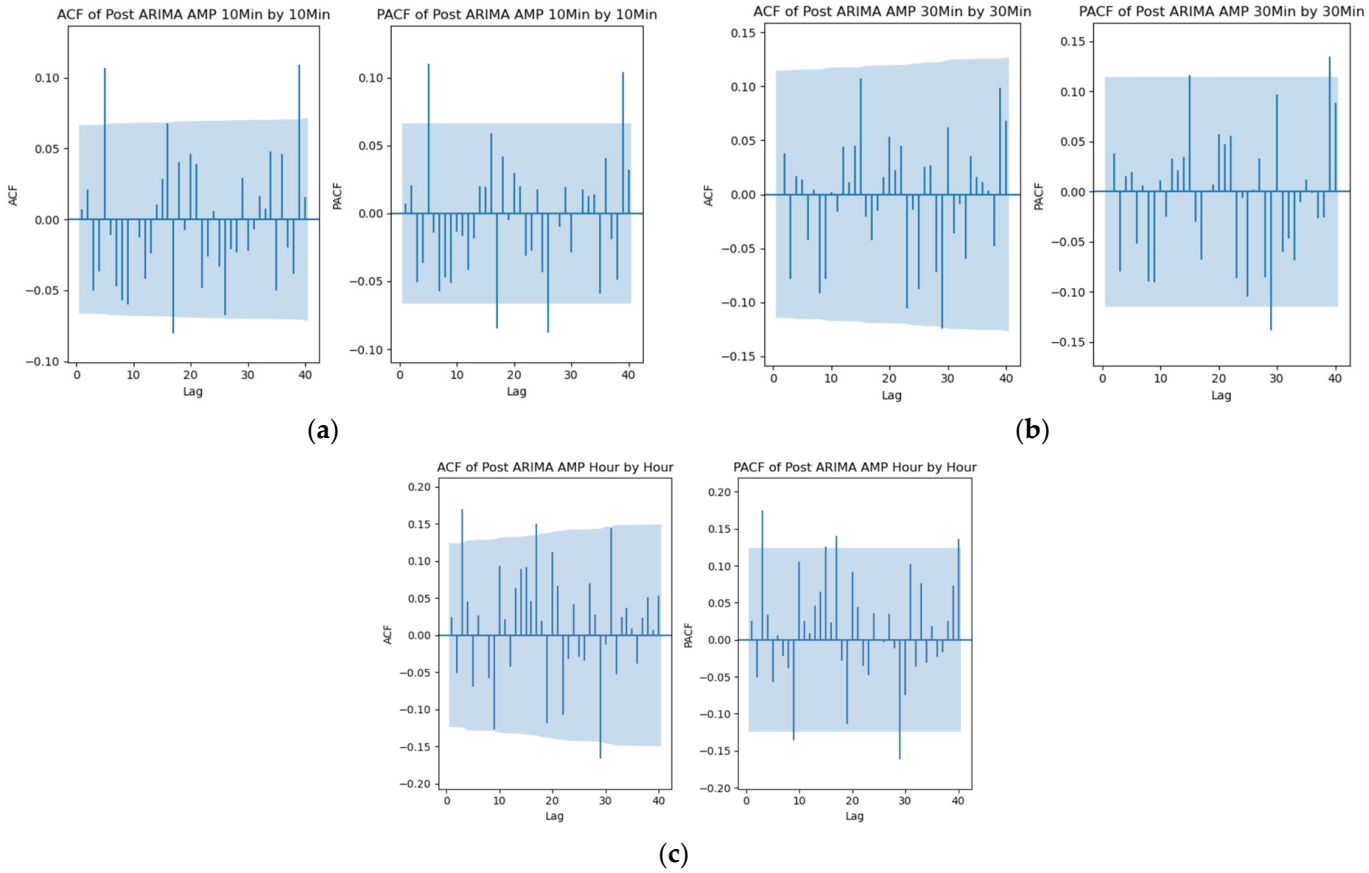

Figure A4. ACF and PACF plots for AMP at different resolutions for an individual. (**a**) At 10-min-by-10-min resolution with ARIMA (2, 1, 3), (**b**) at 30-min-by-30-min resolution with ARIMA (2, 1, 2), (**c**) at hour-by-hour resolution with ARIMA (1, 1, 1).

The figure documents the ACF and PACF of the residuals of the AMP-mapped ARIMA structure in the (a) 10-min-by-10-min, (b) 30-min-by-30-min, and (c) hour-by-hour relationships.

This figure documents the ACF and PACF of the residuals of RAP-mapped AMIRA structure at the minute-by-minute resolution for a particular patient.

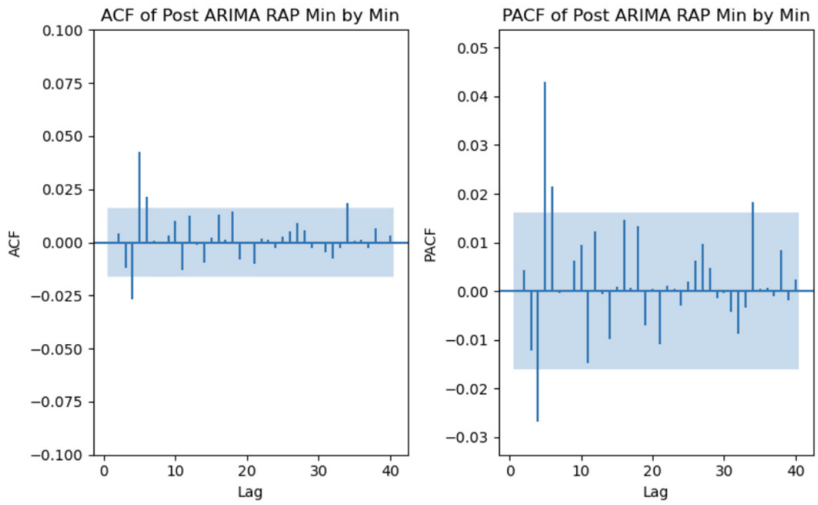

Figure A5. ACF/PACF plots for TBI_071 patient at minute-by-minute resolution.

Table A25. Summary of data variance, residual variance, and significant spike counts (single patient at minute-by-minute resolution).

Var_Data	Var_Model_Res	ACF_Org_Spikes	PACF_Org_Spikes	ACF_Model_Spikes	PACF_Model_Spikes
0.094394	0.067213	7	2	1	1

Table A26. Summary of data variance, residual variance, and significant spike counts (single patient at hour-by-hour resolution).

Var_Data	Var_Model_Res	ACF_Org_Spikes	PACF_Org_Spikes	ACF_Model_Spikes	PACF_Model_Spikes
0.022591	0.026622	5	4	0	0

Table A27. Summary of data variance, residual variance, and significant spike counts (all patients at minute-by-minute resolution for ICP).

Patient	Var_Data	Var_Model_Res	ACF_Org_Spikes	PACF_Org_Spikes	ACF_Model_Spikes	PACF_Model_Spikes
TBI_001	25.48364436	3.63261979	40	10	6	6
TBI_002	25.99239918	3.778211379	40	10	3	4
TBI_003	5.832911742	0.356290631	40	6	3	3
TBI_004	1.54749846	2.001749317	6	7	0	1
TBI_007	22.17284736	3.71386495	40	2	0	0
TBI_008	22.45823401	0.697897216	40	3	2	2
TBI_009	23.04243095	0.596444037	40	12	7	7
TBI_010	29.64771327	0.891392079	40	11	8	7
TBI_011	22.05212994	4.220736902	40	25	4	4
TBI_012	8.013360239	1.38645657	40	9	5	5
TBI_013	11.92649002	1.011265432	40	5	0	0
TBI_014	206.3275595	0.610974052	40	3	1	1
TBI_015	29.38595765	1.487679455	40	8	3	6
TBI_016	28.67873462	3.962485758	40	11	2	3
TBI_017	4.884287991	1.247570184	40	9	5	5
TBI_018	30.26943771	0.710362582	40	9	2	2
TBI_019	64.84611485	3.392462708	40	13	4	7
TBI_020	34.66444142	0.812315036	40	10	8	7
TBI_021	12.99958649	0.304253507	40	8	8	10
TBI_022	41.26722995	0.78598675	40	16	4	4
TBI_023	8.39310931	0.96030019	40	6	0	0
TBI_024	9.937736888	0.737050098	40	6	0	0
TBI_025	5.6131576	0.131189605	40	5	1	1

Table A27. *Cont.*

Patient	Var_Data	Var_Model_Res	ACF_Org_Spikes	PACF_Org_Spikes	ACF_Model_Spikes	PACF_Model_Spikes
TBI_026	13.6038047	3.197814484	40	16	3	3
TBI_027	218.8180735	11.78564682	33	2	0	0
TBI_028	44.69377387	3.839957714	40	9	8	13
TBI_029	153.6065005	2.604778911	40	11	5	5
TBI_030	17.70042196	1.864784494	40	5	1	1
TBI_031	147.8990394	3.600599954	19	14	0	1
TBI_032	123.15142	4.647488278	40	11	4	5
TBI_033	6.812439381	1.480322155	40	4	0	0
TBI_034	5.133167901	0.410004545	40	6	5	4
TBI_036	23.65478526	1.112019449	40	21	16	18
TBI_037	26.11314189	4.098089686	40	15	3	3
TBI_038	30.29076485	2.577853074	40	13	7	12
TBI_039	13.49696824	2.099302804	40	7	1	1
TBI_040	18.745057	1.784692725	40	17	0	0
TBI_041	11.31047671	1.123032534	40	14	7	7
TBI_042	24.22023835	4.499294917	40	9	4	4
TBI_043	2.586822103	0.35153109	40	11	2	2
TBI_044	35.55668495	1.533421164	40	4	1	1
TBI_045	18.5711965	1.337769803	40	8	5	5
TBI_046	47.47698993	1.477596291	40	6	0	0
TBI_047	25.41274556	2.654093577	40	9	3	4
TBI_048	41.20398957	2.262642035	40	6	1	3
TBI_049	6.126654845	0.713296488	40	13	4	3
TBI_050	7.785341194	2.311403027	37	5	4	4
TBI_051	139.8629741	1.426159636	40	3	1	1
TBI_052	33.71746377	1.110466773	40	9	0	0
TBI_053	10.76379679	0.356262064	40	11	3	3
TBI_054	7.084499918	0.976554498	40	8	3	4
TBI_055	10.90634253	1.650016163	40	13	4	5
TBI_056	0.804043501	0.891392712	3	3	0	0
TBI_057	48.87681393	2.8263661	40	16	2	2
TBI_058	16.03008498	0.809140693	40	9	3	3
TBI_059	10.0463926	0.446258303	40	5	0	0
TBI_060	21.93151746	2.3508094	39	4	0	0
TBI_061	1.574957371	0.460113272	40	7	0	0
TBI_062	21.71215414	0.904106032	40	9	4	5
TBI_063	7.333539552	1.204839187	40	10	3	3
TBI_064	8.221775923	2.506947257	40	10	2	3
TBI_065	14.54504238	1.197050539	40	11	3	4
TBI_066	8.034627278	0.383159191	40	13	5	6
TBI_067	5.070425724	1.817565311	40	6	2	2
TBI_068	6.864396674	0.848308599	40	14	0	0
TBI_069	35.0070712	5.026144838	40	22	0	0
TBI_070	48.96745992	1.081846427	40	2	0	0
TBI_071	15.38350768	1.259515207	40	12	4	3
TBI_072	47.61696074	1.285824876	40	6	4	5
TBI_073	11.84341251	0.814264356	40	13	3	3
TBI_074	10.06801951	1.190310723	40	9	1	2
TBI_075	37.67464427	4.419093731	40	5	2	2
TBI_076	25.36052945	3.646337932	40	21	6	4
TBI_077	21.07924879	3.761648412	40	7	3	2
TBI_078	10.01677573	1.160522021	40	6	1	1

Table A27. *Cont.*

Patient	Var_Data	Var_Model_Res	ACF_Org_Spikes	PACF_Org_Spikes	ACF_Model_Spikes	PACF_Model_Spikes
TBI_079	13.38632912	1.168007936	40	21	2	2
TBI_080	12.18723944	1.092091969	40	15	1	1
TBI_081	25.36549213	3.134550556	40	16	6	7
TBI_082	18.58540624	0.866971965	40	5	0	0
TBI_083	6.191120424	0.522826621	40	8	0	0
TBI_084	2.633460518	0.084481815	40	8	1	1
TBI_085	21.4099627	2.655752348	40	17	4	4
TBI_086	18.14679215	1.561314381	40	12	2	2
TBI_087	17.38688637	0.275156772	40	8	0	0
TBI_088	13.49917336	2.496028662	40	11	5	4
TBI_089	11.29641513	2.409699601	40	17	0	0
TBI_090	33.01801939	2.613315144	40	12	3	3
TBI_091	53.72778243	3.253103561	40	18	11	10
TBI_092	31.4890452	3.335741747	40	12	4	4
TBI_093	44.3391171	13.77693402	40	14	3	5
TBI_094	5.349989672	1.557513561	40	12	1	1
TBI_095	17.53414062	2.005922702	40	11	6	6
TBI_096	4.949354682	5.212009008	2	2	0	1
TBI_097	3.614231929	0.188247537	40	10	0	2
TBI_098	5.924771008	0.363675998	40	8	0	0
TBI_099	2.475207307	0.268928986	40	17	1	1
TBI_100	89.16902401	1.661882098	40	8	5	4
TBI_101	87.41789332	1.418430854	40	5	0	0
TBI_102	14.0938089	1.427338644	40	14	4	3
TBI_103	45.75361448	3.819852429	40	9	4	4
TBI_104	20.5961258	2.816142324	40	13	0	1
TBI_105	50.47620147	1.197399697	40	10	4	5
TBI_106	4.879338329	0.657268511	40	18	2	2
TBI_107	40.24937834	0.962644128	40	18	3	3
TBI_108	2.319360483	0.353460811	40	10	0	1
TBI_109	8.947088338	1.604656406	16	6	1	5
TBI_110	8.727249953	1.257566832	40	16	0	0
TBI_111	62.13325546	5.096635243	40	6	3	3
TBI_112	73.74613264	0.351517298	40	5	2	3

Table A28. Summary of data variance, residual variance, and significant spike counts (all patients at minute-by-minute resolution for AMP).

Patient	Var_Data	Var_Model_Res	ACF_Org_Spikes	PACF_Org_Spikes	ACF_Model_Spikes	PACF_Model_Spikes
TBI_001	1.343340132	0.328208076	40	16	3	4
TBI_002	2.293270228	0.277561938	40	4	2	2
TBI_003	0.033950971	0.0034604	40	14	2	2
TBI_004	0.098123741	0.120967039	0	0	1	1
TBI_007	0.421577478	0.065190038	40	8	3	3
TBI_008	0.043892222	0.005038925	40	11	1	1
TBI_009	0.996906165	0.032187021	40	15	6	6
TBI_010	6.347041183	0.129213776	40	6	2	3
TBI_011	1.312277596	0.213840339	40	15	3	3
TBI_012	0.462132863	0.080305173	40	7	0	0
TBI_013	1.157081169	0.118919687	40	9	0	0
TBI_014	6.235668395	0.039473745	40	8	2	2
TBI_015	0.373739971	0.036940885	40	16	7	14

Table A28. *Cont.*

Patient	Var_Data	Var_Model_Res	ACF_Org_Spikes	PACF_Org_Spikes	ACF_Model_Spikes	PACF_Model_Spikes
TBI_016	0.535529751	0.173978637	40	12	3	6
TBI_017	0.129681475	0.05467037	40	16	8	10
TBI_018	0.244679665	0.031328531	40	10	4	6
TBI_019	0.53535602	0.043162029	40	9	2	2
TBI_020	0.418860809	0.012523453	40	10	6	6
TBI_021	0.360069051	0.009375457	40	8	3	3
TBI_022	0.087812623	0.00649149	40	17	4	3
TBI_023	0.298002913	0.015042653	40	8	2	3
TBI_024	0.375828388	0.022713953	40	9	4	4
TBI_025	0.014143672	0.000972211	40	6	0	0
TBI_026	0.870126311	0.337256464	40	20	4	4
TBI_027	11.92212472	0.571789381	34	2	0	0
TBI_028	0.428491724	0.072199329	40	5	4	4
TBI_029	9.222276076	0.702653347	40	12	3	3
TBI_030	0.678317463	0.09170899	40	9	3	1
TBI_031	3.879065959	0.131475377	22	9	3	6
TBI_032	2.693738731	0.156684223	40	9	3	4
TBI_033	0.031237055	0.013479086	40	9	5	5
TBI_034	0.013505549	0.000891985	40	10	6	6
TBI_036	0.458545478	0.033138241	40	33	20	19
TBI_037	0.726783589	0.112287341	40	16	7	7
TBI_038	1.415467662	0.158541956	40	10	2	3
TBI_039	0.754187829	0.129954483	40	4	1	1
TBI_040	2.199989172	0.060258868	40	11	0	0
TBI_041	0.312547527	0.025969651	40	15	6	6
TBI_042	0.387784218	0.176371158	40	12	4	4
TBI_043	0.009088899	0.002822772	40	12	3	3
TBI_044	1.406372939	0.048415965	40	5	0	0
TBI_045	0.357953808	0.028984966	40	9	7	7
TBI_046	2.831491488	0.046052391	40	5	0	0
TBI_047	0.603317169	0.055163774	40	16	8	10
TBI_048	0.229417096	0.028562629	40	6	3	3
TBI_049	0.092535061	0.012429916	40	16	5	5
TBI_050	0.131344992	0.048349435	40	10	5	5
TBI_051	0.272216109	0.005253891	40	8	3	3
TBI_052	0.178086479	0.041510795	40	9	0	0
TBI_053	0.17703771	0.007135714	40	13	9	11
TBI_054	0.120238129	0.01331251	40	5	1	1
TBI_055	0.04458949	0.004439325	40	8	4	5
TBI_056	0.014316729	0.012281975	3	2	0	0
TBI_057	3.569392538	0.197457524	40	22	10	11
TBI_058	0.440942255	0.029971244	40	9	3	3
TBI_059	0.06431319	0.032033161	40	16	1	3
TBI_060	0.948292182	0.10982955	40	5	0	0
TBI_061	0.007634516	0.003148153	40	13	1	1
TBI_062	0.155563678	0.011886941	40	8	4	4
TBI_063	0.307571865	0.03461314	40	8	0	0
TBI_064	0.18061462	0.020803133	40	8	0	0
TBI_065	0.753440961	0.057827397	40	14	7	6
TBI_066	0.073513213	0.005912603	40	17	7	8
TBI_067	0.979082546	0.086219373	40	3	1	1
TBI_068	0.641463939	0.013394464	40	13	1	1

Table A29. Summary of data variance, residual variance, and significant spike counts (all patients at minute-by-minute resolution for AMP).

Patient	Var_Data	Var_Model_Res	ACF_Org_Spikes	PACF_Org_Spikes	ACF_Model_Spikes	PACF_Model_Spikes
TBI_069	1.318329346	0.101846174	40	23	1	1
TBI_070	0.185022046	0.02727362	40	4	0	1
TBI_071	2.530668095	0.067842403	40	10	3	3
TBI_072	6.710503387	0.214237447	40	14	8	10
TBI_073	0.484636139	0.011947037	40	12	7	7
TBI_074	0.277096685	0.095297557	40	18	7	7
TBI_075	1.486125557	0.116571414	40	4	0	0
TBI_076	0.645418044	0.148216566	40	23	2	2
TBI_077	0.629424092	0.133246137	40	9	1	1
TBI_078	0.019209186	0.00221262	40	8	1	1
TBI_079	0.417676325	0.057531593	40	14	3	3
TBI_080	0.044791897	0.017220055	40	21	1	1
TBI_081	1.183804719	0.082886153	40	15	8	8
TBI_082	0.103996832	0.018424478	40	7	0	0
TBI_083	0.04395137	0.013358484	40	16	2	2
TBI_084	0.016857147	0.007414626	40	17	1	1
TBI_085	0.61498222	0.052421746	40	17	9	9
TBI_086	0.190603289	0.026546363	40	10	5	5
TBI_087	0.373547952	0.010920271	40	15	2	1
TBI_088	0.427141836	0.068219118	40	11	3	3
TBI_089	0.198899172	0.019610697	40	12	2	3
TBI_090	1.384396796	0.077851899	40	14	10	12
TBI_091	3.328747757	0.130482218	40	16	10	9
TBI_092	1.823582958	0.121793733	40	11	2	1
TBI_093	0.630876397	0.199425558	40	20	2	2
TBI_094	0.280304083	0.148654574	40	6	0	0
TBI_095	0.359190123	0.043814102	40	13	5	5
TBI_096	0.140210439	0.252006422	3	4	0	0
TBI_097	0.063993143	0.003781466	40	9	1	1
TBI_098	0.034260407	0.010855786	40	19	3	3
TBI_099	0.022710951	0.004343759	40	17	2	1
TBI_100	4.757124998	0.09389492	40	13	6	7
TBI_101	0.44398893	0.111418776	40	12	6	6
TBI_102	3.341908617	0.229569975	40	14	3	3
TBI_103	4.664995835	0.417131024	40	16	7	6
TBI_104	0.582508647	0.31994129	40	17	2	3
TBI_105	2.726413542	0.056364906	40	9	3	3
TBI_106	0.077123613	0.042809749	40	27	1	1
TBI_107	0.079593997	0.054014426	40	17	7	7
TBI_108	0.040924208	0.010816167	40	8	0	0
TBI_109	0.078921504	0.052309563	26	5	1	1
TBI_110	0.275766739	0.069077438	40	14	1	1
TBI_111	7.722836378	0.385442009	40	7	2	3
TBI_112	0.274307466	0.008567303	40	13	4	4

Table A30. Summary of data variance, residual variance, and significant spike counts (all patients at minute-by-minute resolution for RAP).

Patient	Var_Data	Var_Model_Res	ACF_Org_Spikes	PACF_Org_Spikes	ACF_Model_Spikes	PACF_Model_Spikes
TBI_001	0.1412515	0.070159938	40	17	6	6
TBI_002	0.129468786	0.070973082	22	6	4	5
TBI_003	0.303736781	0.099534592	40	8	2	2
TBI_004	0.081088963	0.081802522	1	1	0	0
TBI_007	0.220394564	0.104454374	25	4	3	4
TBI_008	0.243247676	0.131983562	11	4	2	2
TBI_009	0.265758508	0.128971031	40	15	3	2
TBI_010	0.065567075	0.041179102	8	4	0	0
TBI_011	0.156122664	0.075908695	40	18	10	9
TBI_012	0.137185019	0.062191102	21	4	2	1
TBI_013	0.038380234	0.020769834	6	5	0	0
TBI_014	0.226988344	0.097216753	20	6	7	7
TBI_015	0.249062888	0.114315375	40	9	7	7
TBI_016	0.245432782	0.103552744	40	10	3	3
TBI_017	0.270157474	0.141310431	33	1	1	2
TBI_018	0.433322242	0.122960649	40	8	1	3
TBI_019	0.270802434	0.097354065	40	11	2	3
TBI_020	0.178845439	0.06900749	40	25	7	6
TBI_021	0.1592727	0.068723601	40	18	6	5
TBI_022	0.241727085	0.108595488	40	15	7	7
TBI_023	0.199574822	0.087205538	35	8	0	0
TBI_024	0.150651424	0.071601673	40	8	3	3
TBI_025	0.360465375	0.160011105	13	6	6	7
TBI_026	0.248670542	0.128177218	40	8	3	4
TBI_027	0.198875002	0.080355394	19	7	2	2
TBI_028	0.267335613	0.124469042	40	9	5	5
TBI_029	0.228487805	0.129658932	40	14	2	2
TBI_030	0.168989639	0.072832695	23	1	2	3
TBI_031	0.570832286	0.121785389	35	6	2	4
TBI_032	0.223697803	0.119528482	25	4	2	2
TBI_033	0.357154683	0.169029392	20	4	3	3
TBI_034	0.299954673	0.146083555	40	5	0	0
TBI_036	0.139018384	0.065390222	40	9	3	3
TBI_037	0.201542126	0.081334675	40	18	5	3
TBI_038	0.159896225	0.069844247	40	12	0	0
TBI_039	0.215899736	0.091512222	34	7	2	3
TBI_040	0.160825525	0.072372323	40	9	4	5
TBI_041	0.180018002	0.081199784	39	6	4	5
TBI_042	0.281391818	0.132910462	40	9	2	3
TBI_043	0.292297839	0.146629363	40	8	5	5
TBI_044	0.201556902	0.099458121	22	6	1	2
TBI_045	0.163299125	0.079140004	40	10	5	6
TBI_046	0.087890007	0.045085374	10	3	3	3
TBI_047	0.294378248	0.141437383	36	4	1	1
TBI_048	0.329537719	0.150167293	37	5	1	1
TBI_049	0.354216239	0.168793758	40	14	6	5
TBI_050	0.237448831	0.127893757	12	6	2	3
TBI_051	0.38789464	0.185095875	25	5	4	3
TBI_052	0.451801269	0.137452089	40	6	1	1
TBI_053	0.29948899	0.097003591	40	14	3	4
TBI_054	0.094393531	0.067212536	10	3	2	2

Table A30. *Cont.*

Patient	Var_Data	Var_Model_Res	ACF_Org_Spikes	PACF_Org_Spikes	ACF_Model_Spikes	PACF_Model_Spikes
TBI_055	0.331569396	0.144918929	40	11	4	5
TBI_056	0.415221004	0.288936762	7	7	1	3
TBI_057	0.12107862	0.060243334	40	20	9	8
TBI_058	0.269206065	0.119063577	40	19	8	8
TBI_059	0.239644162	0.119257502	40	3	0	0
TBI_060	0.183222724	0.106193035	28	3	0	0
TBI_061	0.263170505	0.12546849	32	5	3	3
TBI_062	0.373968292	0.157995046	16	5	1	1
TBI_063	0.189257062	0.098562334	27	4	2	2
TBI_064	0.416873558	0.189968092	36	4	2	3
TBI_065	0.177895434	0.085929203	29	5	3	3
TBI_066	0.22758353	0.106378819	40	14	8	7
TBI_067	0.161076046	0.085550426	12	4	3	3
TBI_068	0.31934334	0.138317772	40	8	3	3
TBI_069	0.147241898	0.072484398	38	10	2	2
TBI_070	0.364200356	0.156315925	17	3	0	0
TBI_071	0.1287753	0.058878032	34	6	4	4
TBI_072	0.250563826	0.106217166	38	4	2	3
TBI_073	0.211912393	0.097517151	40	14	5	5
TBI_074	0.235383185	0.112651905	40	8	2	2
TBI_075	0.251232415	0.105233391	40	8	3	4
TBI_076	0.150319996	0.07557991	40	10	2	3
TBI_077	0.202743169	0.099692366	40	8	2	2
TBI_078	0.350487187	0.181963517	4	3	0	0
TBI_079	0.168253314	0.069700859	35	9	4	4
TBI_080	0.315216263	0.1683715	40	8	4	4
TBI_081	0.146978659	0.057566577	40	11	5	5
TBI_082	0.263233461	0.12987111	14	6	3	3
TBI_083	0.358715999	0.147852695	29	9	6	7
TBI_084	0.315127065	0.141740705	30	11	6	5
TBI_085	0.134127951	0.070830416	39	6	3	3
TBI_086	0.196843926	0.08764298	40	18	5	6
TBI_087	0.18085509	0.081993391	40	15	6	4
TBI_088	0.084775108	0.043740211	35	12	6	7
TBI_089	0.283335967	0.123453535	40	18	2	2
TBI_090	0.222956546	0.076929373	40	17	3	3
TBI_091	0.090112254	0.039253186	40	22	3	3
TBI_092	0.203595545	0.084275289	40	18	4	4
TBI_093	0.190981587	0.085474574	40	12	6	6
TBI_094	0.306490751	0.164434451	18	3	2	2
TBI_095	0.144113211	0.066675476	40	5	1	1
TBI_096	0.301859576	0.158155105	9	6	0	2
TBI_097	0.231525838	0.106497988	40	8	1	1
TBI_098	0.277038629	0.131407275	39	12	5	5
TBI_099	0.259310022	0.141085614	38	8	2	2
TBI_100	0.120183335	0.05448055	40	22	7	7
TBI_101	0.256311834	0.119121748	40	8	2	3
TBI_102	0.289243285	0.137082761	40	15	2	2
TBI_103	0.154182022	0.070261691	40	15	8	7
TBI_104	0.297232126	0.140985497	40	14	0	0
TBI_105	0.288800164	0.10316541	40	15	1	0
TBI_106	0.284772004	0.136019806	40	6	1	0

Table A30. *Cont.*

Patient	Var_Data	Var_Model_Res	ACF_Org_Spikes	PACF_Org_Spikes	ACF_Model_Spikes	PACF_Model_Spikes
TBI_107	0.425581549	0.186041656	40	14	7	8
TBI_108	0.205362702	0.113394438	36	4	0	0
TBI_109	0.375330545	0.217200451	8	4	5	9
TBI_110	0.242788623	0.120073816	40	6	4	4
TBI_111	0.108203624	0.046197093	27	8	4	4
TBI_112	0.176414156	0.085018341	40	7	1	1

Table A31. Median of the data variance, residual variance, and significant spike counts for total population at min-by-min resolution.

Parameters	Var_Data	Var_Model_Res	ACF_Org_Spikes	PACF_Org_Spikes	ACF_Model_Spikes	PACF_Model_Spikes
ICP	18.57120	1.41843	40	9	2	3
AMP	0.41768	0.04842	40	11	3	3
RAP	0.23153	0.10523	40	8	3	3

Table A32. Mean of the data variance, residual variance, and significant spike counts for total population at min-by-min resolution.

Parameters	Var_Data	Var_Model_Res	ACF_Org_Spikes	PACF_Org_Spikes	ACF_Model_Spikes	PACF_Model_Spikes
ICP	29.78738	2.00069	38.48624	10.05505	2.72477	3.07339
AMP	1.15358	0.08891	38.60550	11.56881	3.35780	3.63303
RAP	0.23621	0.10882	32.44954	9	3.16514	3.34862

Table A33. Median of residuals at different resolutions.

Parameter	Minute-by-Minute	10-min-by-10-min	30-min-by-30-min	Hour-by-Hour
ICP	0.17941	0.28646	0.37397	0.41906
AMP	0.13549	0.21710	0.19870	0.19970
RAP	0.12564	0.18085	0.14078	0.11851

Appendix F. A Comparative Analysis Between Clean and Artifact Data Using Optimal ARIMA

This appendix presents the optimal ARIMA models for artifact segments for each patient at both minute-by-minute and 10 min intervals, selected based on the lowest AIC value. Each cell displays four values—the *p*-, *d*-, and *q*-orders, along with the model's AIC score. m refers to minute. Comparative tables and figures between clean and artifact profiles are also provided, showing median and mean values of the optimal ARIMA model orders, as well as scatterplots of these orders.

AIC, Akaike information criterion; AMP, pulse amplitude of ICP; ARIMA, auto-regressive integrated moving average; ICP, intracranial pressure; *p*-, *d*-, and *q*-orders, three components of ARIMA model, defining autoregression, integrated, and a moving average part, respectively; RAP, compensatory reserve index.

Table A34. Optimal ARIMA models of artifact segments.

Patient	ICP m by m	ICP 10 m by 10 m	AMP m by m	AMP 10 m by 10 m	RAP m by m	RAP 10 m by 10 m
TBI_001	[1, 1, 1, '216.851']	[6, 1, 1, '4255.733']	[1, 1, 6, '911.386']	[6, 1, 1, '1332.552']	[1, 1, 6, '59.114']	[6, 1, 5, '−192.534']
TBI_002	[1, 1, 1, '195.969']	[3, 1, 1, '798.246']	[4, 1, 4, '20.000']	[1, 1, 2, '390.750']	[2, 1, 9, '366.023']	[2, 1, 1, '−52.852']
TBI_003	[3, 1, 3, '151.597']	[4, 1, 3, '609.108']	[1, 1, 1, '654.294']	[2, 1, 2, '−613.493']	[1, 1, 1, '341.556']	[3, 1, 4, '102.301']
TBI_004	[1, 1, 1, '380.408']	[8, 1, 5, '19.483']	[1, 1, 2, '1958.890']	[10, 1, 1, '−8.337']	[1, 1, 9, '−184.189']	[1, 1, 1, '7.550']
TBI_007	[1, 1, 1, '260.029']	[1, 1, 1, '341.530']	[1, 1, 5, '1457.070']	[1, 1, 1, '−42.308']	[10, 1, 1, '804.155']	[1, 1, 1, '29.447']

Table A34. *Cont.*

Patient	ICP m by m	ICP 10 m by 10 m	AMP m by m	AMP 10 m by 10 m	RAP m by m	RAP 10 m by 10 m
TBI_008	[2, 1, 4, '1253.486']	[6, 1, 7, '640.823']	[5, 1, 8, '4040.300']	[1, 1, 5, '−234.704']	[1, 1, 3, '−1014.547']	[1, 1, 1, '133.499']
TBI_009	[1, 1, 5, '1390.931']	[3, 1, 1, '2728.697']	[8, 1, 8, '4457.610']	[2, 1, 5, '−198.338']	[4, 1, 10, '838.514']	[2, 1, 3, '405.306']
TBI_010	[3, 1, 4, '302.078']	[2, 1, 8, '829.657']	[1, 1, 2, '1253.633']	[8, 1, 2, '421.414']	[3, 1, 2, '582.267']	[2, 1, 4, '−123.974']
TBI_011	[4, 1, 1, '432.608']	[4, 1, 1, '3969.556']	[9, 1, 5, '1860.488']	[5, 1, 5, '1322.034']	[3, 1, 1, '1183.942']	[9, 1, 1, '−66.064']
TBI_012	[5, 1, 3, '1207.493']	[3, 1, 3, '932.354']	[10, 1, 10, '5313.922']	[3, 1, 4, '170.531']	[9, 1, 10, '2074.735']	[1, 1, 1, '34.510']
TBI_013	[6, 1, 6, '90.568']	[1, 1, 1, '285.451']	[9, 1, 5, '75.752']	[1, 1, 1, '116.816']	[3, 1, 1, '11.060']	[1, 1, 1, '−111.659']
TBI_014	[6, 1, 1, '981.569']	[6, 1, 2, '705.939']	[10, 1, 10, '4907.600']	[4, 1, 1, '170.705']	[9, 1, 10, '319.266']	[1, 1, 1, '149.620']
TBI_015	[1, 1, 4, '1744.311']	[4, 1, 10, '3273.361']	[8, 1, 3, '7903.675']	[6, 1, 7, '887.067']	[9, 1, 1, '1431.264']	[4, 1, 1, '325.832']
TBI_016	[1, 1, 1, '221.447']	[4, 1, 5, '577.298']	[5, 1, 10, '821.869']	[2, 1, 6, '92.695']	[6, 1, 1, '564.081']	[3, 1, 5, '35.309']
TBI_017	[1, 1, 1, '260.924']	[1, 1, 2, '841.047']	[4, 1, 1, '2207.630']	[5, 1, 6, '−46.309']	[8, 1, 4, '28.000']	[5, 1, 5, '144.457']
TBI_018	[1, 1, 1, '162.220']	[1, 1, 3, '433.669']	[3, 1, 2, '1149.084']	[1, 1, 2, '−13.491']	[1, 1, 1, '404.283']	[3, 1, 3, '89.550']
TBI_019	[5, 1, 2, '26.560']	[2, 1, 6, '408.893']	[1, 1, 1, '27.672']	[4, 1, 3, '13.428']	[2, 1, 1, '−74.780']	[8, 1, 7, '18.908']
TBI_020	[1, 1, 3, '1008.423']	[8, 1, 3, '4486.602']	[5, 1, 3, '4279.900']	[1, 1, 3, '5.157']	[9, 1, 9, '1891.217']	[3, 1, 1, '−23.169']
TBI_021	[3, 1, 1, '541.141']	[1, 1, 2, '2075.738']	[9, 1, 2, '1821.910']	[1, 1, 3, '−1094.246']	[1, 1, 2, '511.206']	[1, 1, 2, '−105.751']
TBI_022	[1, 1, 4, '672.260']	[3, 1, 4, '2732.960']	[7, 1, 9, '2462.705']	[6, 1, 3, '−1294.473']	[3, 1, 6, '839.036']	[1, 1, 2, '339.065']
TBI_023	[1, 1, 1, '251.917']	[5, 1, 8, '2102.452']	[1, 1, 4, '949.311']	[2, 1, 2, '286.001']	[2, 1, 5, '503.681']	[1, 1, 1, '140.425']
TBI_024	[3, 1, 7, '630.735']	[2, 1, 2, '1977.338']	[10, 1, 8, '2840.440']	[3, 1, 7, '213.528']	[7, 1, 9, '770.870']	[5, 1, 1, '46.978']
TBI_025	[1, 1, 4, '268.862']	[5, 1, 7, '673.930']	[6, 1, 3, '940.446']	[2, 1, 1, '−187.712']	[4, 1, 10, '161.285']	[1, 1, 1, '182.025']
TBI_026	[4, 1, 1, '366.193']	[3, 1, 1, '3079.708']	[2, 1, 5, '1669.426']	[4, 1, 7, '884.406']	[6, 1, 7, '845.558']	[2, 1, 1, '282.125']
TBI_027	[10, 1, 1, '4099.958']	[6, 1, 6, '3432.804']	[3, 1, 3, '18617.367']	[8, 1, 9, '1810.299']	[9, 1, 9, '6422.273']	[3, 1, 2, '46.304']
TBI_028	[3, 1, 8, '1982.529']	[6, 1, 5, '2481.023']	[10, 1, 10, '1639.158']	[1, 1, 1, '558.722']	[10, 1, 7, '3723.586']	[1, 1, 1, '228.778']
TBI_029	[2, 1, 4, '1868.183']	[9, 1, 9, '3676.162']	[7, 1, 5, '8724.573']	[4, 1, 6, '1817.830']	[7, 1, 7, '4065.914']	[3, 1, 1, '323.412']
TBI_030	[1, 1, 1, '840.829']	[2, 1, 5, '1440.883']	[1, 1, 2, '4871.952']	[2, 1, 1, '424.745']	[2, 1, 4, '2217.295']	[1, 1, 1, '125.002']
TBI_031	[6, 1, 1, '3583.410']	[1, 1, 1, '116.934']	[4, 1, 4, '11342.088']	[9, 1, 1, '65.009']	[9, 1, 10, '5250.503']	[10, 1, 1, '12.878']
TBI_032	[3, 1, 2, '629.617']	[4, 1, 6, '1243.360']	[1, 1, 9, '3071.748']	[8, 1, 6, '414.222']	[3, 1, 1, '871.735']	[1, 1, 1, '90.492']
TBI_033	[2, 1, 2, '99.774']	[1, 1, 2, '556.279']	[2, 1, 4, '420.894']	[1, 1, 1, '−196.827']	[2, 1, 1, '235.039']	[1, 1, 1, '134.205']
TBI_034	[1, 1, 2, '880.048']	[2, 1, 5, '608.336']	[6, 1, 2, '3311.861']	[2, 1, 1, '−560.840']	[1, 1, 1, '1979.590']	[1, 1, 1, '118.680']
TBI_036	[1, 1, 1, '603.420']	[5, 1, 7, '6284.400']	[2, 1, 2, '2793.023']	[10, 1, 8, '2447.168']	[6, 1, 10, '812.963']	[1, 1, 1, '−40.093']
TBI_037	[6, 1, 1, '1049.940']	[1, 1, 1, '3174.555']	[1, 1, 9, '6439.643']	[1, 1, 2, '692.762']	[1, 1, 1, '2653.677']	[6, 1, 7, '186.534']
TBI_038	[1, 1, 2, '327.503']	[3, 1, 10, '3651.071']	[1, 1, 1, '1631.377']	[2, 1, 8, '1418.069']	[2, 1, 5, '793.073']	[1, 1, 1, '163.865']
TBI_039	[1, 1, 3, '248.396']	[1, 1, 1, '1373.530']	[3, 1, 10, '1548.009']	[1, 1, 2, '461.798']	[7, 1, 5, '699.469']	[1, 1, 1, '147.763']
TBI_040	[2, 1, 2, '597.103']	[1, 1, 3, '2388.786']	[7, 1, 9, '2358.536']	[3, 1, 4, '507.213']	[6, 1, 9, '853.780']	[1, 1, 2, '98.532']
TBI_041	[7, 1, 1, '624.256']	[1, 1, 1, '2322.222']	[1, 1, 1, '4350.928']	[1, 1, 3, '218.837']	[1, 1, 3, '1400.580']	[3, 1, 1, '215.685']
TBI_042	[1, 1, 1, '132.493']	[1, 1, 1, '1491.790']	[1, 1, 1, '846.594']	[4, 1, 1, '275.034']	[4, 1, 7, '370.171']	[2, 1, 3, '229.795']
TBI_043	[6, 1, 1, '3412.524']	[1, 1, 1, '583.359']	[9, 1, 10, '4393.327']	[1, 1, 1, '−742.371']	[8, 1, 8, '−10858.220']	[1, 1, 2, '159.959']
TBI_044	[5, 1, 1, '899.183']	[3, 1, 4, '712.394']	[10, 1, 1, '8831.879']	[2, 1, 1, '165.178']	[6, 1, 1, '1444.800']	[6, 1, 1, '70.514']
TBI_045	[2, 1, 6, '688.985']	[4, 1, 3, '1595.632']	[1, 1, 1, '3162.513']	[2, 1, 1, '125.979']	[1, 1, 4, '−2944.605']	[2, 1, 5, '13.006']
TBI_046	[1, 1, 4, '57.821']	[2, 1, 8, '745.024']	[1, 1, 1, '125.272']	[2, 1, 10, '340.444']	[1, 1, 1, '−21.288']	[2, 1, 2, '−91.210']
TBI_047	[1, 1, 4, '95.827']	[1, 1, 1, '233.857']	[1, 1, 1, '725.657']	[1, 1, 2, '−20.787']	[1, 1, 1, '249.664']	[3, 1, 2, '43.998']
TBI_048	[2, 1, 1, '−9.027']	[1, 1, 3, '1656.563']	[10, 1, 1, '68.995']	[2, 1, 1, '−669.049']	[10, 1, 1, '33.094']	[1, 1, 2, '436.151']
TBI_049	[1, 1, 2, '488.865']	[2, 1, 4, '543.931']	[1, 1, 1, '2721.889']	[6, 1, 9, '7.473']	[9, 1, 2, '875.675']	[2, 1, 4, '75.450']
TBI_050	[1, 1, 1, '117.525']	[2, 1, 2, '779.306']	[1, 1, 1, '767.686']	[2, 1, 1, '−239.027']	[1, 1, 1, '210.167']	[1, 1, 2, '129.049']
TBI_051	[1, 1, 5, '414.880']	[1, 1, 1, '420.971']	[1, 1, 4, '2888.338']	[2, 1, 10, '−111.112']	[4, 1, 1, '248.949']	[1, 1, 1, '120.369']
TBI_052	[5, 1, 5, '136.822']	[4, 1, 8, '1055.686']	[1, 1, 2, '665.639']	[8, 1, 10, '−414.364']	[1, 1, 2, '291.463']	[3, 1, 7, '171.868']
TBI_053	[2, 1, 3, '105.092']	[4, 1, 3, '248.705']	[1, 1, 1, '230.665']	[2, 1, 2, '−69.739']	[1, 1, 1, '−60.925']	[2, 1, 3, '−34.805']
TBI_054	[1, 1, 1, '134.648']	[1, 1, 1, '1387.897']	[3, 1, 1, '−1697.984']	[1, 1, 4, '−662.759']	[1, 1, 2, '−1830.949']	[2, 1, 1, '240.594']
TBI_055	[6, 1, 1, '495.105']	[8, 1, 1, '26.408']	[9, 1, 3, '28.000']	[6, 1, 1, '−13.890']	[5, 1, 8, '203.978']	[9, 1, 1, '17.316']
TBI_056	[2, 1, 1, '327.771']	[9, 1, 9, '7011.416']	[1, 1, 2, '2266.753']	[7, 1, 1, '2779.937']	[1, 1, 8, '968.387']	[5, 1, 1, '443.905']
TBI_057	[4, 1, 3, '2222.079']	[1, 1, 1, '1432.209']	[5, 1, 5, '10260.114']	[2, 1, 2, '−44.341']	[3, 1, 5, '3337.734']	[1, 1, 1, '146.171']
TBI_058	[2, 1, 1, '322.791']	[2, 1, 2, '383.868']	[1, 1, 1, '2050.290']	[1, 1, 1, '−221.804']	[1, 1, 1, '599.655']	[1, 1, 1, '73.161']
TBI_059	[3, 1, 1, '58.209']	[1, 1, 2, '1363.277']	[1, 1, 5, '189.682']	[1, 1, 5, '471.852']	[2, 1, 1, '87.081']	[2, 1, 4, '35.108']
TBI_060	[2, 1, 1, '143.785']	[3, 1, 2, '258.540']	[2, 1, 5, '453.600']	[1, 1, 7, '−451.396']	[2, 1, 5, '204.925']	[2, 1, 1, '84.490']

Table A34. *Cont.*

Patient	ICP m by m	ICP 10 m by 10 m	AMP m by m	AMP 10 m by 10 m	RAP m by m	RAP 10 m by 10 m
TBI_061	[4, 1, 3, '95.894']	[1, 1, 1, '401.476']	[3, 1, 2, '195.117']	[3, 1, 7, '19.553']	[1, 1, 1, '−149.068']	[3, 1, 3, '88.883']
TBI_062	[4, 1, 2, '92.239']	[1, 1, 1, '1489.315']	[2, 1, 1, '−887.826']	[1, 1, 2, '35.883']	[4, 1, 1, '−721.733']	[2, 1, 2, '40.785']
TBI_063	[4, 1, 1, '467.747']	[1, 1, 1, '274.303']	[5, 1, 10, '3628.414']	[2, 1, 2, '−79.875']	[1, 1, 1, '1415.880']	[1, 1, 1, '76.839']
TBI_064	[1, 1, 1, '194.979']	[1, 1, 2, '465.404']	[5, 1, 4, '22.000']	[1, 1, 1, '120.083']	[1, 1, 1, '241.505']	[1, 1, 1, '10.605']
TBI_065	[5, 1, 1, '239.342']	[4, 1, 3, '1368.894']	[1, 1, 1, '1666.025']	[2, 1, 1, '−896.379']	[1, 1, 1, '782.385']	[1, 1, 1, '150.551']
TBI_066	[1, 1, 1, '240.558']	[7, 1, 1, '385.927']	[1, 1, 1, '1617.437']	[2, 1, 10, '158.461']	[1, 1, 1, '563.820']	[1, 1, 1, '33.999']
TBI_067	[3, 1, 3, '645.248']	[1, 1, 1, '1229.778']	[1, 1, 1, '4416.943']	[1, 1, 3, '−217.419']	[1, 1, 2, '1180.296']	[3, 1, 3, '296.879']
TBI_068	[1, 1, 4, '146.175']	[3, 1, 4, '4544.290']	[1, 1, 1, '906.955']	[1, 1, 2, '1296.419']	[1, 1, 1, '290.948']	[10, 1, 1, '15.428']
TBI_069	[2, 1, 1, '605.122']	[1, 1, 4, '126.313']	[7, 1, 4, '4050.266']	[1, 1, 1, '−26.652']	[1, 1, 2, '1771.818']	[2, 1, 1, '49.412']
TBI_070	[4, 1, 1, '73.125']	[7, 1, 4, '6316.318']	[1, 1, 1, '−93.274']	[2, 1, 2, '2622.449']	[2, 1, 1, '−71.552']	[1, 1, 1, '−38.552']
TBI_071	[3, 1, 3, '304.884']	[7, 1, 9, '36.000']	[5, 1, 2, '1276.778']	[6, 1, 9, '288.003']	[4, 1, 1, '552.057']	[3, 1, 1, '75.470']
TBI_072	[1, 1, 1, '155.511']	[2, 1, 3, '5265.377']	[4, 1, 2, '16.000']	[3, 1, 5, '−1026.621']	[1, 1, 2, '309.501']	[1, 1, 1, '602.585']
TBI_073	[2, 1, 4, '307.419']	[1, 1, 2, '2353.766']	[10, 1, 5, '34.000']	[6, 1, 10, '−38.469']	[1, 1, 2, '755.731']	[1, 1, 1, '72.476']
TBI_074	[3, 1, 3, '126.786']	[8, 1, 10, '40.000']	[1, 1, 1, '−50.894']	[3, 1, 6, '244.269']	[1, 1, 1, '−639.540']	[3, 1, 3, '93.193']
TBI_075	[3, 1, 3, '323.676']	[1, 1, 2, '3795.065']	[1, 1, 5, '2518.804']	[6, 1, 5, '668.983']	[5, 1, 1, '401.281']	[3, 1, 1, '37.733']
TBI_076	[2, 1, 2, '153.266']	[1, 1, 1, '2098.357']	[1, 1, 3, '1149.362']	[3, 1, 3, '643.225']	[1, 1, 3, '347.456']	[3, 1, 1, '119.313']
TBI_077	[2, 1, 6, '235.293']	[1, 1, 1, '561.375']	[1, 1, 1, '1869.856']	[3, 1, 9, '−312.053']	[1, 1, 1, '433.423']	[1, 1, 1, '131.781']
TBI_078	[10, 1, 8, '40.000']	[1, 1, 1, '989.121']	[5, 1, 4, '22.000']	[1, 1, 1, '140.132']	[1, 1, 10, '−4685.873']	[4, 1, 1, '37.465']
TBI_079	[4, 1, 6, '200.652']	[3, 1, 1, '2914.104']	[4, 1, 1, '630.640']	[1, 1, 1, '−1450.861']	[5, 1, 5, '−53.220']	[1, 1, 2, '532.785']
TBI_080	[2, 1, 2, '526.633']	[8, 1, 8, '5232.541']	[9, 1, 7, '1413.642']	[3, 1, 4, '1931.642']	[2, 1, 4, '−95.125']	[1, 1, 1, '49.576']
TBI_081	[1, 1, 1, '410.170']	[2, 1, 2, '324.380']	[1, 1, 2, '1671.767']	[1, 1, 3, '−106.536']	[6, 1, 1, '326.753']	[1, 1, 1, '76.542']
TBI_082	[1, 1, 1, '142.962']	[4, 1, 4, '615.931']	[8, 1, 4, '701.148']	[1, 1, 1, '−480.234']	[1, 1, 7, '16.887']	[1, 1, 6, '182.994']
TBI_083	[4, 1, 2, '192.671']	[1, 1, 1, '254.656']	[3, 1, 3, '519.270']	[1, 1, 1, '−724.082']	[1, 1, 1, '−70.222']	[1, 1, 1, '227.432']
TBI_084	[7, 1, 2, '176.973']	[9, 1, 8, '3805.534']	[1, 1, 1, '1396.861']	[8, 1, 7, '282.638']	[1, 1, 1, '675.169']	[1, 1, 1, '−56.330']
TBI_085	[4, 1, 5, '164.428']	[4, 1, 9, '4333.346']	[1, 1, 1, '794.102']	[4, 1, 1, '43.771']	[5, 1, 1, '141.663']	[1, 1, 2, '148.433']
TBI_086	[1, 1, 3, '653.506']	[1, 1, 2, '2362.099']	[1, 1, 1, '2196.813']	[4, 1, 2, '−1591.208']	[1, 1, 1, '−8.758']	[1, 1, 1, '99.391']
TBI_087	[3, 1, 1, '254.955']	[3, 1, 4, '5733.186']	[9, 1, 2, '350.266']	[7, 1, 1, '1185.601']	[9, 1, 10, '−338.154']	[1, 1, 1, '−719.332']
TBI_088	[2, 1, 1, '313.831']	[1, 1, 2, '2767.672']	[3, 1, 4, '2097.287']	[1, 1, 1, '−898.413']	[1, 1, 1, '799.464']	[1, 1, 1, '361.620']
TBI_089	[5, 1, 5, '374.758']	[2, 1, 7, '2391.440']	[2, 1, 2, '3375.603']	[7, 1, 3, '605.383']	[1, 1, 3, '1499.648']	[1, 1, 1, '212.776']
TBI_090	[2, 1, 9, '627.030']	[7, 1, 2, '6128.983']	[6, 1, 9, '4000.068']	[5, 1, 7, '2342.235']	[1, 1, 7, '980.755']	[6, 1, 8, '−668.544']
TBI_091	[1, 1, 4, '492.351']	[1, 1, 5, '3760.560']	[1, 1, 1, '4113.294']	[3, 1, 4, '1543.450']	[2, 1, 9, '2720.688']	[7, 1, 2, '261.090']
TBI_092	[3, 1, 1, '377.535']	[1, 1, 2, '5118.541']	[2, 1, 1, '2346.761']	[3, 1, 1, '1003.610']	[1, 1, 1, '802.367']	[1, 1, 2, '279.230']
TBI_093	[1, 1, 1, '440.220']	[6, 1, 6, '394.269']	[1, 1, 1, '2516.182']	[1, 1, 1, '54.721']	[2, 1, 1, '1282.904']	[1, 1, 1, '127.756']
TBI_094	[4, 1, 2, '244.423']	[1, 1, 1, '2364.346']	[1, 1, 5, '692.869']	[1, 1, 3, '126.146']	[4, 1, 3, '418.360']	[4, 1, 9, '9.800']
TBI_095	[1, 1, 1, '222.588']	[1, 1, 1, '96.413']	[10, 1, 8, '40.000']	[1, 1, 2, '34.204']	[2, 1, 3, '317.848']	[1, 1, 4, '4.547']
TBI_096	[1, 1, 4, '1859.860']	[2, 1, 7, '539.291']	[1, 1, 6, '6557.346']	[3, 1, 3, '−861.808']	[1, 1, 3, '3169.689']	[2, 1, 1, '164.963']
TBI_097	[4, 1, 3, '197.839']	[1, 1, 2, '1453.918']	[4, 1, 2, '768.896']	[9, 1, 6, '−722.735']	[1, 1, 1, '545.407']	[3, 1, 1, '291.945']
TBI_098	[1, 1, 4, '341.200']	[4, 1, 6, '1044.266']	[1, 1, 1, '2084.600']	[5, 1, 5, '−1355.549']	[6, 1, 6, '642.491']	[4, 1, 4, '28.276']
TBI_099	[4, 1, 4, '296.096']	[5, 1, 1, '5978.417']	[1, 1, 1, '2039.579']	[2, 1, 9, '2860.168']	[1, 1, 2, '960.570']	[4, 1, 6, '−204.319']
TBI_100	[6, 1, 1, '1032.526']	[8, 1, 6, '32.000']	[8, 1, 8, '4341.087']	[1, 1, 3, '135.282']	[7, 1, 3, '1694.936']	[1, 1, 2, '55.751']
TBI_101	[5, 1, 1, '833.134']	[1, 1, 1, '1168.088']	[1, 1, 2, '5578.883']	[6, 1, 2, '409.388']	[1, 1, 3, '1230.939']	[7, 1, 1, '166.367']
TBI_102	[9, 1, 1, '21.916']	[8, 1, 8, '8422.112']	[2, 1, 2, '118.470']	[1, 1, 9, '4707.190']	[2, 1, 1, '106.422']	[6, 1, 2, '55.531']
TBI_103	[9, 1, 10, '42.000']	[7, 1, 10, '1789.902']	[1, 1, 1, '1871.172']	[1, 1, 1, '486.303']	[3, 1, 1, '953.341']	[1, 1, 2, '242.016']
TBI_104	[4, 1, 3, '170.430']	[1, 1, 2, '1976.162']	[8, 1, 5, '763.837']	[1, 1, 2, '737.405']	[9, 1, 7, '169.564']	[1, 1, 1, '204.868']
TBI_105	[1, 1, 4, '531.766']	[3, 1, 5, '1840.146']	[3, 1, 3, '2150.159']	[8, 1, 9, '−964.441']	[10, 1, 8, '932.014']	[1, 1, 1, '458.617']
TBI_106	[3, 1, 3, '126.549']	[5, 1, 6, '1661.255']	[3, 1, 1, '470.235']	[5, 1, 1, '−602.737']	[1, 1, 1, '101.765']	[1, 1, 1, '545.032']
TBI_107	[10, 1, 7, '38.000']	[1, 1, 1, '648.972']	[4, 1, 8, '2108.791']	[1, 1, 1, '−625.873']	[10, 1, 2, '1380.588']	[2, 1, 1, '96.404']
TBI_108	[1, 1, 1, '176.033']	[1, 1, 1, '335.184']	[9, 1, 10, '516.831']	[3, 1, 3, '14.186']	[8, 1, 4, '141.479']	[1, 1, 6, '55.569']
TBI_109	[1, 1, 1, '212.494']	[4, 1, 8, '2406.468']	[10, 1, 10, '998.789']	[6, 1, 5, '369.640']	[5, 1, 5, '396.094']	[1, 1, 2, '367.743']
TBI_110	[5, 1, 6, '398.988']	[5, 1, 1, '3183.328']	[2, 1, 4, '1697.653']	[5, 1, 1, '1905.199']	[7, 1, 7, '1046.452']	[1, 1, 1, '−224.253']
TBI_111	[5, 1, 1, '1689.427']	[2, 1, 7, '1897.303']	[1, 1, 4, '12588.356']	[9, 1, 10, '−324.208']	[3, 1, 1, '1771.921']	[3, 1, 1, '58.025']
TBI_112	[1, 1, 2, '930.173']	[3, 1, 1, '1124.876']	[10, 1, 8, '3149.498']	[7, 1, 10, '1.010']	[8, 1, 7, '−708.170']	[1, 1, 1, '179.101']

Table A35. Median of the orders of optimal ARIMA models.

Parameter	Minute-by-Minute				10-min-by-10-min			
	Clean		Artifact		Clean		Artifact	
	p-Order	*q*-Order	*p*-Order	*q*-Order	*p*-Order	*q*-Order	*p*-Order	*q*-Order
ICP	3	5	2	3	3	3	2	1
AMP	3	3	2	2	2	3	1	1
RAP	5	1	2	2	1	1	1	1

Table A36. Mean of the orders of optimal ARIMA models.

Parameter	Minute-by-Minute				10-min-by-10-min			
	Clean		Artifact		Clean		Artifact	
	p-Order	*q*-Order	*p*-Order	*q*-Order	*p*-Order	*q*-Order	*p*-Order	*q*-Order
ICP	3.91743	5.28440	3.82569	3.78899	3.23077	3.69231	3.65385	1.87500
AMP	4.49541	4.20183	3.57798	3.72477	3.26923	3.72115	3.34615	2.35577
RAP	5.12844	2.06422	2.95413	2.62385	2.34615	2.02885	2.93269	2.44231

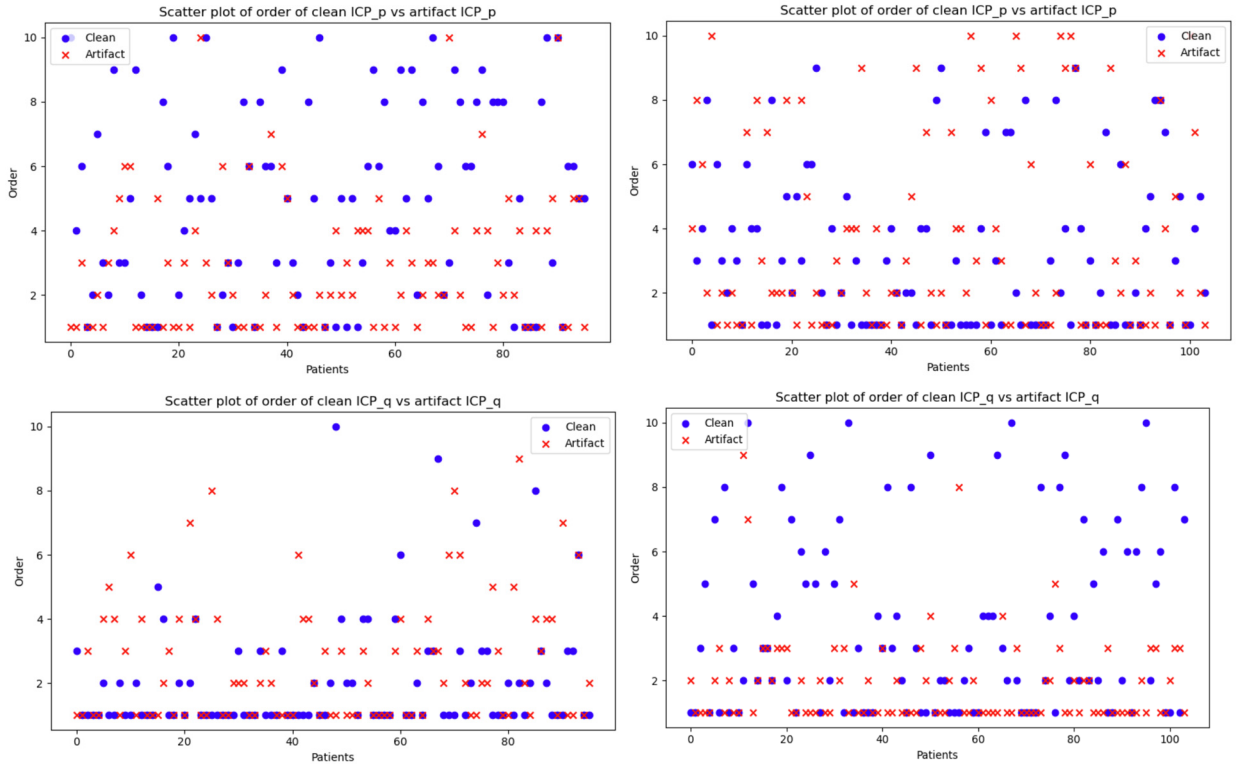

(**a**) (**b**)

Figure A6. Scatterplots for ICP *p*-orders and *q*-orders at different resolutions for each patient. (**a**) is minute-by-minute resolution and (**b**) is 10-mine-by-min resolution.

The figure demonstrates the value of the *p*-orders and *q*-orders from the optimal ARIMA models of ICP's clean vs. artifact data at (a) minute-by-minute resolution and (b) 10-min-by-10-min resolution. The blue circles correspond to the orders of the clean data, whereas the red crosses represent the orders of the artifact segment. If a red cross overlaps a blue circle, the value of the order for that patient is the same. If they do not overlap, the values differ.

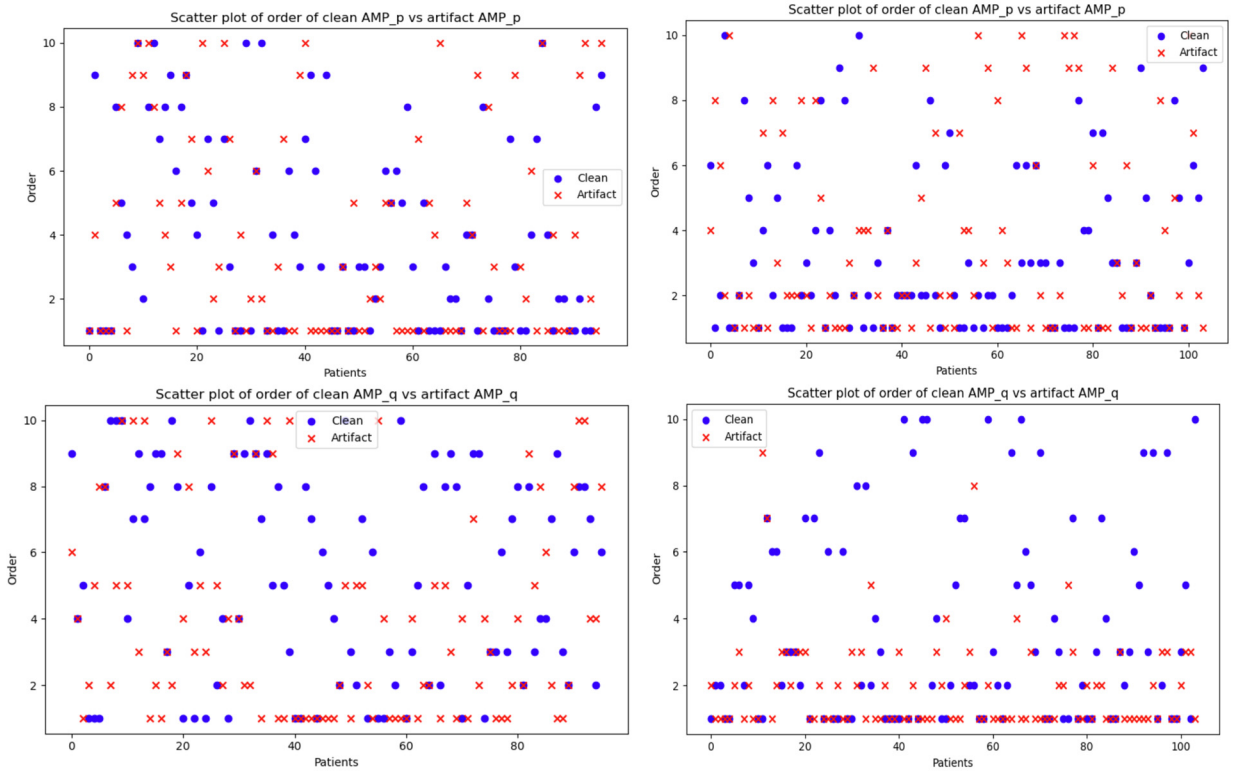

Figure A7. Scatterplots for AMP p-orders and q-orders at different resolutions for each patient. (**a**) is minute-by-minute resolution and (**b**) is 10-min-by-min resolution.

The figure demonstrates the value of the q orders from the optimal ARIMA models of RAP's clean vs. artifact group at (a) minute-by-minute resolution and (b) 10-min-by-10-min resolution.

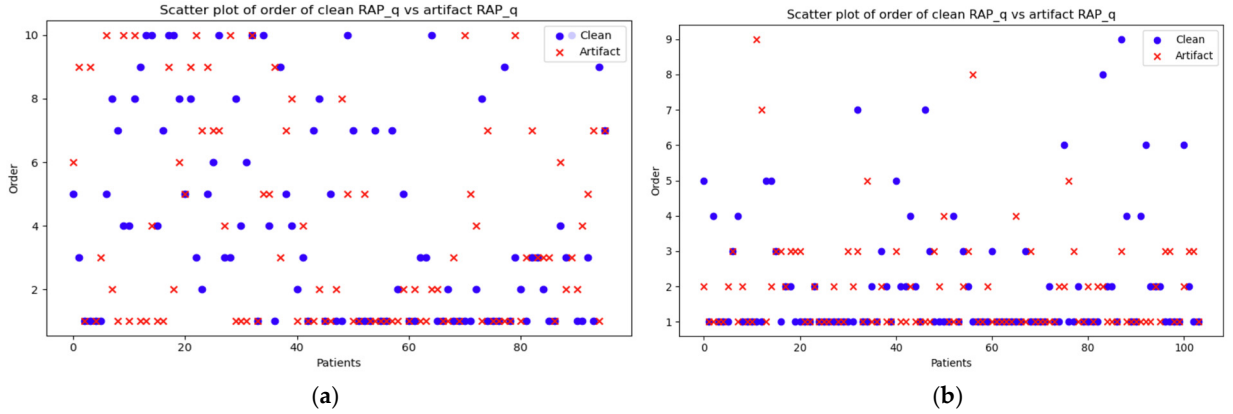

Figure A8. Scatterplots for RAP q-orders at different resolutions for each patient. (**a**) is minute-by-minute resolution and (**b**) is 10-min-by-min resolution.

The figure demonstrates the values of the q-orders from the optimal ARIMA models of RAP's clean vs. artifact group at (a) minute-by-minute resolution and (b) 10-min-by-10-min resolution.

Appendix G. Evaluation of the Potential Features for Identifying Artifacts

This appendix presents the values of the evaluation parameters for the potential features used in identifying artifacts at the minute-by-minute resolution and 10-min-by-10-min resolution.

AMP, pulse amplitude of ICP; ARIMA, auto-regressive integrated moving average; ICP, intracranial pressure, RAP, compensatory reserve index; RAP–ICP, cross-correlation between residuals of RAP and ICP; RAP–AMP, cross-correlation between residuals of RAP and AMP.

Table A37. Evaluation of potential features at the minute-by-minute resolution.

	Total Data	True Artifacts	Predicted Artifacts	False Positives	Success Rate (%)
Difference of the optimal ARIMA models					
ICP	4129	238	155	2398	65.258
AMP			148	2335	62.115
RAP			200	2212	84.038
Medians of the variance of residuals					
ICP	4129	238	167	1997	70.212
AMP			136	1897	56.916
RAP			218	1846	91.666
Median of the maximum cross-correlation of residuals					
RAP–ICP	4129	238	88	1985	37.011
RAP–AMP			146	1856	61.6

Table A38. Evaluation of potential features at the 10-min-by-10-min resolution.

Parameter	Total Data	True Artifacts	Predicted Artifacts	False Positives	Success Rate (%)
Difference of the optimal ARIMA models					
ICP	415	19	11	290	55.336
AMP			10	298	54.128
RAP			8	312	43.089
Medians of the variance of residuals					
ICP	415	19	16	223	85.092
AMP			14	222	74.264
RAP			16	219	84.411
Median of the maximum cross-correlation of residuals					
RAP–ICP	415	19	1	240	6.512
RAP–AMP			7	240	35.829

References

1. Maas, A.I.R.; Menon, D.K.; Adelson, P.D.; Andelic, N.; Bell, M.J.; Belli, A.; Bragge, P.; Brazinova, A.; Büki, A.; Chesnut, R.M.; et al. Traumatic brain injury: Integrated approaches to improve prevention, clinical care, and research. *Lancet Neurol.* **2017**, *16*, 987–1048. [CrossRef]
2. Carney, N.; Totten, A.M.; O'Reilly, C.; Ullman, J.S.; Hawryluk, G.W.; Bell, M.J.; Bratton, S.L.; Chesnut, R.; Harris, O.A.; Kissoon, N.; et al. Guidelines for the Management of Severe Traumatic Brain Injury, Fourth Edition. *Neurosurgery* **2017**, *80*, 6–15. [CrossRef] [PubMed]
3. Hawryluk, G.W.J.; Aguilera, S.; Buki, A.; Bulger, E.; Citerio, G.; Cooper, D.J.; Arrastia, R.D.; Diringer, M.; Figaji, A.; Gao, G.; et al. A management algorithm for patients with intracranial pressure monitoring: The Seattle International Severe Traumatic Brain Injury Consensus Conference (SIBICC). *Intensive Care Med.* **2019**, *45*, 1783. [CrossRef]
4. Chesnut, R.; Aguilera, S.; Buki, A.; Bulger, E.; Citerio, G.; Cooper, D.J.; Arrastia, R.D.; Diringer, M.; Figaji, A.; Gao, G.; et al. A management algorithm for adult patients with both brain oxygen and intracranial pressure monitoring: The Seattle International Severe Traumatic Brain Injury Consensus Conference (SIBICC). *Intensive Care Med.* **2020**, *46*, 919–929. [CrossRef]
5. Le Roux, P.; Menon, D.K.; Citerio, G.; Vespa, P.; Bader, M.K.; Brophy, G.M.; Diringer, M.N.; Stocchetti, N.; Videtta, W.; Armonda, R.; et al. Consensus summary statement of the International Multidisciplinary Consensus Conference on Multimodality Monitoring

in Neurocritical Care: A statement for healthcare professionals from the Neurocritical Care Society and the European Society of Intensive Care Medicine. *Intensive Care Med.* **2014**, *40*, 1189–1209. [CrossRef]
6. Budohoski, K.P.; Czosnyka, M.; de Riva, N.; Smielewski, P.; Pickard, J.D.; Menon, D.K.; Kirkpatrick, P.J.; Lavinio, A. The relationship between cerebral blood flow autoregulation and cerebrovascular pressure reactivity after traumatic brain injury. *Neurosurgery* **2012**, *71*, 652–660; discussion 660–661. [CrossRef] [PubMed]
7. Calviello, L.; Donnelly, J.; Cardim, D.; Robba, C.; Zeiler, F.A.; Smielewski, P.; Czosnyka, M. Compensatory-Reserve-Weighted Intracranial Pressure and Its Association with Outcome After Traumatic Brain Injury. *Neurocrit. Care* **2018**, *28*, 212–220. [CrossRef] [PubMed]
8. Kim, D.-J.; Czosnyka, Z.; Keong, N.; Radolovich, D.K.; Smielewski, P.; Sutcliffe, M.P.; Pickard, J.D.; Czosnyka, M. Index of cerebrospinal compensatory reserve in hydrocephalus. *Neurosurgery* **2009**, *64*, 494–501; discussion 501–502. [CrossRef] [PubMed]
9. Islam, A.; Froese, L.; Bergmann, T.; Gomez, A.; Sainbhi, A.S.; Vakitbilir, N.; Stein, K.Y.; Marquez, I.; Ibrahim, Y.; A Zeiler, F. Continuous monitoring methods of cerebral compliance and compensatory reserve: A scoping review of human literature. *Physiol. Meas.* **2024**, *45*, 06TR01. [CrossRef] [PubMed]
10. Maksymowicz, W.; Czosnyka, M.; Koszewski, W.; Szymanska, A.; Traczewski, W. The role of cerebrospinal compensatory parameters in the estimation of functioning of implanted shunt system in patients with communicating hydrocephalus (preliminary report). *Acta Neurochir.* **1989**, *101*, 112–116. [CrossRef] [PubMed]
11. Czosnyka, M.; Czosnyka, Z.; Keong, N.; Lavinio, A.; Smielewski, P.; Momjian, S.; Schmidt, E.A.; Petrella, G.; Owler, B.; Pickard, J.D. Pulse pressure waveform in hydrocephalus: What it is and what it isn't. *Neurosurg. Focus.* **2007**, *22*, E2. [CrossRef] [PubMed]
12. Czosnyka, Z.; Keong, N.; Kim, D.; Radolovich, D.; Smielewski, P.; Lavinio, A.; Schmidt, E.A.; Momjian, S.; Owler, B.; Pickard, J.D.; et al. Pulse amplitude of intracranial pressure waveform in hydrocephalus. *Acta Neurochir. Suppl.* **2008**, *102*, 137–140. [CrossRef] [PubMed]
13. Czosnyka, M.; Guazzo, E.; Whitehouse, M.; Smielewski, P.; Czosnyka, Z.; Kirkpatrick, P.; Piechnik, S.; Pickard, J.D. Significance of intracranial pressure waveform analysis after head injury. *Acta Neurochir* **1996**, *138*, 531–541; discussion 541–542. [CrossRef] [PubMed]
14. Sainbhi, A.S.; Vakitbilir, N.; Gomez, A.; Stein, K.Y.; Froese, L.; Zeiler, F.A. Time-Series autocorrelative structure of cerebrovascular reactivity metrics in severe neural injury: An evaluation of the impact of data resolution. *Biomed. Signal Process Control* **2024**, *95*, 106403. [CrossRef]
15. Froese, L.; Gomez, A.; Sainbhi, A.S.; Batson, C.; Stein, K.; Alizadeh, A.; Zeiler, F.A. Dynamic Temporal Relationship Between Autonomic Function and Cerebrovascular Reactivity in Moderate/Severe Traumatic Brain Injury. *Front. Netw. Physiol.* **2022**, *2*, 837860. [CrossRef]
16. Czosnyka, M.; Smielewski, P.; Timofeev, I.; Lavinio, A.; Guazzo, E.; Hutchinson, P.; Pickard, J.D. Intracranial Pressure: More Than a Number. *Neurosurg. Focus* **2007**, *22*, 1–7. [CrossRef]
17. Holm, S.; Eide, P.K. The frequency domain versus time domain methods for processing of intracranial pressure (ICP) signals. *Med. Eng. Phys.* **2008**, *30*, 164–170. [CrossRef] [PubMed]
18. Carrera, E.; Kim, D.-J.; Castellani, G.; Zweifel, C.; Czosnyka, Z.; Kasprowicz, M.; Smielewski, P.; Pickard, J.D.; Czosnyka, M. What Shapes Pulse Amplitude of Intracranial Pressure? *J. Neurotrauma* **2010**, *27*, 317–324. [CrossRef] [PubMed]
19. Islam, A.; Marquez, I.; Froese, L.; Vakitbilir, N.; Gomez, A.; Stein, K.Y.; Bergmann, T.; Sainbhi, A.S.; Zeiler, F.A. Association of RAP Compensatory Reserve Index with Continuous Multimodal Monitoring Cerebral Physiology, Neuroimaging, and Patient Outcome in Adult Acute Traumatic Neural Injury: A Scoping Review. *Neurotrauma Rep.* **2024**, *5*, 813–823. [CrossRef]
20. Weersink, C.S.A.; Aries, M.J.H.; Dias, C.; Liu, M.X.; Kolias, A.G.M.; Donnelly, J.M.B.; Czosnyka, M.; van Dijk, J.M.C.; Regtien, J.; Menon, D.K.P.; et al. Clinical and Physiological Events That Contribute to the Success Rate of Finding "Optimal" Cerebral Perfusion Pressure in Severe Brain Trauma Patients. *Crit. Care Med.* **2015**, *43*, 1952. [CrossRef]
21. Lee, H.-J.; Kim, H.; Kim, Y.-T.; Won, K.; Czosnyka, M.; Kim, D.-J. Prediction of Life-Threatening Intracranial Hypertension During the Acute Phase of Traumatic Brain Injury Using Machine Learning. *IEEE J. Biomed. Health Inform.* **2021**, *25*, 3967–3976. [CrossRef] [PubMed]
22. Tsigaras, Z.A.; Weeden, M.; McNamara, R.; Jeffcote, T.; Udy, A.A.; Anstey, J.; Plummer, M.; Bellapart, J.; Chow, A.; Delaney, A.; et al. The pressure reactivity index as a measure of cerebral autoregulation and its application in traumatic brain injury management. *Crit. Care Resusc.* **2023**, *25*, 229–236. [CrossRef] [PubMed]
23. Needham, E.; McFadyen, C.; Newcombe, V.; Synnot, A.J.; Czosnyka, M.; Menon, D. Cerebral Perfusion Pressure Targets Individualized to Pressure-Reactivity Index in Moderate to Severe Traumatic Brain Injury: A Systematic Review. *J. Neurotrauma* **2017**, *34*, 963–970. [CrossRef] [PubMed]
24. Gaasch, M.; Schiefecker, A.J.; Kofler, M.; Beer, R.; Rass, V.; Pfausler, B.; Thomé, C.; Schmutzhard, E.; Helbok, R. Cerebral Autoregulation in the Prediction of Delayed Cerebral Ischemia and Clinical Outcome in Poor-Grade Aneurysmal Subarachnoid Hemorrhage Patients*. *Crit. Care Med.* **2018**, *46*, 774. [CrossRef] [PubMed]
25. Sykora, M.; Czosnyka, M.; Liu, X.; Donnelly, J.; Nasr, N.; Diedler, J.; Okoroafor, F.; Hutchinson, P.; Menon, D.; Smielewski, P. Autonomic Impairment in Severe Traumatic Brain Injury: A Multimodal Neuromonitoring Study. *Crit. Care Med.* **2016**, *44*, 1173. [CrossRef]

26. Sorrentino, E.; Diedler, J.; Kasprowicz, M.; Budohoski, K.P.; Haubrich, C.; Smielewski, P.; Outtrim, J.G.; Manktelow, A.; Hutchinson, P.J.; Pickard, J.D.; et al. Critical thresholds for cerebrovascular reactivity after traumatic brain injury. *Neurocrit. Care* **2012**, *16*, 258–266. [CrossRef] [PubMed]
27. Anonymous. Pandas-Python Data Analysis Library. Available online: https://pandas.pydata.org/ (accessed on 17 December 2024).
28. Anonymous. Pandas. DataFrame. Describe—Pandas 2.2.3 Documentation. Available online: https://pandas.pydata.org/docs/reference/api/pandas.DataFrame.describe.html (accessed on 1 November 2024).
29. Zeiler, F.A.; Donnelly, J.; Menon, D.K.; Smielewski, P.; Hutchinson, P.J.; Czosnyka, M. A Description of a New Continuous Physiological Index in Traumatic Brain Injury Using the Correlation between Pulse Amplitude of Intracranial Pressure and Cerebral Perfusion Pressure. *J. Neurotrauma* **2018**, *35*, 963–974. [CrossRef] [PubMed]
30. Howells, T.; Lewén, A.; Sköld, M.K.; Ronne-Engström, E.; Enblad, P. An evaluation of three measures of intracranial compliance in traumatic brain injury patients. *Intensive Care Med.* **2012**, *38*, 1061–1068. [CrossRef]
31. Varsos, G.V.; Czosnyka, M.; Smielewski, P.; Garnett, M.R.; Liu, X.; Kim, D.-J.; Donnelly, J.; Adams, H.; Pickard, J.D.; Czosnyka, Z. Cerebral critical closing pressure in hydrocephalus patients undertaking infusion tests. *Neurol. Res.* **2015**, *37*, 674–682. [CrossRef]
32. Kiening, K.L.; Schoening, W.N.; Stover, J.F.; Unterberg, A. Continuous monitoring of intracranial compliance after severe head injury: Relation to data quality, intracranial pressure and brain tissue PO2. *Br. J. Neurosurg.* **2003**, *17*, 311–318. [CrossRef] [PubMed]
33. Anonymous. Mannwhitneyu—SciPy v1.14.1 Manual. Available online: https://docs.scipy.org/doc/scipy/reference/generated/scipy.stats.mannwhitneyu.html (accessed on 1 November 2024).
34. Anonymous. F_oneway—SciPy v1.14.1 Manual. Available online: https://docs.scipy.org/doc/scipy/reference/generated/scipy.stats.f_oneway.html (accessed on 1 November 2024).
35. Lütkepohl, H. *New Introduction to Multiple Time Series Analysis*; Springer Science & Business Media: Berlin/Heidelberg, Germany, 2005.
36. Chatfield, C. *The Analysis of Time Series: An Introduction*, 6th ed.; Chapman and Hall/CRC: New York, NY, USA, 2003. [CrossRef]
37. Sharma, R.R.; Kumar, M.; Maheshwari, S.; Ray, K.P. EVDHM-ARIMA-Based Time Series Forecasting Model and Its Application for COVID-19 Cases. *IEEE Trans. Instrum. Meas.* **2021**, *70*, 6502210. [CrossRef] [PubMed]
38. Li, Z.; Li, Y. A comparative study on the prediction of the BP artificial neural network model and the ARIMA model in the incidence of AIDS. *BMC Med. Inform. Decis. Mak.* **2020**, *20*, 143. [CrossRef] [PubMed]
39. Perktold, J.; Seabold, S.; Sheppard, K.; Quackenbush, P.; Arel-Bundock, V.; McKinney, W.; Langmore, I.; Baker, B.; Gommers, R.; Zhurko, Y.; et al. Statsmodels/Statsmodels: Release 0.14.2, Version v0.14.2. 2024. Available online: https://zenodo.org/records/10984387 (accessed on 13 January 2025).
40. Huang, L.; Sullivan, L.; Yang, J. Analyzing the impact of a state concussion law using an autoregressive integrated moving average intervention analysis. *BMC Health Serv. Res.* **2020**, *20*, 898. [CrossRef]
41. Mohamadi, S.; Amindavar, H.; Tayaranian Hosseini, S.M.A. ARIMA-GARCH Modeling for Epileptic Seizure Prediction. In Proceedings of the 2017 IEEE International Conference on Acoustics, Speech and Signal Processing (ICASSP), New Orleans, LA, USA, 5–9 March 2017; pp. 994–998. [CrossRef]
42. Kębłowski, P.; Welfe, A. The ADF–KPSS test of the joint confirmation hypothesis of unit autoregressive root. *Econ. Lett.* **2004**, *85*, 257–263. [CrossRef]
43. Anonymous. Pandas. DataFrame. Resample—Pandas 2.2.3 Documentation. Available online: https://pandas.pydata.org/docs/reference/api/pandas.DataFrame.resample.html (accessed on 1 November 2024).
44. Eide, P.K.; Sroka, M.; Wozniak, A.; Sæhle, T. Morphological characterization of cardiac induced intracranial pressure (ICP) waves in patients with overdrainage of cerebrospinal fluid and negative ICP. *Med. Eng. Phys.* **2012**, *34*, 1066–1070. [CrossRef]
45. Froese, L.; Dian, J.; Batson, C.; Gomez, A.; Unger, B.; Zeiler, F.A. The impact of hypertonic saline on cerebrovascular reactivity and compensatory reserve in traumatic brain injury: An exploratory analysis. *Acta Neurochir* **2020**, *162*, 2683–2693. [CrossRef] [PubMed]
46. Dias, C.; Silva, M.J.; Pereira, E.; Silva, S.; Cerejo, A.; Smielewski, P.; Rocha, A.P.; Gaio, A.R.; Paiva, J.-A.; Czosnyka, M. Post-traumatic multimodal brain monitoring: Response to hypertonic saline. *J. Neurotrauma* **2014**, *31*, 1872–1880. [CrossRef] [PubMed]
47. Zeiler, F.A.; Aries, M.; Cabeleira, M.; van Essen, T.A.; Stocchetti, N.; Menon, D.K.; Timofeev, I.; Czosnyka, M.; Smielewski, P.; Hutchinson, P.; et al. Statistical Cerebrovascular Reactivity Signal Properties after Secondary Decompressive Craniectomy in Traumatic Brain Injury: A CENTER-TBI Pilot Analysis. *J. Neurotrauma* **2020**, *37*, 1306–1314. [CrossRef] [PubMed]